

# MADDEN-JULIAN OSCILLATION

Chidong Zhang  
*Rosenstiel School of Marine and Atmospheric Science*  
*University of Miami*  
*Miami, Florida, USA*

Received 5 August 2004; revised 8 January 2005; accepted 25 May 2005; published 30 June 2005.

[1] The Madden-Julian Oscillation (MJO) is the dominant component of the intraseasonal (30–90 days) variability in the tropical atmosphere. It consists of large-scale coupled patterns in atmospheric circulation and deep convection, with coherent signals in many other variables, all propagating eastward slowly ( $\sim 5 \text{ m s}^{-1}$ ) through the portion of the Indian and Pacific oceans where the sea surface is warm. It constantly interacts with the underlying ocean and influences many weather and climate systems. The past decade has witnessed an expeditious progress in the study of the MJO: Its large-scale and multiscale structures are better described, its scale interaction is recognized, its broad influences on tropical and extratropical weather and climate are increasingly appreciated, and its mechanisms for

disturbing the ocean are further comprehended. Yet we are facing great difficulties in accurately simulating and predicting the MJO using sophisticated global weather forecast and climate models, and we are unable to explain such difficulties based on existing theories of the MJO. It is fair to say that the MJO remains an unmet challenge to our understanding of the tropical atmosphere and to our ability to simulate and predict its variability. This review, motivated by both the acceleration and gaps in our knowledge of the MJO, intends to synthesize what we currently know and what we do not know on selected topics: its observed basic characteristics, mechanisms, numerical modeling, air-sea interaction, and influences on the El Niño and Southern Oscillation.

**Citation:** Zhang, C. (2005), Madden-Julian Oscillation, *Rev. Geophys.*, 43, RG2003, doi:10.1029/2004RG000158.

## 1. INTRODUCTION

[2] A remarkable feature of the atmospheric circulation and moist convection in the tropics is their tendency to be organized at *planetary scales* and to propagate eastward at an averaged speed of  $5 \text{ m s}^{-1}$  across the equatorial Indian and western/central Pacific oceans, with a local intraseasonal period of 30–90 days. (Italicized terms are defined in the glossary, after the main text. Not all terms are explained according to standard meteorological and oceanographic definitions. Instead, the explanations are tailored to this article.) This phenomenon (Figure 1) is known as the Madden-Julian Oscillation (MJO). Since first documented by *Madden and Julian* [1971, 1972], the MJO has intrigued many atmospheric scientists and oceanographers all over the world.

[3] The MJO is intriguing for many reasons. It influences the variability of rainfall over the Pacific islands, in the monsoon regions of Asia [e.g., *Lau and Chan*, 1986; *Sui and Lau*, 1992; *Lawrence and Webster*, 2002] and Australia [e.g., *Hendon and Liebmann*, 1990], along the west coast of North America [e.g., *Mo and Higgins*, 1998; *Jones*, 2000; *Bond and Vecchi*, 2003], in South America [e.g., *Paegle et al.*, 2000; *Liebmann et al.*, 2004], and in Africa [*Matthews*, 2004]. It modulates the genesis of tropical cyclones in the Pacific Ocean and the Caribbean Sea [e.g., *Liebmann et al.*, 1994; *Nieto Ferreira et al.*, 1996; *Maloney and Hartmann*, 2000; *Hall et al.*, 2001; *Higgins and Shi*, 2001] and affects equatorial surface winds in the Atlantic Ocean [*Foltz and*

*McPhaden*, 2004]. Owing to its connection to these and other weather systems the MJO affects global medium and extended range weather forecasts [e.g., *Ferranti et al.*, 1990; *Hendon et al.*, 2000; *Jones and Schemm*, 2000]. It also modulates the global angular momentum [e.g., *Langley et al.*, 1981; *Gutzler and Ponte*, 1990; *Weickmann et al.*, 1997] and Earth's electric and magnetic fields [*Anyamba et al.*, 2000]. As will be discussed in this review, the dynamics of the MJO involves atmospheric planetary-scale circulations and its interaction with *mesoscale* convective activities; the MJO also interacts with the ocean and thereby may influence the evolution of El Niño–Southern Oscillation (ENSO); it is very difficult to simulate the MJO correctly by state-of-the-art global weather prediction models and global climate models (GCM). The MJO therefore tests our understanding of how the atmosphere operates in the tropics. Failing to explain, simulate, and predict the MJO exposes gaps in our knowledge of critical processes in the tropical climate system. The MJO might have even helped shape human history. The episodic strong *westerly* surface winds lasting up to 30 days, a distinct feature of the MJO, might have been the critical weather conditions for the courageous and gifted Polynesian seamen to sail eastward in the trade wind–dominated equatorial Pacific to reach and settle in Polynesia almost 4500 years ago [*Hostetter*, 1991; *Finney*, 1994].

[4] This review article does not imagine the MJO that might have occurred 4500 years ago. Nor does it recite the history of the study of the MJO since it was first docu-

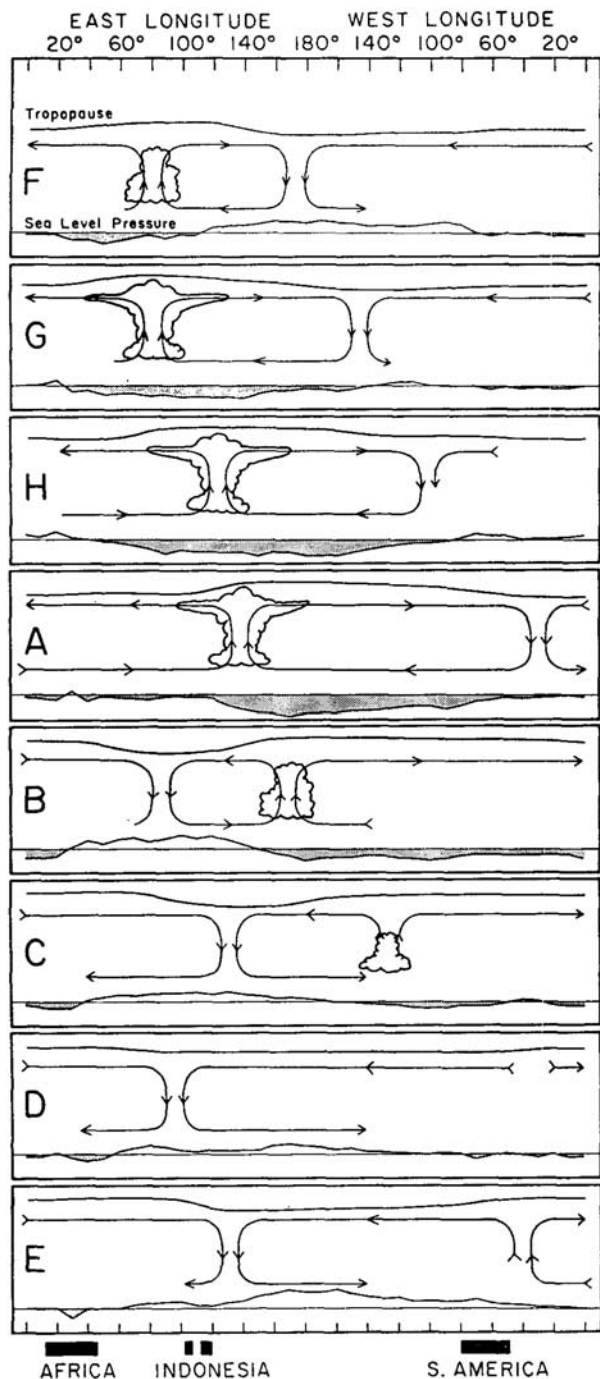


**Figure 1.** Longitude-height schematic diagram along the equator illustrating the fundamental large-scale features of the Madden-Julian Oscillation (MJO) through its life cycle (from top to bottom). Cloud symbols represent the convective center, arrows indicate the zonal circulation, and curves above and below the circulation represent perturbations in the upper tropospheric and sea level pressure. From *Madden and Julian* [1972].

mented using modern observations in 1971. The purpose of this review is to synthesize our current knowledge on the MJO, reflecting especially the progress made during the past decade to complement an earlier review on this subject by *Madden and Julian* [1994], and to summarize the

unknowns that urgently need to be addressed. An inevitable challenge to this review is a balance between depth and breadth. This review focuses on five topics: basic observed features, mechanisms, numerical simulations, air-sea interaction, and influences on ENSO. These topics have been strikingly advanced since Tropical Ocean–Global Atmosphere Coupled Ocean–Atmosphere Response Experiment (TOGA COARE) (November 1992 to February 1993) [Webster and Lukas, 1992], an international research program that in many ways has furthered the study of the MJO as never seen before.

[5] It is important to point out that the MJO is a dominant but not the only component of tropical intraseasonal variations. For example, prominent intraseasonal oscillations exhibit a northward propagation during the Asian summer monsoon [e.g., Yasunari, 1979; Lau and Chan, 1986; Wang and Rui, 1990b]. Many intraseasonal phenomena not included in this review are covered by two recent publications on general tropical intraseasonal variability [European Centre for Medium-Range Weather Forecasts, 2004; Lau and Waliser, 2005].

[6] This review is organized in the following way: Basic observed features of the MJO are first described in section 2. Theories and hypotheses on mechanisms for the MJO are discussed conceptually in section 3. Discussions on numerical simulations of the MJO in section 4 emphasize current successes and failures instead of detailed numerical schemes that sensitively affect the simulations. Air-sea interaction associated with the MJO is reviewed in section 5 mainly from an observational point of view. Possible effects of the MJO on ENSO, very controversial but potentially important to ENSO prediction, are discussed in section 6. As a conclusion, issues in the current study of the MJO that urgently need to be addressed are raised in section 7. A glossary is provided to explain the terminology that may not be commonly used outside the atmospheric and oceanic sciences.

## 2. OBSERVED BASICS

[7] The most basic observed features of the MJO are illustrated in Figure 1. In the equatorial Indian and western Pacific oceans an MJO event features a *large-scale*, eastward moving center of strong deep convection and precipitation (“active phase”), flanked to both east and west by regions of weak deep convection and precipitation (“inactive” or “suppressed phases”). The two phases of the MJO are connected by overturning zonal circulations that extend vertically through the entire troposphere. In the lower troposphere (below 10 km, typically at the 1.5-km or 850-hPa level) and near the surface, anomalously strong westerly winds exist in and to the west of the large-scale convective center with anomalous *easterly* winds to the east. The zonal winds reverse the directions in the upper troposphere (above 10 km, typically at the 13-km or 200-hPa level). This close association between the large-scale circulation and convective center, commonly referred to as the coupling

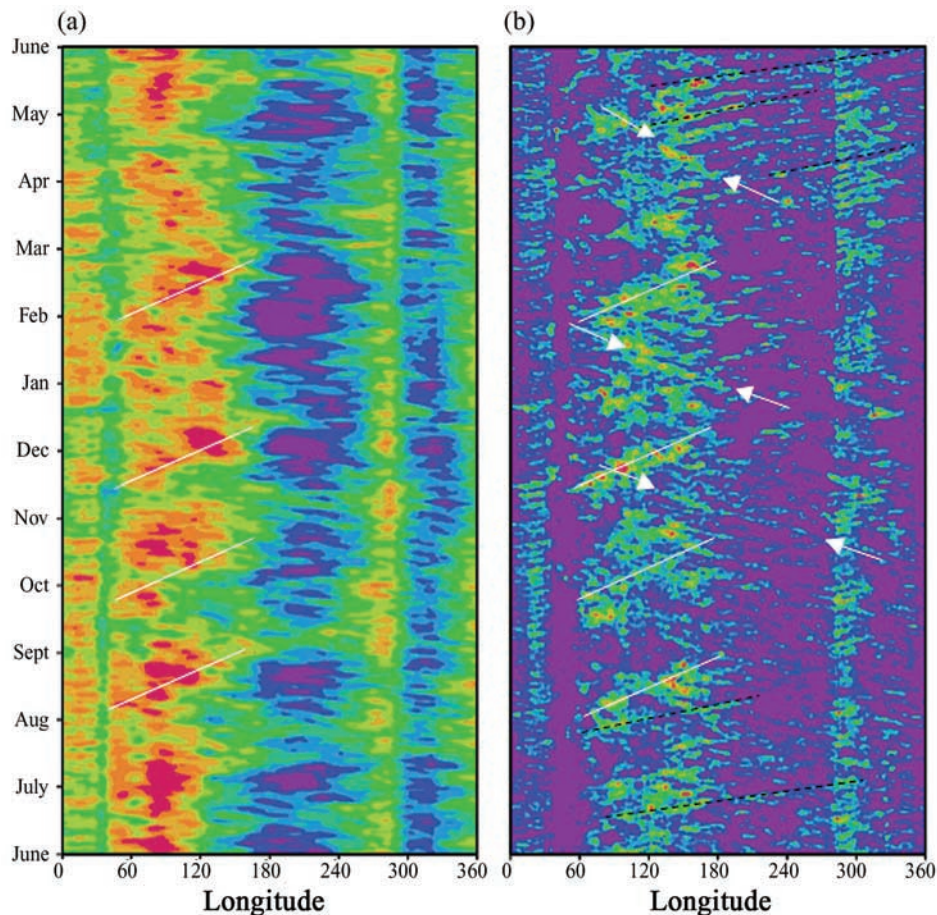


**Figure 2.** Longitude-time plots of daily (a) zonal wind ( $2.5^\circ \times 2.5^\circ$ ,  $\text{m s}^{-1}$ ) at 850 hPa (roughly 1.5 km above sea level) from the National Centers for Environmental Prediction/National Center for Atmospheric Research (NCEP/NCAR) reanalysis [Kalnay *et al.*, 1996] and (b) precipitation ( $1^\circ \times 1^\circ$ ,  $\text{mm d}^{-1}$ ) from the GPCP combined data set [Huffman *et al.*, 1997] for June 2000 to May 2001, both averaged over  $10^\circ\text{N}$ – $10^\circ\text{S}$ . The white straight lines mark identified MJO events, with a slope corresponding to an eastward propagation speed of  $5 \text{ m s}^{-1}$ . Notice that each MJO event may propagate eastward at a slightly different speed. The faster eastward moving ( $15 \text{ m s}^{-1}$ ) signals with shorter periods (5–10 days) (examples marked with black dashed lines) are of convectively coupled Kelvin waves and should not be mistaken for the MJO [e.g., Takayabu *et al.*, 1999]. The westward moving synoptic signals (examples marked with white arrows) are likely of Rossby or mixed Rossby-gravity waves.

between the two, is central to the MJO dynamics (section 3). This coupled pattern propagates eastward at an averaged speed of  $5 \text{ m s}^{-1}$ .

[8] So prominent a phenomenon is the MJO that its existence can be discerned from observations without any filtering, especially in precipitation (Figure 2). The spectral peaks of the MJO at 30–90 days in precipitation and zonal wind at 850 hPa are clearly distinguished from the lower-frequency peaks (Figure 3). The power at the negative intraseasonal frequency (periods around  $-50$  days) and the same zonal wave number is much weaker, signaling eastward propagation [Hayashi, 1979]. The MJO also exhibits a distinctive multiscale structure, geographic preference, seasonal cycle, and interannual variability. The combination of these primary features distinguishes the MJO from other types of intraseasonal phenomena in the tropics. These basic characteristics of the MJO are further discussed in this section.

## 2.1. Intraseasonal Period

[9] The dominant period of the MJO spreads over a range of roughly 30–100 days (Figure 3). Its power peak is highly variable within this range. These reflect a fundamental but often neglected nature of the MJO. Although referred to as an “oscillation,” the MJO by no means oscillates regularly. It is highly episodic or discrete [Salby and Hendon, 1994]. The range of its local period (30–100 days) suggests the interval between two consecutive events is irregular and their propagation speeds may vary (section 2.3). The MJO undergoes a seasonal cycle (section 2.8) and interannual fluctuations (section 2.9) with its occurrence frequency higher in certain times than others. All these result in a spread of its spectral peak.

## 2.2. Planetary Zonal Scale

[10] The typical zonal extent of an MJO event, measured by its regions of positive and negative anomalies in cloud

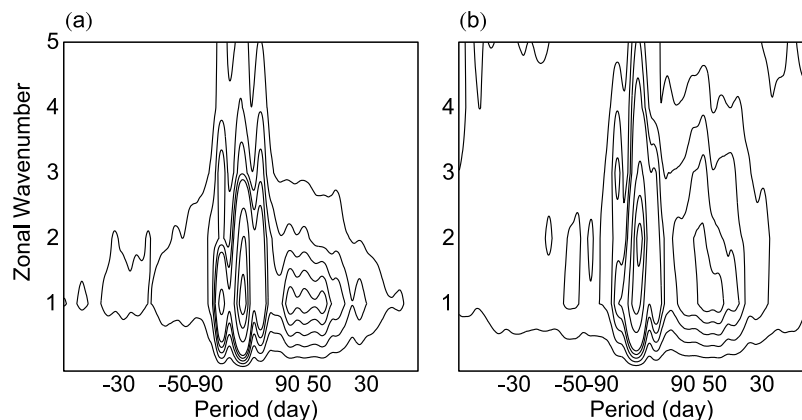


**Figure 3.** Time-space power spectra of (a) 850 hPa zonal wind (NCEP/NCAR reanalysis) and (b) precipitation [Xie and Arkin, 1997] for 1979 through 1998, averaged over 20°N–20°S and 60°–180°E. Positive (negative) periods correspond to eastward (westward) propagating power. Data resolutions for the spectra are pentad in time and 10° in longitude.

covers, is roughly 12,000–20,000 km (see the composite of Rui and Wang [1990]). Only one fully developed MJO event exists in the tropics at a given time. Occasionally, two weak convective centers of the MJO with weak circulations may coexist, one being just initiated in the Indian Ocean and the other decaying in the central Pacific [e.g., Wheeler and Hendon, 2004]. The zonal scale of the convective component is much less than that of the circulation because of the nature of atmospheric response to localized heating [Salby *et al.*, 1994]. The spectral peak is thus at zonal wave number 1 for the zonal wind but spreads over zonal wave numbers 1–3 for precipitation (Figure 3). Meanwhile, the zonal extent of active phase of the MJO is much smaller than that of inactive phase. The MJO is therefore more an isolated or discrete pulse-like event than a sinusoidal wave [Salby and Hendon, 1994; Yano *et al.*, 2004].

### 2.3. Eastward Propagation

[11] The slow eastward propagation at an averaged speed of  $5 \text{ m s}^{-1}$  [e.g., Weickmann *et al.*, 1985; Knutson *et al.*, 1986] is one of the most fundamental features that distinguishes the MJO from other phenomena in the tropical atmosphere, especially convectively coupled Kelvin waves, which propagate eastward at greater speeds of  $15\text{--}17 \text{ m s}^{-1}$  [e.g., Wheeler and Kiladis, 1999; Straub and Kiladis, 2002] (Figure 2b). The phase speed of the MJO varies slightly among individual events and during different stages of the life cycle of a given event [Hendon and Salby, 1994] (Figure 2). While the convective signals of the MJO normally vanish in the eastern Pacific (Figure 2b), its signals in wind and surface pressure continue to propagate farther east as free (uncoupled with convection) waves at much higher speeds of about  $30\text{--}35 \text{ m s}^{-1}$  [Milliff and Madden, 1996; Matthews, 2000] (Figure 4). A continuous, global circumferential propagation of the MJO along the equator exists only in its upper level fields [e.g., Krishnamurti *et al.*, 1985; Knutson and Weickmann, 1987] as atmospheric responses to the convective perturbations. Issues related to the stationary intraseasonal oscillation in the tropics are discussed in section 3.1.1.

### 2.4. Convection-Wind Coupling

[12] The large-scale wind structure (Figure 1) is often described in terms of *equatorial waves* coupled to deep convection. East of the convective center, the low-level easterlies and upper level westerlies resemble the equatorial Kelvin wave. To the west, low-level westerlies (upper level easterlies) and the associated pair of cyclonic (anticyclonic) circulation or gyres straddling the equator are the characteristics of the equatorial Rossby wave [Madden, 1986; Nogués-Paegle *et al.*, 1989] (Figure 5). Both Kelvin and Rossby wave structures have been considered dynamically essential to the MJO (section 3.2.1).

[13] Observations have revealed that the relative phase between the large-scale surface zonal wind and convective center varies during the life cycle of the MJO [e.g., Knutson and Weickmann, 1987; Rui and Wang, 1990; Hendon and Salby, 1994; Sperber, 2003]. When the MJO

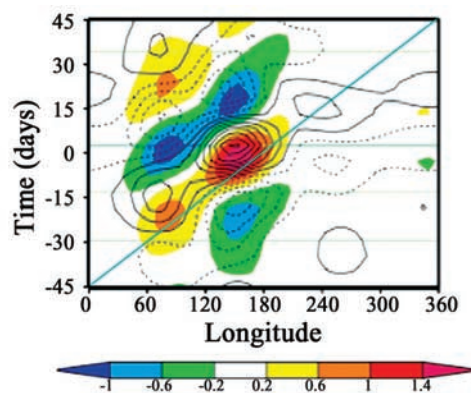


**Figure 4.** MJO composite based on regression of equatorial band-pass (30–90 days) filtered 850-hPa zonal wind (contours, interval  $0.2 \text{ m s}^{-1}$ ) and precipitation (colors,  $\text{mm d}^{-1}$ ) upon 850-hPa zonal wind of the MJO at 160°E and the equator. The MJO zonal wind was extracted from the band-pass filtered time series using its four leading modes of singular vector decomposition [Zhang and Dong, 2004]. The straight line from the lower left to upper right corners indicates the eastward phase speed of  $5 \text{ m s}^{-1}$ .

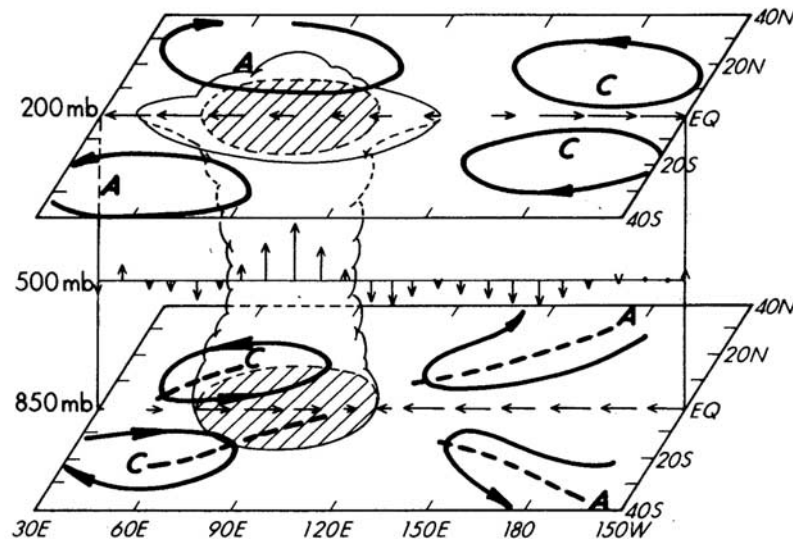


**Figure 5.** Schematic depiction of the large-scale wind structure of the MJO. The cloud symbol indicates the convective center. Arrows represent anomalous winds at 850 and 200 hPa and the vertical motions at 500 hPa. “A” and “C” mark the anticyclonic and cyclonic circulation centers, respectively. Dashed lines mark troughs and ridges. From *Rui and Wang* [1990].

is in the Indian Ocean, its convective center is more likely to be in between the surface westerlies to the west and easterlies to the east, as depicted in Figure 1, which is synthesized as MJO model I in Figure 6. When the MJO moves to the Pacific, surface westerlies are likely to prevail through the convective center (Figure 4). This structure is referred to as MJO model II in Figure 6. In reality, the structure of an MJO event may be of either model I or II or anything in between.

## 2.5. Large-Scale Vertical Structure

[14] Many fundamental large-scale features of the MJO are not included in the MJO schematics in Figures 1, 5, and 6. Water vapor, temperature, divergence, and *adiabatic heating* all show large-scale patterns coherent with the wind and deep convection of the MJO [e.g., *Chen and Yen*, 1991; *Hendon and Salby*, 1994; *Lin and Johnson*, 1996a, 1996b; *Mote et al.*, 2000; *Kemball-Cook and Weare*, 2001; *Myers and Waliser*, 2003; *Weare*, 2003; *Lin et al.*, 2004]. These fields, as well as the winds, also show marked zonal asymmetry and westward tilt in the vertical with respect to the convective center [*Sperber*, 2003; *Kiladis et al.*, 2005] (Figure 7). Immediately ahead (to the east) of the convective center are low-level convergence, ascending motions, and positive anomalies in humidity; low-level divergence, descending motions, and negative anomalies in humidity occur immediately behind (to the west). Such zonal asymmetry provides favorable large-scale conditions for the development of new convective systems east of the existing ones and discourages such development to the west, resulting in the eastward propagation of the convective center. Some of these features have been taken into consideration in MJO theories and hypotheses (section 3). However, it is not clear whether the zonal asymmetry is due to the

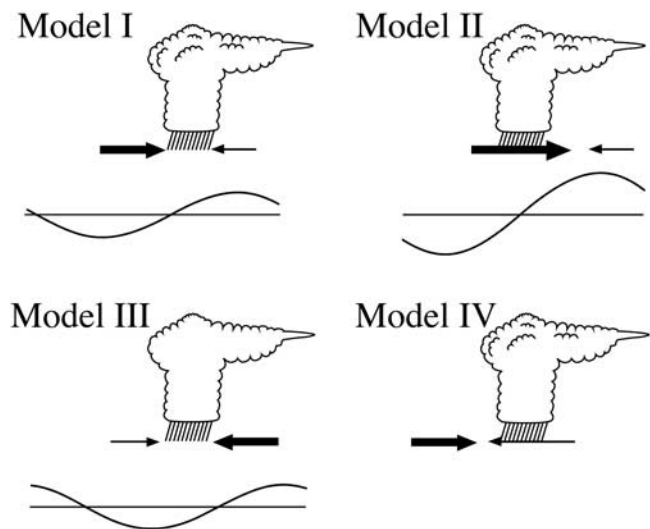


**Figure 6.** Schematic diagrams of four MJO models describing the phase relationship between its convective centers (represented by the cloud symbols) and surface zonal wind (arrows) synthesized from observations, theories, and numerical simulations. Maximum surface zonal wind is marked by thick arrows. Curves at the bottom of each panel depict intraseasonal perturbations in sea surface temperature induced by the MJO, with positive anomalies above the horizontal lines (see section 5.2). Model I is consistent with the classic conceptual model of *Madden and Julian* [1972] shown in Figure 1, which is more often observed in the Indian Ocean than in the Pacific Ocean. Model II is more observed in the Pacific Ocean. Model III is predicted by the wind-induced surface heat exchange/evaporation-wind feedback theory (section 3.2.2). Model IV is produced by some numerical models (section 4.1). Neither model III nor IV has been observed. From *Zhang and Anderson* [2003].

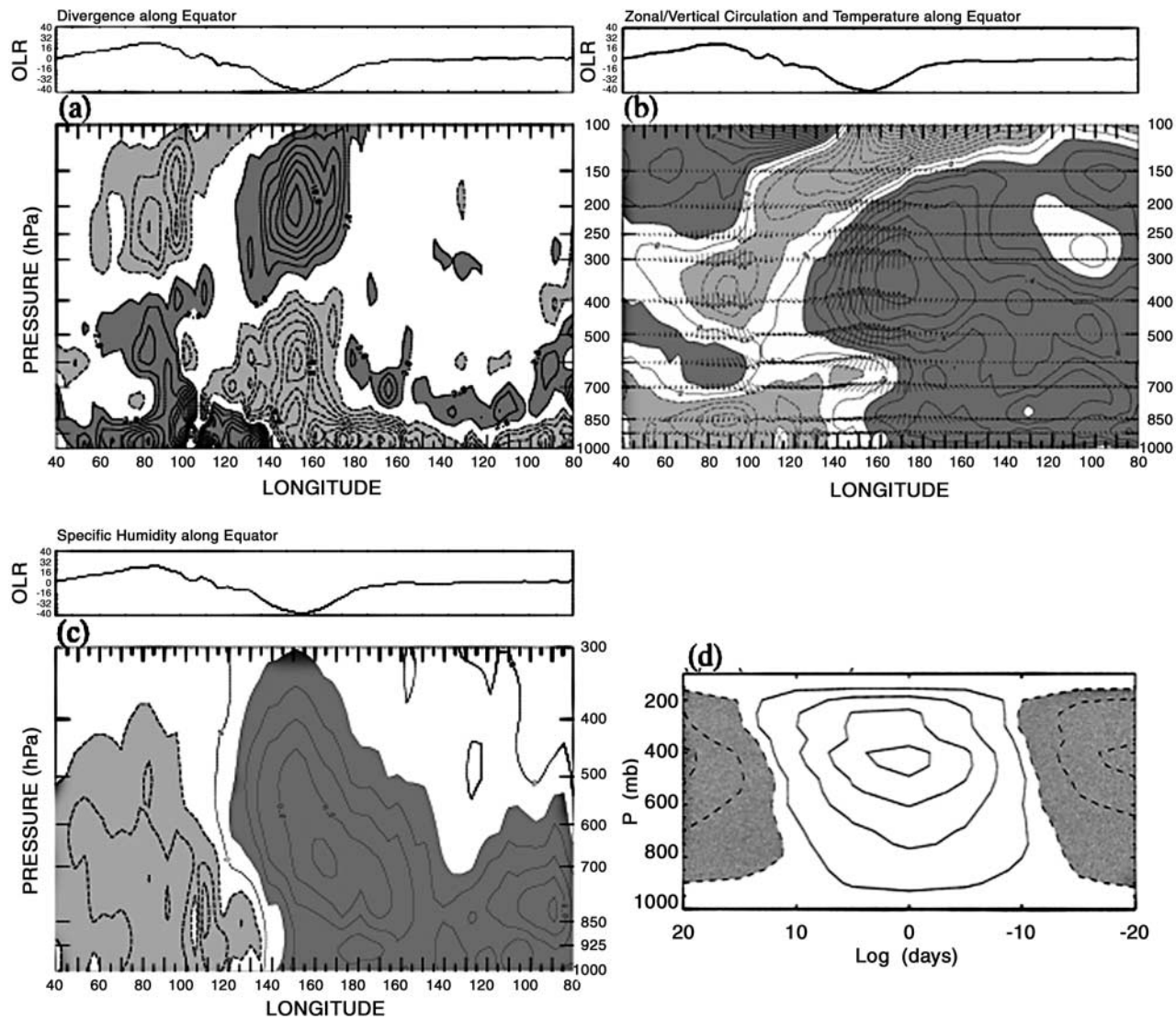


**Figure 7.** Longitude-height composite of the MJO along the equator. (a) Mass divergence ( $\rho \nabla \cdot \mathbf{V}$ ,  $2 \times 10^{-7} \text{ kg m}^{-3} \text{ s}^{-1}$ ), (b) mass flux vectors ( $pu$ ,  $\rho \omega \times 1200$ ) and temperature contours (0.1 K), and (c) specific humidity ( $10^{-1} \text{ g kg}^{-1}$ ), all based on an MJO index of outgoing longwave radiation (OLR) plotted at the top of each panel [from Kiladis et al., 2005]. (d) Lag-pressure composite of diabatic heating anomalies of the MJO with negative lags corresponding to east of the convective center, which is the reference point with 0 lag [from Lin et al., 2004]. A westward tilt is a common feature in these variables.

large-scale circulation (Kelvin versus Rossby waves) or embedded mesoscale systems (sections 2.6 and 3.3.4).

## 2.6. Multiscale Structure

[15] The eastward moving convective center or active phase of the MJO can be viewed as a large-scale ensemble of myriad higher-frequency, small-scale convective systems moving in all directions [e.g., Nakazawa, 1988; Hendon and Liebmann, 1994] (Figure 8). The apparent eastward propagation of the large-scale convective center of the MJO is due to consecutive development of new convective systems, each on average slightly to the east of the previous one. Among others the most noticeable high-frequency variability within the large-scale ensemble of cloud clusters are eastward propagating synoptic-scale disturbances [Dunkerton and Crum, 1995] at the speed of the coupled

Kelvin wave, which has been referred to as the supercluster or supercloud cluster [Nakazawa, 1988; Lau et al., 1989], and westward moving disturbances with apparent periods of 2 and 5 days. The 2-day disturbances are likely manifestations of the diurnal cycle of deep convection [Chen and Houze, 1997] and inertio-gravity waves [Takayabu, 1994; Liebmann et al., 1997; Haertel and Kiladis, 2004]. The westward propagating 5-day waves might be related to equatorial Rossby waves and mixed Rossby-gravity waves [Wheeler and Kiladis, 1999]. In addition, other types of disturbances, such as easterly waves and tropical storms, also propagate westward. However, all can exist independently of the MJO [Clayson et al., 2002] (Figures 2b and 8).

[16] The large-scale enhancement of convection during active phases of the MJO is mostly a manifestation of an increase in the occurrence of large ( $>90,000 \text{ km}^2$ ) and deep

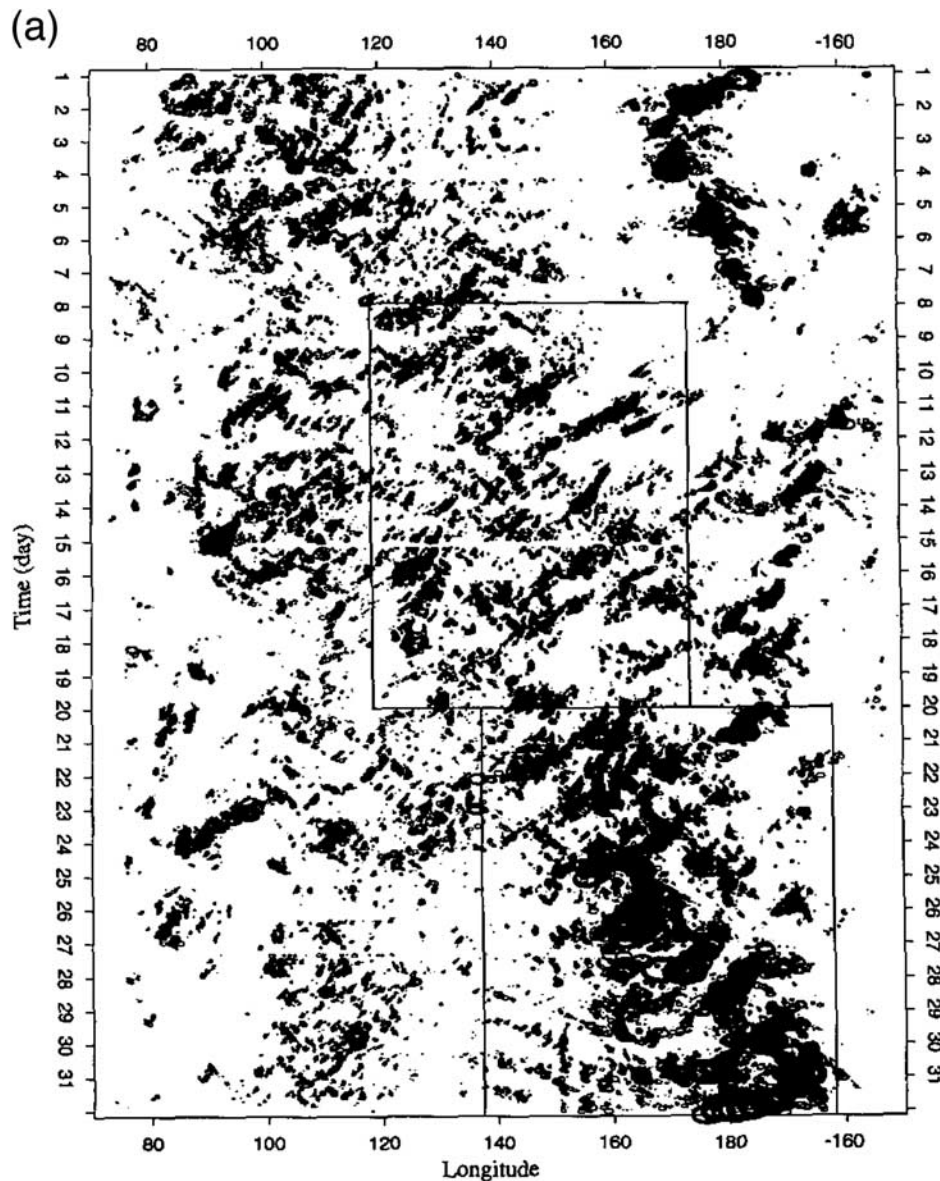


**Figure 8.** Longitude-time diagrams of deep cloud clusters (cloud top infrared temperature  $<208$  K) over  $0^{\circ}$ – $10^{\circ}$ S for (a) 1–31 December 1992 during which an MJO event propagated through the eastern Indian and western Pacific oceans [Yanai *et al.*, 2000]. (b) Details for 20–31 December as marked by the lower right box in Figure 8a. (c) Details for 22–28 December as marked by the box in Figure 8b. Sizes of ovals are proportional to the actual sizes of cloud clusters. From Chen *et al.* [1996].

(cloud top temperature  $<208$  K) cloud clusters [Mapes and Houze, 1993; Chen *et al.*, 1996]. During inactive phases, there are plenty of deep but small ( $<3000$  km<sup>2</sup>) convective systems and far fewer deep and large ones. Convective clouds whose tops reach only to the middle troposphere because of an *inversion* at the *melting level* are also common during inactive phases [Johnson *et al.*, 1999].

[17] The diurnal cycle in deep convection is modulated by the MJO. Over the Maritime Continent the diurnal cycle is the strongest during the inactive phase of the MJO and becomes diminished during the active phase [Sui and Lau, 1992], possibly because of the interruption of the local sea breeze circulation by the large-scale

circulation of the MJO (see also section 2.7). Over the open ocean, deep convective signals exhibit a nocturnal peak during active phases of the MJO when long-lived, organized mesoscale systems prevail; during inactive phases the cloud population is dominated by isolated, short-lived small convective systems that tend to peak in the afternoon [Chen and Houze, 1997].

[18] The low-level westerly wind component of the MJO is composed of synoptic-scale westerly wind bursts (WWB) [Luther *et al.*, 1983]. The WWB might be stationary [Hartten, 1996; Harrison and Vecchi, 1997], but within an MJO envelope each on average tends to occur slightly east of the previous one (August–September and November–December 2000 and February–March

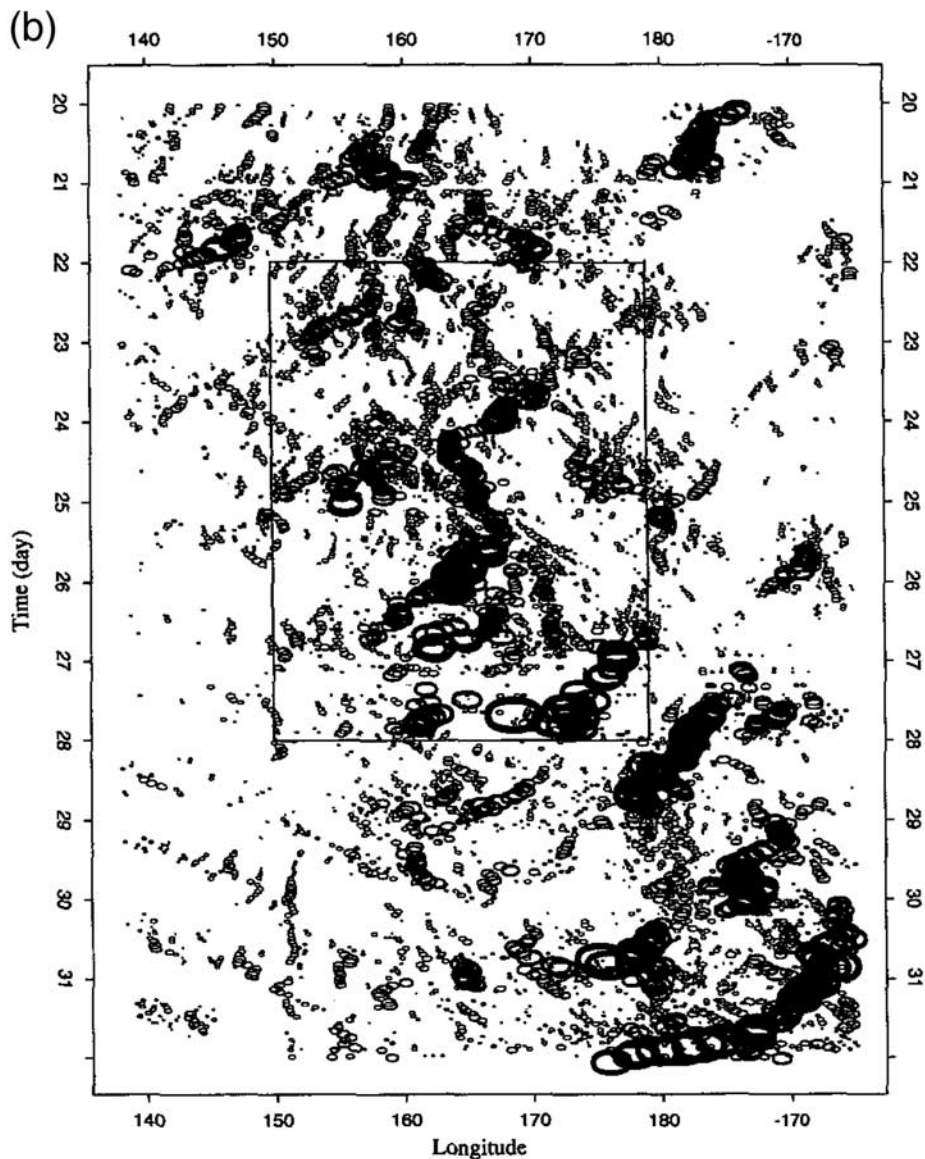


Figure 8. (continued)

2001 in Figure 2a). See section 5 for more discussion on WWB.

## 2.7. Geographical Preference

[19] MJO signals in convection are normally confined to the Indian and western Pacific oceans (Figures 2, 4, and 9), because convective instability can be sustained only over the warm sea surface known as the “warm pool.” MJO signals in some other fields can be detected in the rest of the tropics [e.g., *Knutson and Weickmann*, 1987; *Chen and Chen*, 1997; *Sperber*, 2003]. The effect of the warm sea surface in determining the location of the MJO can be further illustrated by two examples. One is the zonal displacement of the MJO in concert with ENSO (section 2.9). The other is the MJO signal in the eastern Pacific north of the *equatorial cold tongue* and adjacent to the Central American coast, which is nontrivial only in boreal summer when the sea surface temperature there is sufficiently high [*Maloney and Kiehl*, 2002] (Figures 9c and 9d).

[20] The convective component of the MJO over the Maritime Continent is generally much weaker than over the surrounding oceans (Figure 9). Possible explanations [*Salby and Hendon*, 1994; *Wang and Li*, 1994; *Zhang and Hendon*, 1997; *Maloney and Sobel*, 2004] for this are the following: (1) The strong diurnal cycle in convection due to diurnal heating over land tends to compete with the MJO for moisture and energy. (2) Topography interferes with low-level moisture convergence believed to be crucial to the MJO (section 3.2.1). (3) Surface evaporation, another possible crucial factor for the MJO (section 3.2.2), is severely reduced over land. These possible explanations may also be applied to tropical South America, where deep convection in local summer is almost as strong as in the western Pacific but MJO signals are intriguingly weak.

## 2.8. Seasonal Cycle

[21] The MJO undergoes a strong seasonal cycle in both its strength and latitudinal locations [*Madden*, 1986; *Gutzler*

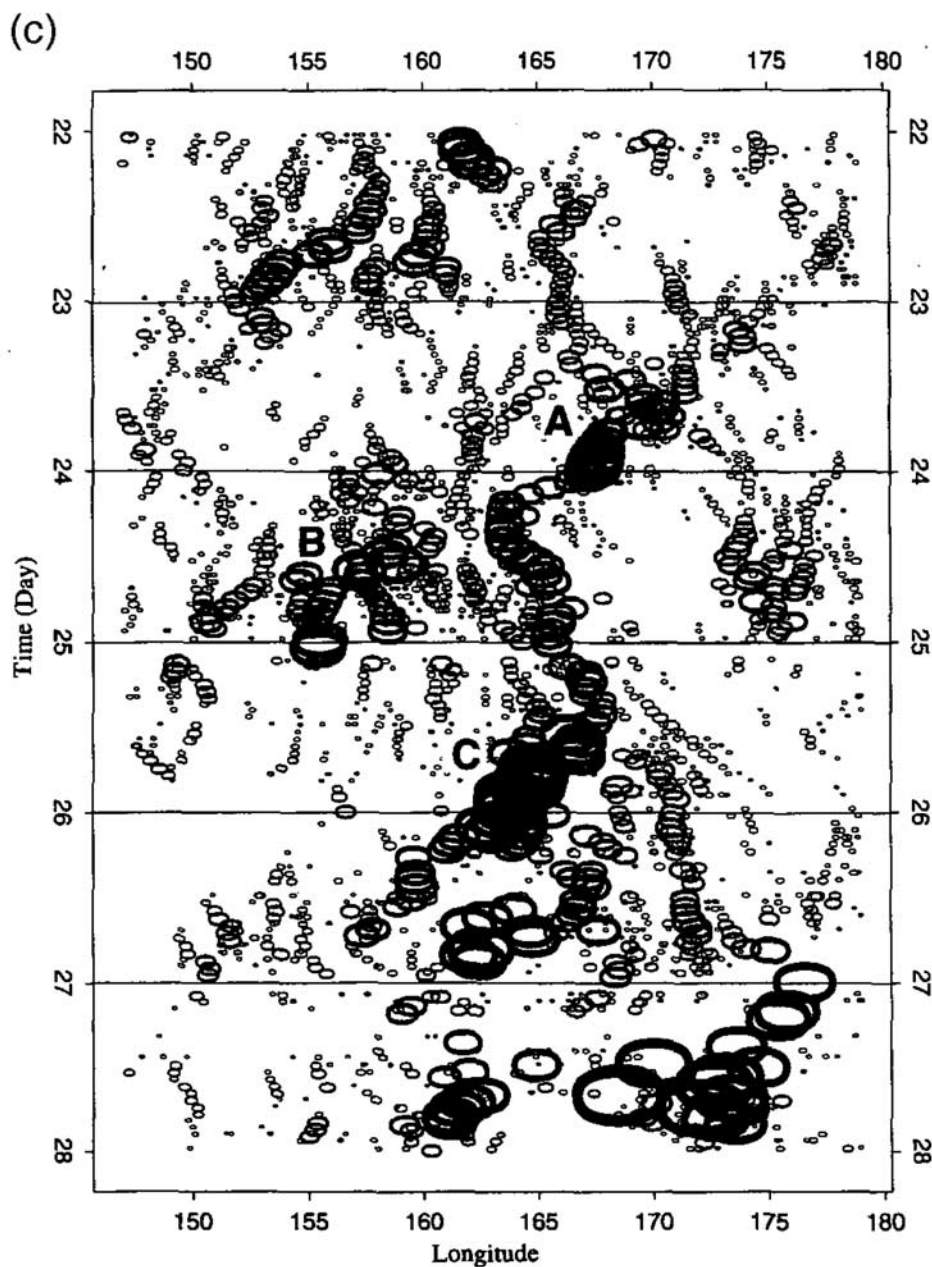


Figure 8. (continued)

and Madden, 1989; Salby and Hendon, 1994; Zhang and Dong, 2004], as illustrated in Figures 9 and 10. Its primary peak season is austral summer/fall when the strongest MJO signals are immediately south of the equator; the second peak season is boreal summer when its strongest signals are north of the equator. The primary peak season in austral summer is related to the Australian summer monsoon [Hendon and Liebmann, 1990], while the secondary peak season in boreal summer is related to the Asian summer monsoon [e.g., Lawrence and Webster, 2002]. The seasonal migration of the MJO in latitude is much stronger in the western Pacific Ocean than in the Indian Ocean [Zhang and Dong, 2004]. In a narrow latitudinal band (e.g.,  $5^{\circ}\text{N}$ – $5^{\circ}\text{S}$ ) the seasonal cycle of the MJO shows a single peak in austral summer/fall. In the eastern Pacific a separated MJO peak

exists only in boreal summer [Kayano and Kousky, 1998; Maloney and Kiehl, 2002].

## 2.9. Interannual Variability

[22] In the Pacific, interannual variability in zonal wind variance of the MJO is more prominent in the lower than upper troposphere [Gutzler, 1991]. During a warm event of ENSO (El Niño), as the eastern edge of the warm pool extends eastward [Picaut et al., 1996], so does MJO activity [e.g., Anyamba and Weare, 1995; Fink and Speth, 1997; Gualdi et al., 1999; Hendon et al., 1999; Woolnough et al., 2000; Bergman et al., 2001]. The MJO in the Pacific appears to be extraordinarily vigorous prior to the peak of an ENSO warm event and anomalously weak after the peak and during a cold event [Zhang and Gottschalck, 2002].

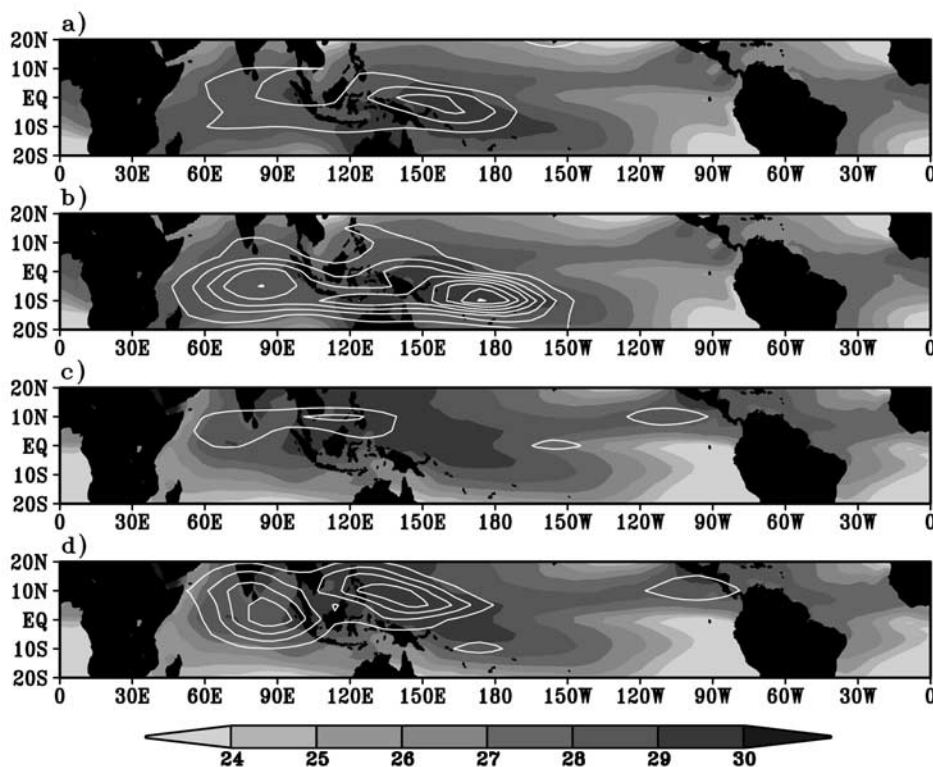


**Figure 9.** Variance of the MJO (contours) in (a) 850-hPa zonal wind and (b) precipitation during December–March and (c) 850 hPa zonal wind and (d) precipitation during June–September, overlaid with mean sea surface temperature (SST) ( $^{\circ}\text{C}$ ). Contour intervals are  $1 \text{ m}^2 \text{ s}^{-2}$  for the wind starting from  $2 \text{ m}^2 \text{ s}^{-2}$  and  $2 \text{ mm}^2 \text{ d}^{-2}$  for precipitation starting from  $2 \text{ mm}^2 \text{ d}^{-2}$ . See *Zhang and Dong* [2004] for details of defining the MJO.

Simultaneous relationship between the level of global MJO activity and sea surface temperature (SST) indices representing ENSO has been found to be very weak [*Slingo et al.*, 1999; *Hendon et al.*, 1999]. This suggests that globally the interannual variability of the MJO might be driven more by the atmospheric internal dynamics than surface conditions. Possible connections between the MJO and ENSO are further discussed in section 6.

### 3. MECHANISMS

[23] Explaining the primary observed features described in section 2 tests our understanding of the MJO. Because the Kelvin wave is the only equatorial mode with an eastward propagating, planetary-scale zonal wind field resembling that of the observed MJO (Figure 1), it has been taken as the dynamical backbone of the MJO from day one. However, convectively coupled Kelvin waves propagate eastward at a much faster speed than does the MJO (section 2.3). The reduction in the phase speed of the Kelvin wave by damping [*Chang*, 1977] is insufficient to bridge the gap. Therefore key questions that must be addressed by any MJO theory are as follows: What are the mechanisms that distinguish the MJO from the convectively coupled Kelvin waves? What processes must take place to supply energy against dissipation selectively to the intraseasonal, planetary-scale, and slowly eastward propagating disturbances known as the

MJO? The MJO can be regarded as the “holy grail” of the tropical atmospheric dynamics [*Raymond*, 2001], and it has motivated many hypotheses describing potential roles of certain physical processes in it and many idealized numerical models generating MJO-like signals with a chosen set of parameters to isolate a certain processes. Few theories, however, explain the mechanisms that quantitatively select the frequency/period, zonal scales, and eastward propagation speed of the MJO.

[24] There are two major schools of thought on the energy source of the MJO. One considers the MJO to be an atmospheric response to an independently existing forcing mechanism. The eastward propagation and coupling between convection and wind are secondary by-products of the atmospheric response. In the other school of thought the MJO creates its own energy source through atmospheric instability. The coupling between convection and circulation is at the center of the instability. Here theories and hypotheses are discussed conceptually without mathematical details, even though they often are the key to the success of a theory. *Wang* [2005] provides a review with more details on theories of the intraseasonal variability.

#### 3.1. Atmospheric Response to Independent Forcing

##### 3.1.1. Tropical Intraseasonal Stationary Forcing

[25] Intraseasonal fluctuations in precipitation associated with the Asian summer monsoon, which are relatively fixed in longitude and can result from the local hydrological cycle

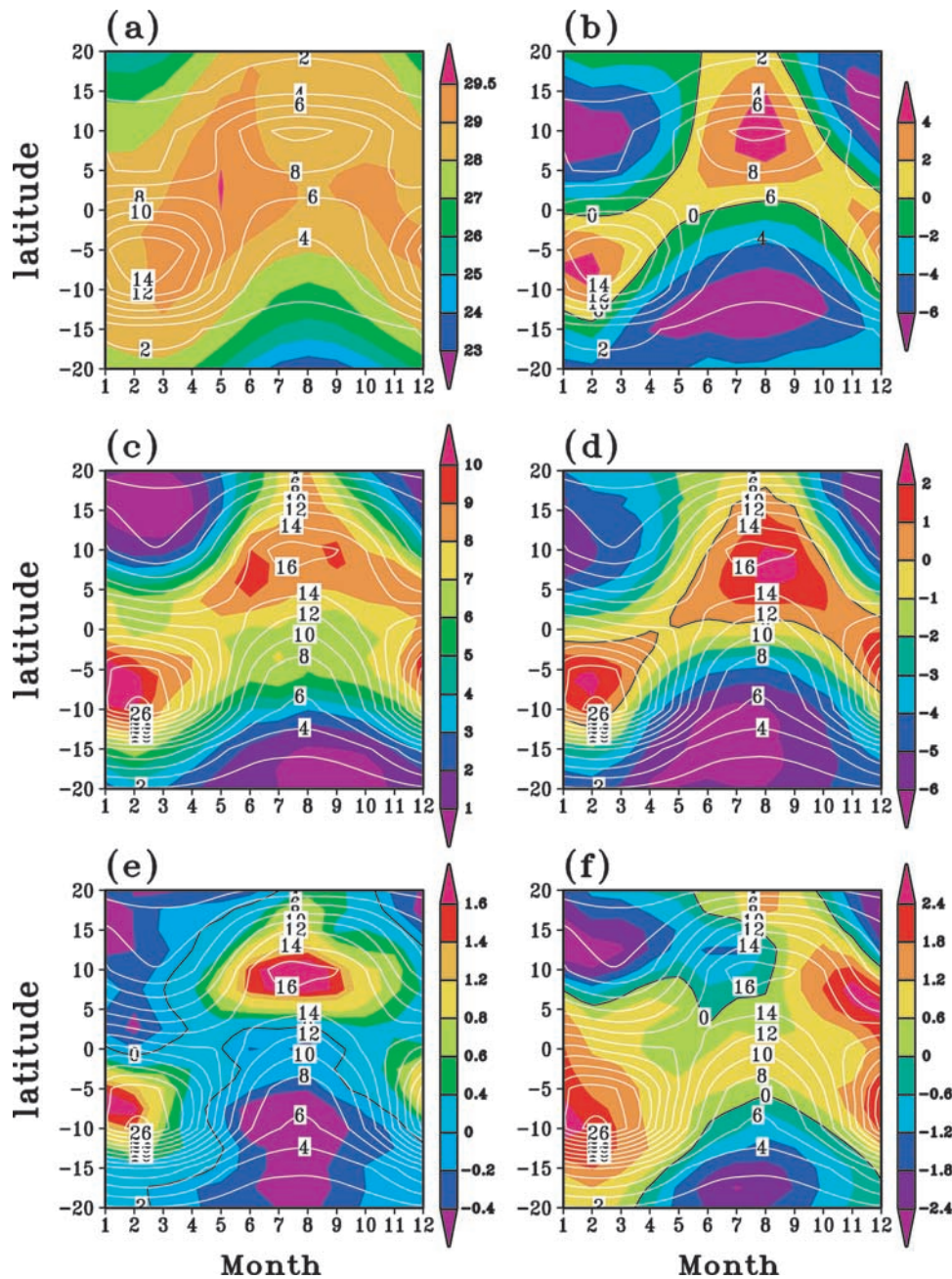


**Figure 10.** Seasonal cycle of the MJO (white contours) measured by variance in its (top) 850-hPa zonal wind ( $\text{m}^2 \text{s}^{-2}$ ) and (middle and bottom) precipitation ( $\text{mm}^2 \text{d}^{-2}$ ) averaged over  $60^\circ\text{--}180^\circ\text{E}$  and each month for 1979–1998. The background colors (with zero indicated by black contours) are mean (a) SST ( $^\circ\text{C}$ ), (b) zonal wind at 850 hPa ( $\text{m s}^{-1}$ ), (c) precipitation ( $\text{mm d}^{-1}$ ), (d) surface zonal wind ( $\text{m s}^{-1}$ ), (e) 850 hPa moisture convergence  $\nabla \cdot (q\mathbf{V})_{850}$  ( $\text{g kg}^{-1} \text{s}^{-1}$ ), and (f) 925 hPa moisture convergence  $\nabla \cdot (q\mathbf{V})_{925}$  ( $\text{g kg}^{-1} \text{s}^{-1}$ ). From *Zhang and Dong [2004]*.

[Webster, 1983], have been suggested to be a forcing source for the MJO [e.g., Yasunari, 1979]. In a theory an interaction among surface evaporation, convection, and radiation results in a stationary oscillation in precipitation with a period close to 50 days [Hu and Randall, 1994, 1995]. Observations have suggested the existence of intraseasonal standing oscillations in convection [e.g., Lau and Chan, 1985; Hsu et al., 1990; Weickmann and Khalsa, 1990; Zhu and Wang, 1993; Hsu, 1996]. Despite visual impressions,

however, no statistically significant signals of intraseasonal stationary oscillation in equatorial convection can be objectively identified [Zhang and Hendon, 1997]. Numerical simulations of atmospheric responses to prescribed stationary intraseasonal heating cannot reproduce the observed eastward moving Rossby wave structure of the MJO [e.g., Yamagata and Hayashi, 1984; Anderson and Stevens, 1987] because Rossby wave responses to a given forcing source radiate away to the west. Meanwhile, damping makes the

amplitude of atmospheric responses decay rapidly as they move away from their stationary forcing source [Lau and Peng, 1987].

### 3.1.2. Tropical Stochastic Forcing

[26] So dependent on the frequency and spatial scale of forcing are atmospheric responses that a localized, stochastic heating source with a red spectrum can produce a circulation with an intraseasonal spectral peak [Salby and Garcia, 1987]. The Kelvin wave structure associated with the MJO, weakly unstable or even damped, can be vitalized by external energy sources of mesoscale thermal processes with white noise in time and longitude but a meridional distribution of the equatorial Kelvin waves [Yu and Neelin, 1994]. The maximum growth in precipitation due to this stochastic forcing is, however, at smaller scales (zonal wave numbers  $>4$ ). In an analytical model, momentum and energy transfers from synoptic-scale to planetary-scale, intraseasonal perturbations play a critical role in generating the MJO [Majda and Biello, 2004].

### 3.1.3. Lateral Forcing

[27] Intraseasonal perturbations coherent with the MJO exist in the extratropics [e.g., Weickmann, 1983] and are thought to be possible forcing sources of the MJO [Lau and Peng, 1987; Hsu et al., 1990; Lau et al., 1994; Matthews et al., 1996]. Eastward moving extratropical disturbances can indeed excite a variety of equatorial waves [e.g., Yanai and Lu, 1983]. A coupling between extratropical *baroclinic* disturbances and tropical *barotropic* intraseasonal perturbations may amplify the latter [Frederiksen and Frederiksen, 1997]. However, whether relationships between the extratropical and tropical intraseasonal signals are statistically significant is controversial [Ghil and Mo, 1991; Straus and Lindzen, 2000]. Extratropical intraseasonal perturbations can persistently and significantly influence the tropics only in the central and eastern Pacific [Liebmann and Hartmann, 1984; Magana and Yanai, 1991; Matthews and Kiladis, 1999; Yanai et al., 2000] where the *critical latitude* preventing equatorward propagation of extratropical wave energy disappears because of the upper tropospheric mean westerly wind [Webster and Holton, 1982]. On the other hand, other types of high-frequency transients from higher latitudes may act as lateral stochastic forcing to the equatorial waves [Mak, 1969] and energize the MJO [Compo et al., 1999; Lin et al., 2000].

## 3.2. Atmospheric Instability

[28] Instability theories of the MJO seek mechanisms for growing modes that bear characteristics similar to the observed. Nonlinear advection has been shown to be nonessential to the MJO [Van Tuyl, 1987], permitting analytical solutions for linear unstable modes. Sources of the instability inevitably involve deep convective processes, which are highly nonlinear and demand simplifications in their mathematical representations to a degree that solutions are dictated by specific assumptions. A common malady of an instability theory is that its maximum growth rate occurs at smallest scales (the “instability catastrophe” [Crum and Dunkerton, 1992]). Special tricks are needed to remedy this.

Among the popular ones are positive-only heating [Lau and Peng, 1987; Wang and Xue, 1992] and time lags between the energy input (from surface evaporation or moist convergence) and convective heating [e.g., Goswami and Rao, 1994]. The justification of positive-only heating is that precipitation occurs solely in regions of large-scale ascents, which is inconsistent with observed precipitation during inactive phases of the MJO (Figure 2b). The numerical value of the time lag cannot always be chosen independently of desired results.

### 3.2.1. Moisture Convergence

[29] On the basis of the premise of CISK [Charney and Eliassen, 1964; Ooyama, 1964] and wave-CISK [Lindzen, 1974] the equatorial Kelvin wave becomes unstable when its convective heating interacts with its low-level convergence in “mobile wave-CISK” [Lau and Peng, 1987] or “Kelvin wave-CISK” [Chang and Lim, 1988] theories. Without additional assumptions (e.g., positive-only heating), unstable wave-CISK Kelvin modes propagate at speeds ( $16\text{--}19\text{ m s}^{-1}$ ) comparable to the observed speed of the convectively coupled Kelvin waves, not the MJO. The growth rates are the greatest on smallest scales. The direct dependence of convective heating on moisture convergence in the wave-CISK type of theories has been criticized as unphysical [Emanuel et al., 1994; Raymond, 1994]. In global models the wave-CISK mechanism alone appears to be insufficient to generate MJO-like signals [Hayashi and Golder, 1997].

[30] The instability catastrophe of wave-CISK theories has been treated by including the frictional effect on moisture convergence in the atmospheric boundary layer in a “moist Kelvin wave” or “frictional-convergence” theory of the MJO [Wang, 1988a; Salby et al., 1994]. In this theory, *frictional convergence* in the boundary layer leads wave convergence in the lower troposphere and damps small-scale wave-CISK modes. The instability of moisture convergence due to boundary layer viscosity results in slowly eastward moving, planetary-scale, unstable modes in a parameter regime stable to inviscid wave-CISK. The instability depends crucially on the vertical distribution of moist static energy of the basic state.

[31] When the equatorial Rossby wave is included, boundary layer dynamics can generate an unstable mode consisting of coupled Rossby-Kelvin waves [Wang and Rui, 1990a; Wang and Li, 1994] in contrast to other wave-CISK theories where the Rossby waves are stable [e.g., Chang and Lim, 1988]. The inclusion of the Rossby wave helps suppress unrealistic fast growth of pure wave-CISK Kelvin mode (Figure 11). The resulting eastward propagating speed comes from a group velocity of a multiscale structure (section 2.6) that is slower than the propagation speed of the unstable, convectively coupled Kelvin wave [also see Chao, 1987]. The boundary layer convergence leading (east of) the convective center of the MJO, a key feature of this theory, has been confirmed by global data assimilation products (Figure 7a) [Hendon and Salby, 1994; Jones and Weare, 1996; Maloney and Hartmann, 1998; Kiladis et al., 2005]. The frictional-

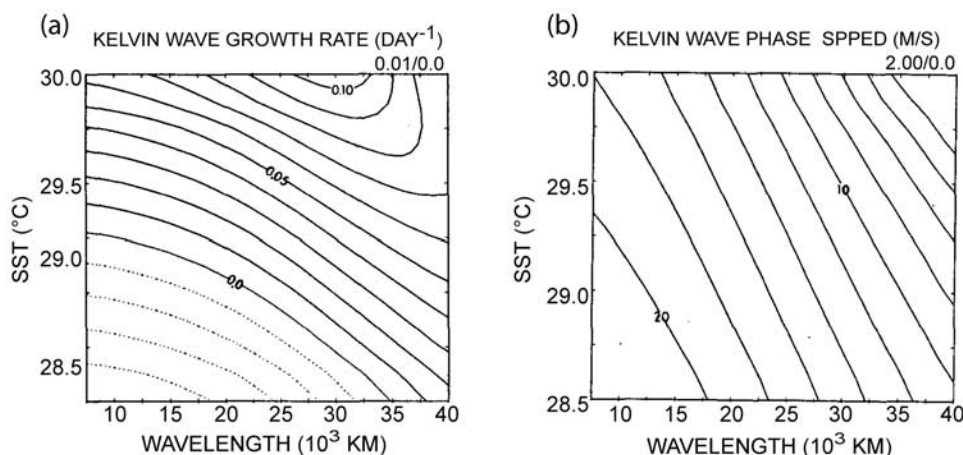


**Figure 11.** (a) Growth rate ( $\text{day}^{-1}$ ) and (b) zonal phase speed ( $\text{m s}^{-1}$ ) of the unstable Kelvin mode from the moist Kelvin-Rossby wave theory of the MJO. From *Wang and Rui [1990a]*.

convergence mechanism has been shown to be sensitive to surface drag but not to *cumulus parameterization* [Moskowitz and Bretherton, 2000]. It may also be responsible for the initiation of the MJO in the Indian Ocean [Seo and Kim, 2003].

### 3.2.2. Surface Evaporation

[32] Surface evaporation interacting with the surface wind component of planetary-scale, intraseasonal Kelvin mode has been considered the source of instability for the MJO in the theory of “wind-induced surface heat exchange” (WISHE) [Emanuel, 1987; Yano and Emanuel, 1991] or “evaporation-wind feedback” (EWF) [Neelin *et al.*, 1987]. Other assumptions, such as wave propagation into the stratosphere [Yano and Emanuel, 1991], are needed in the theory to make the growth rate to peak on the planetary scales. A central feature of the original theory is a requirement of mean surface easterlies, which, when superimposed with surface easterly wind of the MJO, give rise to positive anomalies in surface wind speed and thereby in evaporation east of the convective center. This MJO structure is synthesized as model III in Figure 6. Observations based on in situ surface measurements have shown, however, that, on average, maximum surface evaporation is in or to the west of the convective center of the MJO where its surface westerly wind is [e.g., Zhang, 1996; Lin and Johnson, 1996a; Zhang and McPhaden, 2000]. In boreal winter a mean surface easterly flow is rarely observed in the equatorial Indian and western Pacific oceans, where the MJO signals are the most prominent [Wang, 1988b]. The WISHE/EWF theory has been modified under an assumption of *moist convective adjustment* to provide instability to an intraseasonal, planetary-scale Kelvin mode in a resting basic state [Neelin and Yu, 1994]. Modeling studies have suggested that the WISHE/EWF mechanism may strengthen the MJO if it does not determine its existence [Neelin *et al.*, 1987; Lau and Shen, 1988; Wang and Li, 1994; Lin *et al.*, 2000; Maloney and Sobel, 2004]. In light of the possibility of SST feedback to the MJO

(sections 4.2.4 and 5.3) the sensitivity of the MJO to surface evaporation needs to be quantified.

## 3.3. Other Factors

### 3.3.1. Radiation

[33] In theory, radiation can play an essential role in maintaining local, stationary intraseasonal oscillations in deep convection [Hu and Randall, 1994, 1995]. The atmospheric convective instability could be modified by clear-sky radiation due to water vapor [Zhang and Chou, 1999], which fluctuates with the MJO [Brown and Zhang, 1997; Myers and Waliser, 2003; Weare, 2003]. Radiation feedback is critical to generating MJO signals in a numerical model based on the WISHE/EWF mechanism (section 3.2.2) [Raymond, 2001]. In another model where convective processes are explicitly calculated by a *cloud-resolving model*, interactive radiation can help but is not essential to MJO-like intraseasonal, eastward propagating supercloud clusters [Grabowski, 2003]. Radiation due to low to middle clouds might play a role in the MJO through their contributions to the vertical heating profile (section 3.3.5).

### 3.3.2. Water Vapor

[34] Water vapor can be important to the MJO for different reasons. In some theory the propagation speed of the MJO depends on the time mean *moist stability* [Lau and Peng, 1987; Wang, 1988a] and its time-dependent component [Neelin and Yu, 1994]. Intraseasonal fluctuations in tropospheric water vapor induced by MJO circulation might feed back to its precipitation by directly affecting deep convection [e.g., Tompkins, 2001] or indirectly modulating the moist stability [Myers and Waliser, 2003]. The eastward propagation of the MJO may come from its zonal asymmetry. The atmosphere tends to be more stabilized to the west of the convective center than to the east [Hendon, 1988] partially because the Ekman divergence is related to the equatorial surface westerlies [Matthews, 2000] and partially because extraordinary drying immediately follows the convectively active phase of the MJO [Hendon and Liebmann, 1990] (Figure 7c). Low-level humidity gradually increases

ahead (east of) the convective center [Kemball-Cook and Weare, 2001; Myers and Waliser, 2003], resulting in a westward tilt in the moisture field as shown by observations (Figure 7c) and GCM simulations [Lau et al., 1988; Park et al., 1990; Wang and Schlesinger, 1999; Maloney, 2002]. In some models the water vapor feedback helps organize deep convection into large-scale ensembles moving slowly eastward [Grabowski and Moncrieff, 2005] and determines their propagation speed [Swinbank et al., 1988].

[35] The mechanisms for the low-level moistening and drying are unclear. Large-scale subsidence can efficiently dry the atmosphere with a timescale  $\leq 10$  days [Grabowski and Moncrieff, 2005], but why it is zonally asymmetric with respect to the convective center of the MJO is unclear. The low-level Rossby cyclonic circulations west of the convective center (Figure 5) may bring dryer air from higher latitudes into the equatorial region. However, this has yet to be confirmed by observations. It is questionable whether low-level convergence and surface evaporation are responsible for the moistening east of the convective center [Kemball-Cook and Weare, 2001; Maloney, 2002]. Vertical transport and *detrainment* of moisture by isolated small cumuli [Esbensen, 1978] and middle-level clouds [Johnson et al., 1999] may slowly moisten the lower troposphere prior to an active phase [Slingo et al., 2003]. In a discharge-recharge hypothesis [Hendon and Liebmann, 1990; Blade and Hartmann, 1993] the period of the MJO depends on the time the atmosphere takes to be destabilized again (energy recharge) after the convective stabilization (discharge). The selection of the temporal and spatial scales of the MJO by the water vapor feedback has yet to be included in theories.

### 3.3.3. Sea Surface Temperature

[36] SST can affect the MJO in a number of ways. Mean SST determines the geographical preference of the MJO (section 2.7) by maintaining low moist static stability, a critical factor for the selection of the propagation speed and period of the MJO in some theories [Lau and Shen, 1988; Davey, 1989] (Figure 11). Interannual variability of SST associated with ENSO affects the interannual variability in the MJO in the Pacific (section 2.9), which may lead to an MJO-ENSO interaction (section 6). Fluctuations in SST induced by the MJO may feed back directly to the MJO (sections 4.2.4 and 5.3). The diurnal cycle in SST may be involved in scale interactions with the MJO (sections 3.3.4 and 5.2.1). Wang and Xie [1997] theorized that an air-sea coupled intraseasonal instability is possible only when surface forcing due both to solar radiation and latent heat fluxes is included (section 5.1). The amplitude of intraseasonal perturbations in SST induced solely by latent heat flux associated with the MJO is too small to cause an instability [Hirst and Lau, 1990].

### 3.3.4. Scale Interaction

[37] Possible scale interactions involved with the MJO have recently been discussed by Slingo et al. [2003] and Moncrieff [2004]. The observed rich multiscale structure of the MJO (section 2.6) raises the question as to whether it represents a dynamical hierarchy essential to the large-scale features of the MJO [Majda and Biello, 2004] or simply a

manifestation of large-scale modulation of existing smaller-scale systems [Hendon and Liebmann, 1994]. It is obvious in Figure 2 that the westward moving, 2- to 5-day signals exist in both active and inactive phases of the MJO but are modified by the MJO. In a simple wave-CISK model [Lau et al., 1989] the intraseasonal period of the MJO depends on the time the large-scale atmosphere needs to adjust to finer-scale heating and to make the planetary-scale Kelvin waves dominantly unstable. Of the models that produce MJO-like signals some simulate the multiscale structure [e.g., Hayashi and Sumi, 1986; Itoh, 1989; Wang and Li, 1994]; others do not [e.g., Gustafson and Weare, 2004a, 2004b]. In a two-dimensional (zonal and vertical) large-scale model without the Coriolis force [Chao and Lin, 1994] the eastward moving speed of supercloud clusters embedding westward propagating convective systems is much less than that of convectively coupled Kelvin waves produced in a two-dimensional cloud-resolving model without any multiscale structure [Grabowski and Moncrieff, 2001].

[38] A possible scale interaction may occur between the MJO and the diurnal cycle through the water vapor feedback due to low and midlevel clouds (section 3.3.2). Midlevel clouds in an inactive phase of the MJO [Johnson et al., 1999] may moisten the lower to middle troposphere and create a favorable condition for the upcoming active phase [Inness et al., 2001]. These midlevel clouds undergo a strong diurnal cycle, which may be related to the diurnal cycle in SST [Slingo et al., 2003]. The diurnal cycle could be important to the MJO also through air-sea interaction. The diurnal cycle in surface heating is critical to intraseasonal fluctuations in SST (section 5.2.1) and therefore to the MJO if SST feedback to the MJO is important (sections 4.2.4 and 5.3).

[39] Mesoscale convective systems dominating active phases of the MJO feature *stratiform precipitation* [Houze, 1989] and midlevel rear inflows [Zipser, 1969]. During active phases of the MJO such a rear inflow comes from the west into mesoscale convective systems in the large-scale convective center of the MJO [Kingsmill and Houze, 1999]. There, it descends because of diabatic cooling due to evaporation and melting of stratiform precipitation, and, when reaching into the boundary layer, it enhances large-scale surface westerlies [Houze et al., 2000; Mecham et al., 2005] (Figure 12). This mesoscale downward momentum transport, supplementary to the large-scale momentum transport by the Rossby gyres [Moncrieff, 2004], is another example of scale interaction associated with the MJO. Whether the scale interactions are essential for the scale selection of the MJO is unknown.

### 3.3.5. Heating Profile

[40] The atmospheric large-scale circulation in the tropics is sensitive to the vertical structure of diabatic heating [e.g., Hartmann et al., 1984]. Diabatic heating peaks in the middle troposphere because of convective rain and in the upper troposphere because of stratiform precipitation; their combination yields a top-heavy profile commonly observed in the tropics [Houze, 1989]. It is debatable, however, whether such a deep convective heating profile is effective

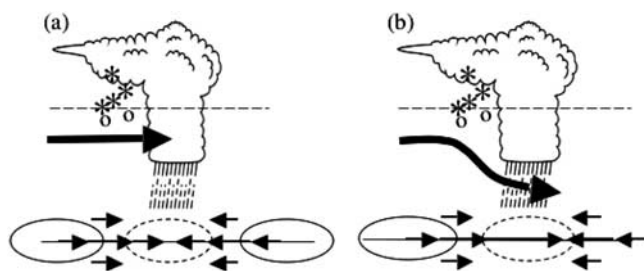


**Figure 12.** Schematic diagrams illustrating the effect of mesoscale downward transport of zonal momentum on the large-scale pattern of surface zonal wind during active phases of the MJO. Cloud symbols represent large-scale convective centers of the MJO. Horizontal dashed lines mark the melting level. Asterisks and circles represent ice crystals (graupels) and raindrops from stratiform clouds. Thick arrows pointing to the right represent the midlevel rear inflows of mesoscale systems embedded in the large-scale convective centers. Thin arrows at bottom represent large-scale surface zonal winds. Ovals indicate high and low (dashed) surface pressure centers. (a) Without the mesoscale downward momentum transport, surface zonal winds, determined by the zonal pressure gradient, distributed as in MJO model I in Figure 6. (b) Mesoscale downward momentum transport due to diabatic cooling of evaporation and melting of stratiform precipitation helping to establish surface westerlies in the convective center as in MJO model II in Figure 6. Based on *Houze et al.* [2000].

in generating surface wind responses that are deemed important to the MJO in some theories (section 3.2). It has been argued that the lower branch of the atmospheric circulation directly responding to the top-heavy heating profile is significant only in the lower troposphere but not near the surface [*Schneider and Lindzen*, 1977; *Wu et al.*, 2000, 2001]. Only if the heating profile peaks in the lower troposphere, can the atmospheric circulation respond with significant amplitude near the surface [*Bergman and Hendon*, 2000]. Shallow heating might be needed if the interaction between surface winds and atmospheric convection is crucial to the MJO [*Wu*, 2003].

[41] The phase speed of the Kelvin wave is given as  $c = (gh)^{1/2}$ , where  $g$  is gravity and  $h$  is the equivalent depth, a measure of the vertical scale [*Matsuno*, 1966]. Deep heating profiles can only force deep (large  $h$ ), fast modes. Slow modes can be produced by heating profiles peaking in the lower troposphere (e.g., between 500 and 700 hPa [*Sui and Lau*, 1989]), which may interact with deep modes to reduce the overall propagation speed of the MJO [*Chang and Lim*, 1988].

[42] The heating profile associated with the MJO exhibits a westward tilt, with a weak maximum in the lower troposphere during the transition between inactive and active phases and a typical top-heavy structure during active phases (Figure 7d). The shallow heating can possibly come from condensation within middle-level precipitating clouds [*Johnson et al.*, 1999] and radiative effects of shallow, nonprecipitating clouds [*Bergman and Hendon*, 2000].

Shallow convection may provide favorable conditions for deep convection [*Mapes*, 2000] followed by stratiform rain [*Lin et al.*, 2004]. The corresponding atmospheric circulation may have to be understood in terms of its interaction with both deep and shallow heating as well as mesoscale convective systems (section 3.3.4). The variation in the heating profile during the life cycle of the MJO has yet to be considered in MJO theories.

#### 4. NUMERICAL MODELING

[43] Simulating a realistic MJO has never ceased to challenge the atmospheric modeling community. Early simulations by primitive models appeared to be promising, with eastward propagating signals in both large-scale circulation and precipitation [*Hayashi and Golder*, 1986; *Hayashi and Sumi*, 1986; *Lau and Lau*, 1986]. However, their eastward propagation speeds were often closer to that of the observed convectively coupled Kelvin waves than to the speed of the MJO. Many more sophisticated models still cannot produce the MJO. It is common that when eastward propagating signals are reproduced, they are too weak, their propagation speeds are too large, their spatial distributions and seasonal cycles are unrealistic, and their convection and wind is decoupled [*Slingo et al.*, 1996; *Sperber et al.*, 1997]. While these problems still plague many GCMs to date [*Sperber*, 2004], marked improvements have been made in others, which provided insights to the physics and dynamics of the MJO and encouraged MJO prediction experiments (section 4.3).

##### 4.1. Realism of Current Simulations

[44] The MJO has been such an elusive modeling trophy that it is hard to resist the temptation of claiming it whenever intraseasonal signals propagating eastward are discerned in numerical simulations. The realism of simulated MJO should, however, be evaluated at the highest possible standard. Otherwise, the risk of misrepresenting the physics and dynamics of the MJO is too high. Only when model simulations are diagnosed following the same procedures as for observations can the simulated MJO be evaluated fairly and model improvement judged objectively. The following progressive procedure, synthesized from previous observational analysis of the MJO, can be used in evaluation of model simulations against observations.

[45] 1. Examine time-space power spectra [*Hayashi*, 1979]. Intraseasonal and planetary-scale eastward propagating power in convection and zonal wind much larger than the corresponding westward propagating power signifies the existence of the MJO [e.g., *Zhang and Hendon*, 1997].

[46] 2. Objectively extract MJO signals using methods such as the empirical orthogonal function [e.g., *Lau and Chan*, 1985] or singular vector decomposition [e.g., *Weare*, 2003]. The leading modes that are supposed to represent the MJO should be separable from the others based on a priori criteria [e.g., *North et al.*, 1982].

[47] 3. Reconstruct the MJO from the leading modes and examine its primary features, such as the zonal scale,

propagation speed, and structure [e.g., *Sperber*, 2003; *Kiladis et al.*, 2005].

[48] 4. Examine the spatial distribution and seasonal cycle of the MJO [e.g., *Zhang and Dong*, 2004].

[49] When used to validate simulations against observations, each of the above steps progressively demands a higher degree of realism from the simulated MJO. The first three should be considered the minimum validation. If simulated MJO signals are too weak for some of these steps, for example, steps 2 and 3, to be applicable, other methods can be adapted to analyze only selected data with identifiable signals [e.g., *Duffe et al.*, 2003; *Sperber*, 2004].

[50] Examples are given in Figures 13 and 14 to illustrate the current stage of MJO simulations. All selected global weather forecast and climate models produce some MJO signals, as evidenced by their eastward propagating power that is greater than the westward propagating power in zonal wind (Figure 13). Even though the intraseasonal peaks are not always distinguishable from the lower-frequency power and the MJO signals in precipitation are much weaker, these power spectra are much more realistic than those produced by many other global models.

[51] A realistic spectrum does not guarantee a realistic structure of the simulated MJO. Figure 14 demonstrates a common problem [e.g., *Itoh*, 1989; *Wang and Li*, 1994]: Positive anomalies in precipitation tend to be in regions of low-level easterly anomalies, contrary to the observations (Figures 4 and 5). This simulated structure of the MJO is synthesized as MJO model IV in Figure 6. Few models can produce the MJO with a structure similar to the observed [e.g., *Sperber et al.*, 1997; *Inness and Slingo*, 2003]. Unrealistic vertical distributions of heating might be a reason. MJO signals in models are often too weak in the Indian Ocean or too strong in the tropical northeastern Pacific [*Maloney*, 2002; *Liess and Bengtsson*, 2004]. The seasonal cycle of the simulated MJO often misses the observed latitudinal migration or peaks at a wrong time [*Slingo et al.*, 1996; *Liess et al.*, 2004]. In short, models that produce dominant eastward propagating power with reasonable zonal scales, periods, and phase speeds may still suffer from unrealistic structures, spatial distributions, and seasonal cycles of their simulated MJO.

## 4.2. Sensitivity to Model Configurations

[52] Simulations of the MJO can be affected by four factors among others.

### 4.2.1. Cumulus Parameterization

[53] *Slingo et al.* [1996] compared simulations of 15 GCMs and concluded that the large range of capability of simulating the MJO by these models could be explained partially in terms of the type of cumulus parameterizations used. The sensitivity of MJO simulations to cumulus parameterizations has been best demonstrated by *Maloney and Hartmann* [2001]. By switching the cumulus parameterization in a GCM they were able to transform the model from one with very weak intraseasonal variability to one that produced prominent MJO signals albeit the wrong structure (Figure 14). Possible reasons for such sensitivity

include types of *closure* (buoyancy versus moisture convergence) [*Slingo et al.*, 1996], the treatment of humidity in the closures [*Wang and Schlesinger*, 1999], and vertical heating profiles [*Park et al.*, 1990].

[54] Isolated convection tended to gather and form eastward propagating large cloud clusters in an idealized large-scale model when its traditional cumulus parameterization is replaced with a two-dimensional cloud-resolving model at each grid point [*Grabowski*, 2001, 2003]. This “superparameterization” approach has proven capable of producing MJO-like signals in a full GCM that showed no such capability when its original cumulus parameterizations were used [*Khairoutdinov and Randall*, 2001; *Randall et al.*, 2003]. It has yet to be determined whether this new treatment of convective processes can improve simulations of the MJO beyond what can result from a switch of conventional parameterization schemes [*Wang and Schlesinger*, 1999; *Maloney and Hartmann*, 2001].

### 4.2.2. Resolutions

[55] Studies on the dependence of the simulated MJO on model horizontal resolutions have yielded inconsistent results [e.g., *Hayashi and Golder*, 1986; *Slingo et al.*, 1996; *Gualdi et al.*, 1997; *Liess and Bengtsson*, 2004]. This inconsistency might come from the dependence of cumulus parameterizations on the resolution [*Wang and Schlesinger*, 1999]. An MJO simulation appeared to be improved as the vertical resolution is increased, possibly because of the moistening effect of middle-level clouds (section 3.3.2) that can be produced only when the vertical resolution is sufficiently high [*Inness et al.*, 2001].

[56] The demonstrated sensitivity to resolutions has motivated the use of regional mesoscale models and cloud-resolving models (CRM) in the study of the MJO. A regional (24°S–24°N, 44°–181°E) mesoscale (60-km resolution) model can simulate the MJO reasonably well without intraseasonal perturbations in the prescribed lateral boundary conditions [*Gustafson and Weare*, 2004a, 2004b]. It has yet to be determined whether the MJO simulated by mesoscale models can be more realistic than that simulated by coarse-resolution global models. A two-dimensional CRM along the equator produces eastward moving signals comparable to the convectively coupled Kelvin waves [*Grabowski and Moncrieff*, 2001]. When the same CRM is used in place of cumulus parameterization at each grid point in a large-scale model, the eastward phase speed is substantially reduced in spite of other remaining unrealistic features [*Grabowski*, 2003]. This suggests the importance of the three-dimensional structure to the MJO even when it is simulated with a high-resolution treatment of circulation-convection interaction.

### 4.2.3. Mean State

[57] The mean background state has been considered crucial to the dynamics of the MJO. The mean distribution of low-level moisture helps determine the phase speed and growth rate of the MJO in some instability theories (section 3.2.1). Comparisons of simulations from different GCMs have suggested that simulated MJO-like signals tend to be stronger in models whose mean

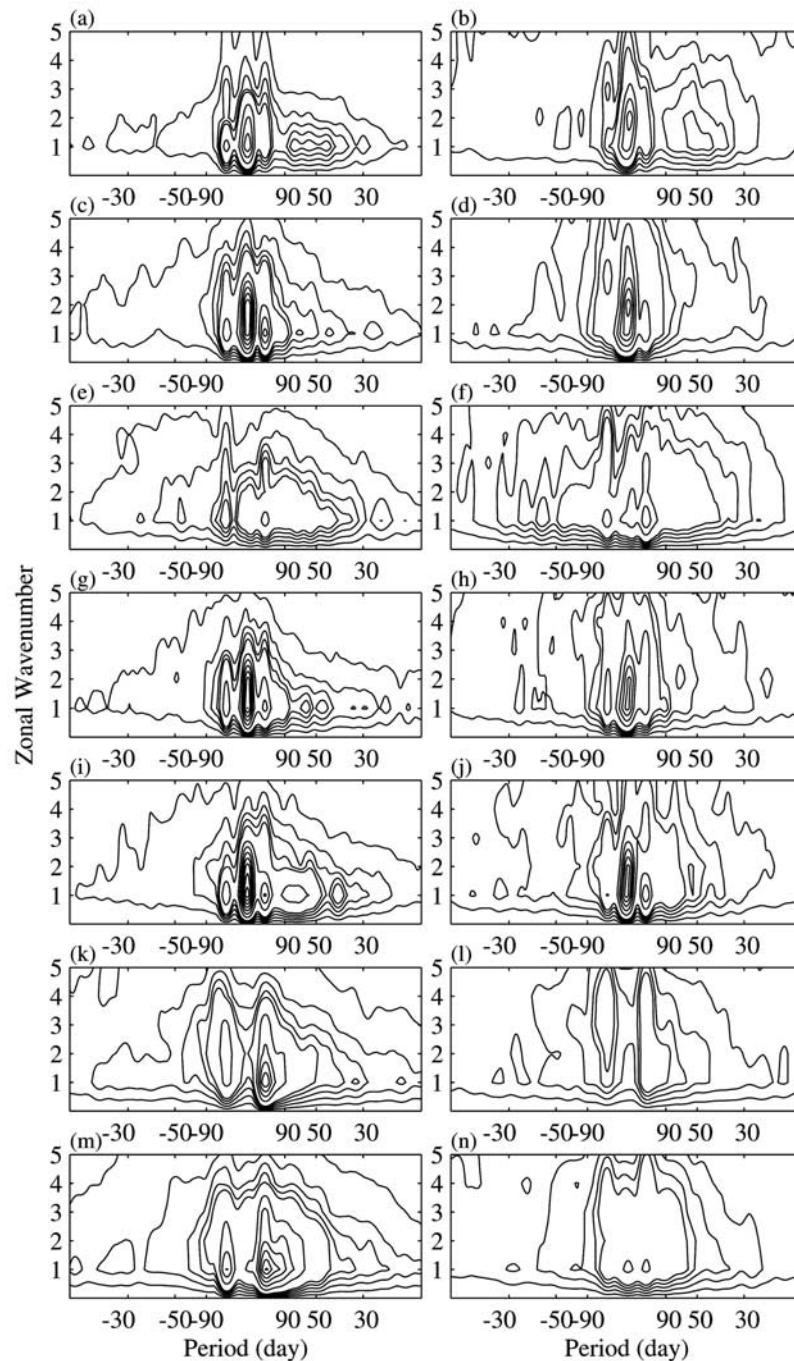


**Figure 13.** Time-space spectra for (left) zonal wind at 850 hPa and (right) precipitation averaged over  $20^{\circ}\text{N}$ – $20^{\circ}\text{S}$  and  $60^{\circ}$ – $180^{\circ}\text{E}$  from (a and b) NCEP/NCAR reanalysis and Xie and Arkin [1997] and from simulations by (c and d) Bureau of Meteorology atmospheric model version 3 [G. Wang *et al.*, 2005], (e and f) European Center/Hamburg model 4 (ECHAM4) and Hamburg ocean primitive equation (HOPE-G) coupled model [Min *et al.*, 2004], (g and h) Global Forecast System Model version 03 of NCEP (GFS03), (i and j) GFS03 coupled with an ocean model [W. Wang *et al.*, 2005], (k and l) Climate Atmosphere Model of NCAR version 2 with a relaxed Arakawa-Schubert cumulus parameterization scheme (CAM2R), (m and n) CAM2R coupled with an ocean mixed layer model [Maloney and Sobel, 2004]. Contour intervals are 1 up to 10 and 5 beyond.

seasonal cycles are stronger and whose mean precipitation is more realistically distributed with respect to SST [Slingo *et al.*, 1996]. The importance of the mean vertical wind shear and low-level zonal wind in a model has also been suggested [e.g., Hendon, 2000; Kemball-Cook *et al.*,

2002; Inness *et al.*, 2003]. The MJO appears to prefer low-level and surface mean westerlies in both simulations [Inness *et al.*, 2003] and observations [Zhang and Dong, 2004]. The exact role of the mean background state in the MJO has yet to be quantified.

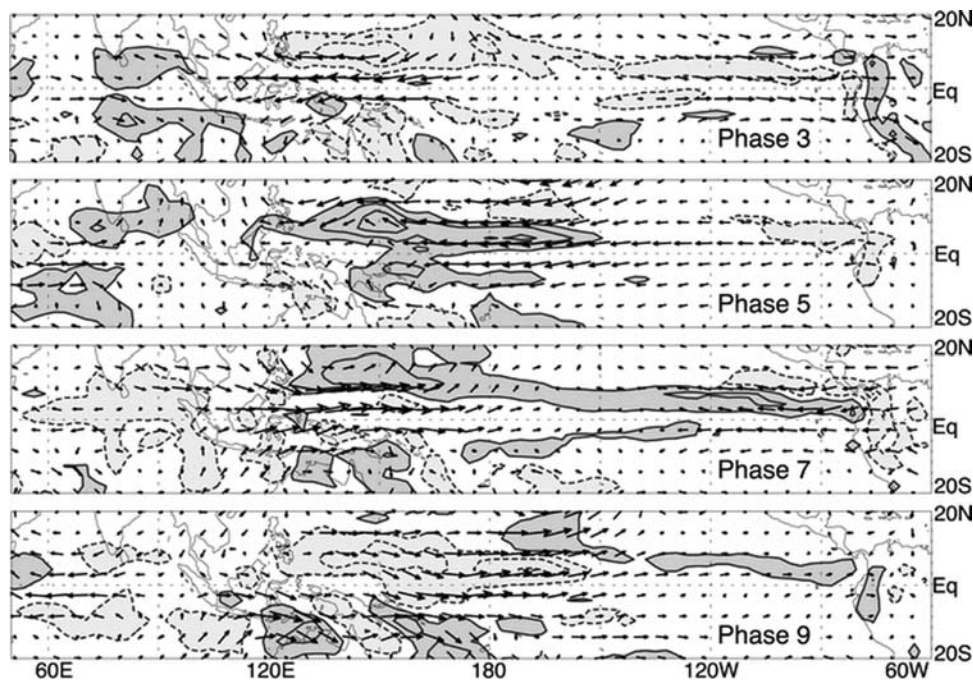


**Figure 14.** MJO composites of 850-hPa wind and convective precipitation anomalies simulated by a global climate model with realistic power spectrum and eastward propagating speed. Regions with positive (negative) anomalies in precipitation are heavily (lightly) shaded. Phases correspond to longitudinal positions of the convective center. From *Maloney and Hartmann* [2001].

#### 4.2.4. Air-Sea Coupling

[58] It has been shown that by including feedback from intraseasonal perturbations in SST the simulated MJO can be obviously improved [Flatau *et al.*, 1997; Waliser *et al.*, 1999b; Inness *et al.*, 2003], improved only slightly [Maloney and Kiehl, 2002; Sperber, 2004], not affected, or even deteriorated [Hendon, 2000; Liess *et al.*, 2004]. The effects of air-sea coupling depend on the season [Kemball-Cook *et al.*, 2002], mean state [Hendon, 2000; Inness *et al.*, 2003], and simulated intraseasonal fluctuations in SST [Watterson, 2002; Maloney and Sobel, 2004]. Air-sea coupling may improve simulated MJOs in terms of the amplitude (larger), phase speed (slower), and seasonality (stronger) only if a model on its own can produce reasonable MJO signals without SST feedback. It is not a panacea for the lack of the MJO in any model [Hendon, 2000]. In fact, even for a model that can produce reasonable MJO signals, an improvement by air-sea coupling is not guaranteed [e.g., Liess *et al.*, 2004]. Possible mechanisms for the SST feedback are discussed in section 5.3.

#### 4.3. Prediction

[59] The ability to simulate the intraseasonal fluctuations associated with the MJO by some models makes it tempting to explore the possibility of extending numerical weather prediction in the tropics beyond the known predictability limit for synoptic-scale systems (7–14 days). Investigations on this subject [Lau and Chang, 1992; Jones *et al.*, 2000; Hendon *et al.*, 2000; Waliser *et al.*, 2003a; Jones *et al.*, 2004] have showed that useful prediction skill for filtered intraseasonal perturbations can last up to 15–20 days, provided models can reproduce the MJO reasonably well.

Better prediction skill is likely to be obtained when an MJO event is in its active phase at the initial time and remains strong during the forecasting period. The extended 15- to 20-day prediction skill is, however, only a quarter of the life cycle of the MJO. In comparison, weather prediction at midlatitudes is limited by the full life cycle (up to 14 days) of the dominant extratropical weather systems. Meanwhile, dynamic models do not outperform statistical models in MJO forecasts [Waliser *et al.*, 1999a; Lo and Hendon, 2000]. The prediction limit demonstrated by these investigations therefore illustrates more the limitation of the numerical model's capability of simulating the MJO than the predictability of the MJO itself. Without further improvement of model simulations of the MJO, empirical methods are more feasible for practical intraseasonal prediction in the tropics [e.g., Wheeler and Weickmann, 2001; Newman *et al.*, 2003].

### 5. AIR-SEA INTERACTION

[60] Episodic, extraordinarily strong surface westerly winds (up to  $10 \text{ m s}^{-1}$ ) in the equatorial western Pacific have long been known to sea-going oceanographers, who named them westerly wind bursts [e.g., Luther *et al.*, 1983]. These WWB can leave significant imprints in the upper ocean [e.g., Meyers *et al.*, 1986; McPhaden *et al.*, 1988]. Some WWB, especially the long-lasting ones, are associated with the MJO. Unfortunately, confusion between the concepts of the MJO and WWB is widespread throughout the literature. Oceanographers usually refer to any strong westerly wind events as WWB, no matter how long they

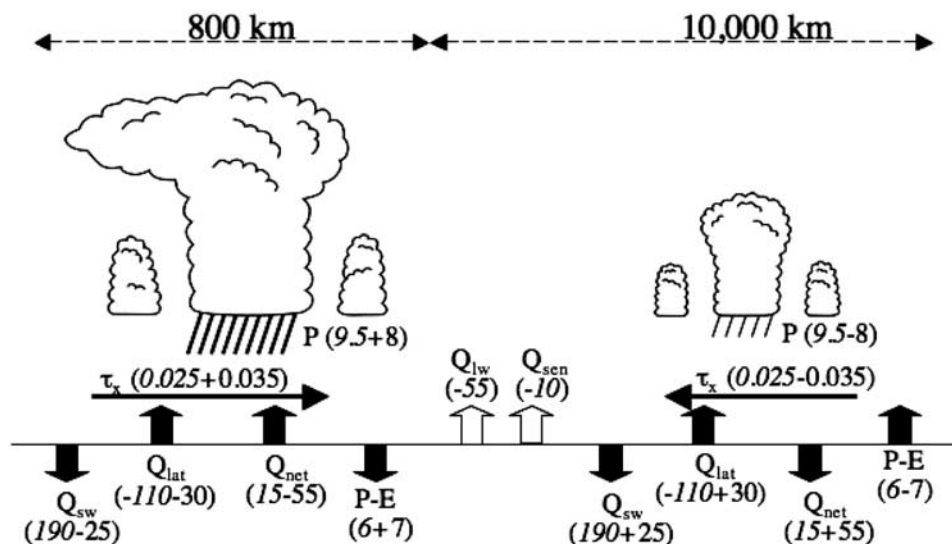


**Figure 15.** Schematic diagram illustrating the amplitudes of surface forcing of the MJO in terms of the mean plus/minus intraseasonal perturbation in solar radiation flux ( $Q_{sw}$ ), latent heat flux ( $Q_{lat}$ ), net heat flux ( $Q_{net}$ ), precipitation ( $P$ ), freshwater input ( $P - E$ ), and zonal stress ( $\tau_x$ ), whose direction is marked by horizontal arrows. Downward (upward) pointing arrows and positive (negative) values indicate fluxes into (from) the ocean. The deep (shallow) cloud symbol at the left (right) represents a convectively active (inactive) phase, whose zonal scale is indicated at the top. Intraseasonal fluctuations in longwave radiation flux ( $Q_{lw}$ ) and sensible heat flux ( $Q_{sen}$ ) are negligibly small and are assumed to be zero. Units are  $W m^{-2}$  for the fluxes,  $mm d^{-1}$  for precipitation and freshwater input, and  $N m^{-2}$  for wind stress. Uncertainties in the net fluxes are  $10 W m^{-2}$ . (Diagram is based on estimates from in situ observations by Zhang [1996], Cronin and McPhaden [1997], Shinoda et al. [1998], and Zhang and McPhaden [2000].)

last. Atmospheric scientists typically consider WWB to be of *synoptic scale* in time. The vertical structure of the zonal wind is predominantly barotropic for synoptic-scale WWB but is baroclinic for the MJO [Fasullo and Webster, 2000]. The MJO propagates eastward; synoptic-scale WWB do not necessarily do so [Hartten, 1996]. The convection-wind coupling is an intrinsic feature for the MJO (section 2.4) not for most synoptic-scale WWB by definition. The MJO undergoes a substantial seasonal cycle (sections 2.8). Most synoptic-scale WWB do not [Harrison and Vecchi, 1997]. Some global models have shown substantial improvement in simulating the MJO (section 4). No such improvement has been documented for simulations of synoptic-scale WWB. Some of these distinctions are important to air-sea interaction and possible interactions with ENSO (section 6). A review on air-sea interaction on intraseasonal timescales in general is given by Hendon [2005].

### 5.1. MJO Forcing

[61] The MJO perturbs the upper ocean through surface fluxes of momentum, latent and sensible heat, radiation, and fresh water [e.g., Krishnamurti et al., 1988; Zhang, 1996; Hendon and Glick, 1997; Lau and Sui, 1997; Jones et al., 1998]. The latter three in combination make up buoyancy flux. A schematic diagram in Figure 15, based on in situ observations in the equatorial western Pacific, illustrates different forcing components during the two phases of the MJO. Amplitudes of these fluxes in the Indian Ocean can be different [Shinoda et al., 1998]. Surface fluxes from global reanalyses suffer from large biases [e.g., Shinoda et al., 1999].

[62] Perturbations in the momentum flux ( $0.02-0.055 N m^{-2}$ ) are dominated by the zonal wind, whose intraseasonal amplitudes are  $5-10 m s^{-1}$  in daily mean observations [McPhaden et al., 1992] and  $2-5 m s^{-1}$  in MJO composites [Zhang and McPhaden, 2000]. The intraseasonal amplitude of surface meridional wind is negligibly weak [Zhang, 1996]. The net freshwater flux into the ocean (precipitation minus evaporation or  $P - E$ ) is mainly controlled by precipitation. Strong evaporation in convective centers of the MJO compensates only slightly the freshwater input of precipitation.

[63] Perturbations in solar radiation flux (controlled by cloudiness) and latent heat flux (mainly controlled by surface winds) have similar amplitudes ( $25-30 W m^{-2}$ ). Intraseasonal perturbations in infrared (longwave) radiation and sensible heat fluxes are smaller than measurement uncertainties ( $\leq 5 W m^{-2}$ ). The intraseasonal amplitude of the net heat flux, composed mainly of the radiation and latent heat fluxes, depends on the relative phase among different components of the MJO [Zhang and Anderson, 2003]. It is the largest ( $50-60 W m^{-2}$ ) when the cooling maxima due to enhanced latent heat flux and reduced solar radiation flux collocate in convective centers of the MJO (model II in Figure 6).

[64] Buoyancy flux into the ocean increases with surface warming by solar radiation and freshening by precipitation. It decreases with cooling by latent heat flux and nighttime infrared radiation and salinizing by evaporation. If during an active phase of the MJO the precipitation center and maximum surface cooling of the MJO are collocated (model

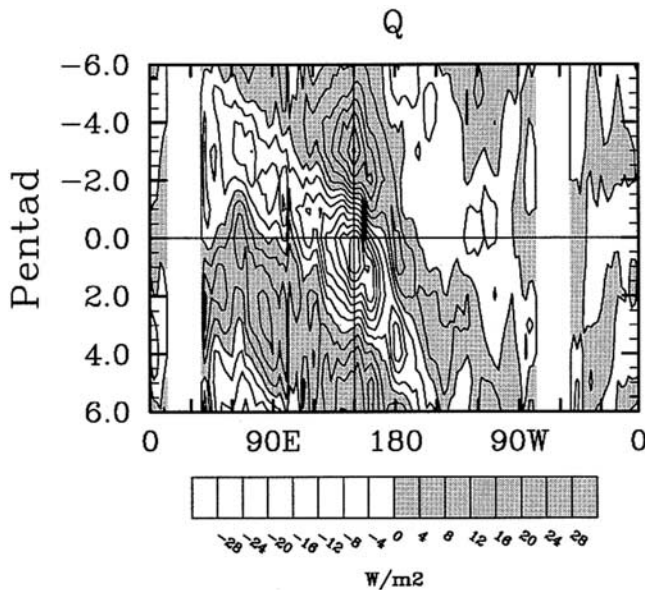


**Figure 16.** Time-longitude composite of anomalies in net surface heat flux associated with the MJO, with flux into the ocean shaded. From Jones *et al.* [1998].

II in Figure 6), then the contribution to total buoyancy flux by the fresh water ( $2.5 \times 10^{-6} \text{ kg m}^{-2} \text{ s}^{-1}$ ) partially cancels that by heat fluxes ( $-5 \times 10^{-6} \text{ kg m}^{-2} \text{ s}^{-1}$ ). The net buoyancy flux ( $-2.5 \times 10^{-6} \text{ kg m}^{-2} \text{ s}^{-1}$ ) reduces the stability of the ocean *mixed layer* [Zhang and McPhaden, 2000]. Fluctuations in these surface fluxes in combination constitute the MJO forcing, which propagates eastward along with the MJO from the Indian Ocean to the western Pacific Ocean (Figure 16), leaving a trail of a disturbed ocean.

## 5.2. Sea Responses

[65] Oceanic responses to MJO forcing can be categorized into two types: mixed layer responses and wave responses. Mixed layer responses in currents, salinity, and temperature profiles in the upper ocean, forced mainly by the perturbations in local surface fluxes, are governed by mixed layer dynamics and energy balance. They are confined where MJO forcing is strong (i.e., the Indian Ocean and western Pacific Ocean). Responses of the oceanic Kelvin wave are forced by the perturbations in surface momentum flux and governed by large-scale geophysical fluid dynamics. They propagate from the western Pacific to the eastern Pacific where MJO forcing is absent. The two are not completely separated in the western and central Pacific.

### 5.2.1. Mixed Layer Responses

[66] One of the most significant footprints of the MJO in the oceanic mixed layer is an intraseasonal fluctuation in its temperature. As a direct consequence of the surface cooling in convective centers of the MJO and warming outside (Figure 15), fluctuations in SST propagate eastward in tandem with the MJO; their phases are in quadrature, with the maximum SST leading convective centers of the MJO (Figure 17). This MJO-related fluctuation in SST is on

average about  $0.5^\circ\text{C}$  from the minimum to maximum [e.g., Zhang, 1996; Jones *et al.*, 1998] but can be greater than  $2^\circ\text{C}$  in individual cases [Krishnamurti *et al.*, 1988; McPhaden *et al.*, 1992].

[67] This seemingly simple, clear picture of the mixed layer responses to MJO forcing is sometimes blurred by other processes, such as horizontal advection by ocean currents, surface freshwater flux, cold water *entrainment* at the bottom of the mixed layer, the effect of the diurnal cycle, and the structure of the MJO. Strong surface wind of the MJO forces ocean currents and hence the possible effect of horizontal advection. Because the vertical component of the Coriolis force vanishes, strong surface westerly winds force eastward equatorial ( $3^\circ\text{N}$ – $3^\circ\text{S}$ ) currents of about  $1 \text{ m s}^{-1}$  near the surface [Yoshida, 1959], which penetrate downward as deep as 100 m [Lindstrom *et al.*, 1987; McPhaden *et al.*, 1992]. Its horizontal thermal advection associated with active phases of the MJO can be strong in cases [Cronin and McPhaden, 1997; Wijesekera and Gregg, 1996; Feng *et al.*, 2000], especially in a deeper layer [Song and Friehe, 1997]. Near the eastern edge of the warm pool, where the zonal SST gradient is strong, the eastward thermal advection can push the warm pool farther to the east, which may affect ENSO [Picaut *et al.*, 1996] (section 6). Within the warm pool, horizontal thermal advection is generally incoherent on the scale of the MJO; its inclusion is not essential to the overall simulation of the intraseasonal fluctuations in SST [Shinoda and Hendon, 2001]. The role of horizontal saline advection in the mixed layer salt budget is significant [Smyth *et al.*, 1996; Cronin and McPhaden, 1998; Feng *et al.*, 2000], mainly because of the large saline gradient at the surface caused by localized rainfall events.

[68] Surface freshwater flux increases the stability of the mixed layer, which reduces the strength of buoyancy-driven mixing. Strong surface winds during active phases of the MJO minimize the sensitivity of the mixed layer temperature to freshwater flux [Shinoda *et al.*, 1998]. This sensitivity can be amplified if surface wind is weak, for example, when its maximum is dislocated away from a convective center of the MJO [Zhang and Anderson, 2003].

[69] A direct consequence of buoyancy flux is the *barrier layer* [Godfrey and Lindstrom, 1989], which tends to prevent entrainment cooling from affecting the heat budget of the mixed layer and makes the latter more sensitive to surface heat fluxes [Lukas and Lindstrom, 1991; Sprintall and Tomczak, 1992]. A barrier layer usually forms when positive buoyancy flux due to precipitation and surface heating is accompanied by light surface wind, which is typical during inactive phases of the MJO. It can also form because of horizontal advection and vertical shear caused by strong surface wind [Cronin and McPhaden, 2002]. Extraordinarily strong surface winds during active phases of the MJO can generate sufficient mixing to erode away the barrier layer [Lukas and Lindstrom, 1991] and thus evoke entrainment cooling [Cronin and McPhaden, 1997]. The barrier layer therefore fluctuates intraseasonally: it is the thickest during inactive phases of the MJO [Sprintall and McPhaden, 1994; Zhang and McPhaden, 2000].

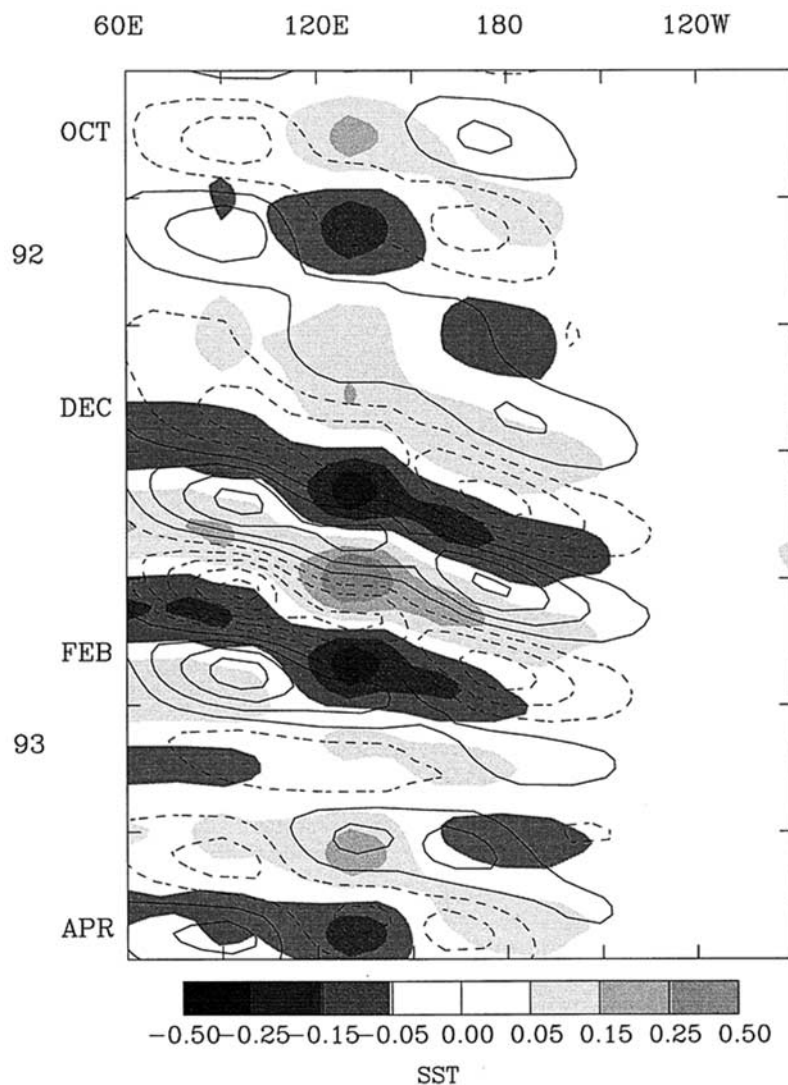


**Figure 17.** Time-longitude diagram of anomalies in OLR (contours with interval of  $10 \text{ W m}^{-2}$ ) and SST (shaded,  $^{\circ}\text{C}$ ) associated with the MJO along  $5^{\circ}\text{S}$  for 1 October 1992 through 15 April 1992. From *Hendon and Glick [1997]*.

[70] The role of entrainment in the heat balance of the upper ocean during the life cycle of the MJO is difficult to estimate accurately. Direct measurements of microscale turbulence have been made only for few cases [*Smyth et al.*, 1996; *Wijesekera and Gregg*, 1996]. These estimates suggest that entrainment heat flux at the base of the mixed layer varies between  $-25 \text{ W m}^{-2}$  (heat imported upward into the mixed layer) during inactive phases of the MJO and  $35 \text{ W m}^{-2}$  (heat exported downward from the mixed layer) during active phases. The heat flux is normally downward as the mixed layer, warmer than the water below, is deepened by enhanced turbulence due to wind work and/or oceanic convection. Upward heat flux occurs when a large fraction of solar radiation penetrates through a very thin mixed layer during inactive phases of the MJO and creates a temperature inversion at its bottom [*Anderson et al.*, 1996; *Shinoda and Hendon*, 1998].

[71] The contrast between daytime heating (dominated by solar radiation) and nighttime cooling (by longwave radia-

tion) leads to a profound diurnal cycle in the depth of the mixed layer, which can shoal to a few meters during the day (with weak winds) and deepens to 60 m or more at night [*Anderson et al.*, 1996]. During active phases, owing to a combination of strong surface winds and nocturnal cooling, the mixed layer deepening at night can break a weak barrier layer and evoke entrainment and thus enhance the mixed layer cooling on intraseasonal timescales. This diurnal cycle is critical to the amplitude of the intraseasonal fluctuation in SST in response to the MJO forcing [*Anderson et al.*, 1996; *Sui et al.*, 1997; *Shinoda and Hendon*, 1998]. Without it the mixed layer would become constantly thin, lose a certain amount of solar radiation because of its penetration during inactive phases, and experience no entrainment cooling (or even experience entrainment warming) during active phases. In consequence, the intraseasonal fluctuations in the mixed layer temperature would be less. This is an excellent example of scale interaction (section 3.3.4). Another example of scale interaction associated with the MJO

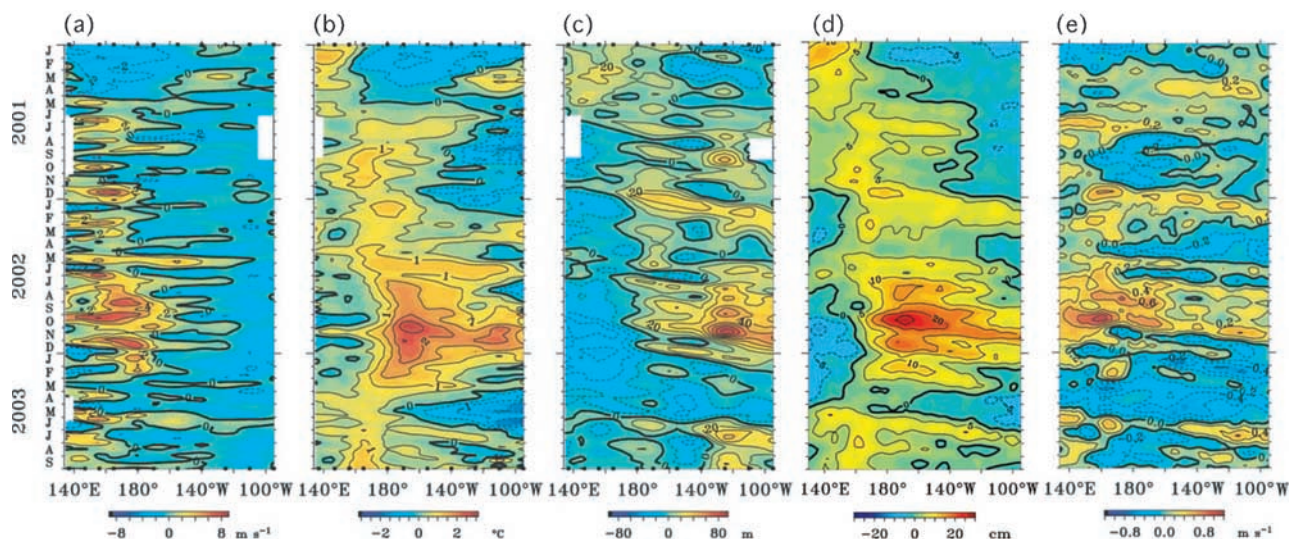


**Figure 18.** Anomalies (relative to the mean seasonal cycle) of (a) zonal wind, (b) SST, (c) 20°C depth (an index for the depth of the thermocline), (d) sea surface height, and (e) surface zonal current velocity averaged between 2°N and 2°S for January 2001 to September 2003. From McPhaden [2004].

is its rectification effects on lower-frequency variability of the ocean [Kessler and Kleeman, 2000; Waliser et al., 2003b], which may lead to an interaction with ENSO (section 6).

[72] Surface westerlies associated with the MJO also induce local responses below the mixed layer. A westward countercurrent can develop to 20–40 cm s<sup>-1</sup> between the surface jet and the equatorial undercurrent; the thermocline can be depressed by 20–30 m by a downwelling of 2–3 m d<sup>-1</sup> [McPhaden et al., 1992]. The associated temperature perturbations near the thermocline are of about 1°C and are disconnected from those in the mixed layer induced by surface heat fluxes [Zhang, 1997]. Oceanic Kelvin waves are responsible for the thermocline perturbations.

### 5.2.2. Wave Responses

[73] Intraseasonal equatorial Kelvin waves stand out as another distinct footprint of the MJO in the ocean. Their signals can be detected from the current [Johnson and McPhaden, 1993a], thermocline depth [Kessler et al., 1995], and sea level height [Enfield, 1987; Delcroix et al., 1991]. The pulse-like structure of the MJO, with its westerly wind much stronger than its easterly wind, forces pulses of downwelling Kelvin waves. They propagate from their birthplace in the western Pacific into the eastern Pacific (Figure 18) where the MJO is very weak or absent. The associated vertical displacement in the thermocline is typically 20–30 m but can be as great as 60 m [Lukas et al., 1984; McPhaden et al., 1988, 1992]. This may have significant consequences in its interaction with ENSO (section 6).

[74] The power of the intraseasonal Kelvin wave is centered at 70–90 days with zonal scale of 13,000–15,000 km [Hendon et al., 1998] and its maximum in the central Pacific (~140°W) [Cravatte et al., 2003]. Observed propagation speeds of the Kelvin wave are about 2.1–2.8 m s<sup>-1</sup> [McPhaden and Taft, 1988; Delcroix et al., 1991;

Johnson and McPhaden, 1993b; Kessler et al., 1995; Kutsuwada and McPhaden, 2002]. The phase speed expected from linear theories is about 2–3 m s<sup>-1</sup> [Cane and Sarachik, 1981], with higher values in the west than in the east because of the sloping equatorial thermocline [Giese and Harrison 1990]. The speed can also be affected by the phase of ENSO [Benestad et al., 2002] and nonlinearity [Ripa, 1985]. In addition, there may be a slight enhancement of eastward zonal phase speeds because of Doppler shifting by the equatorial undercurrent [Johnson and McPhaden, 1993b].

[75] The dominant period of the Kelvin wave (70–90 days) is at the low-frequency end of the spectrum for its forcing wind (30–90 days) [McPhaden and Taft, 1988; Hendon et al., 1998]. This can be explained in terms of the eastward propagation of the MJO. The energy received by the Kelvin wave is an integration of zonal stress along the characteristic line of the Kelvin wave [Kessler et al., 1995; Boulanger and Menkes, 1995]. Surface westerly winds propagating eastward cover a longer range of longitude (the fetch) and spend a longer “contact time” with the Kelvin wave. This would make the low-frequency (periods > 60 days) part of intraseasonal wind stress forcing, their weak amplitude notwithstanding, nearly resonant with the gravest baroclinic Kelvin wave and therefore able to force Kelvin waves of longer periods than if it were stationary [Kessler et al., 1995; Hendon et al., 1998].

[76] The Kelvin wave may affect the energy balance of the mixed layer in different ways. In the central Pacific near the eastern edge of the western Pacific warm pool, where the zonal SST gradient is large, the eastward surface current of the Kelvin wave can advect warmer water eastward [Picaut et al., 1996; McPhaden, 2002]. In the eastern Pacific, where the zonal SST gradient is weak but the mean thermocline is shallow, the displacement of the

thermocline associated with the downwelling Kelvin waves weakens the cooling of equatorial *upwelling* that counteracts solar heating [McPhaden, 2002]. Both effects can lead positive anomalies in equatorial SST there [Johnson and McPhaden, 1993a; Zhang, 2001].

### 5.3. Oceanic Feedback

[77] The MJO is sometimes incorrectly labeled as a coupled mode simply because there is intraseasonal coherence between atmospheric variables and SST [Kawamura, 1991]. Whether the MJO is a coupled mode depends on whether the intraseasonal feedback from SST is essential to its dynamics. This is an issue much less certain than SST responses to the MJO. While numerical simulations have shown different degrees of improvement in MJO simulations when SST feedback is included (section 4.2.4), the mechanism for the improvement is unclear. It has been proposed that energizing effects of the positive anomaly in SST ahead (east of) convective centers of the MJO, through an enhancement in either surface latent flux [Flatau *et al.*, 1997] or low-level moisture convergence [Waliser *et al.*, 1999b; Kemball-Cook *et al.*, 2002], help improve MJO simulations. While the destabilizing effect of the positive SST anomaly east of the convective center may enhance the eastward propagation of the MJO [Inness and Slingo, 2003], it is unclear why this reduces the eastward propagation speed in some simulations [e.g., Waliser *et al.*, 1999b] and increases it in others [e.g., Watterson, 2002]. The atmosphere does not see SST; it only senses it through surface fluxes. The net effect of SST perturbations is to reduce the amplitude of intraseasonal perturbations in surface fluxes, because of the phase relations between SST and surface winds [Shinoda *et al.*, 1998]. MJO simulations can be degraded by intraseasonal perturbations in surface fluxes [Colon *et al.*, 2002]. An understanding of intraseasonal feedback of SST to the MJO needs to be achieved in tandem with an improved understanding of the sensitivity of the MJO to surface heat fluxes and SST effects on the MJO on the annual and interannual timescales (sections 2.8 and 2.9).

## 6. INFLUENCES ON ENSO

[78] Possible influences on ENSO by high-frequency equatorial anomalous wind events were first speculated by Keen [1982], Lukas *et al.* [1984], and Lau and Chan [1985]. Such speculations have received increasing research interest lately. Even though ENSO prediction by dynamical models has been continuously improved [Latif *et al.*, 1998], their forecasts of a recent ENSO event were unsatisfactory [Barnston *et al.*, 1999; Landsea and Knaff, 2000]. It has been speculated that a lack of the MJO in those models ails the predictions. Newly available data provide detailed observations of how the MJO and ENSO are related. Among the most useful are the global model reanalysis products [e.g., Kalnay *et al.*, 1996] and the surface and subsurface observations from the Tropical Atmosphere-Ocean mooring array in the equatorial Pacific [McPhaden *et al.*, 1998]. Extraordinarily strong MJO events have been

repeatedly observed during the onset and growth stages of recent major ENSO warm events [e.g., Lau and Chan, 1988; Kindle and Phoebus, 1995; Kessler and McPhaden, 1995; McPhaden, 1999, 2004; Wang and Weisberg, 2000; Bergman *et al.*, 2001]. Commonly, the interannual warming of the equatorial sea surface in the central and eastern Pacific is composed of a series of intraseasonal events associated with the MJO. In each of such events the eastern edge of the western Pacific warm pool is displaced eastward because of thermal advection, and the thermocline is deepened in the eastern Pacific because of the downwelling Kelvin waves (Figure 18). Meanwhile, since first proposed by Lau [1985], theories on stochastic forcing of ENSO have been advanced [Penland and Sardeshmukh, 1995; Jin *et al.*, 1996; Penland, 1996; Kleeman and Moore, 1997]. The MJO has been considered a dominant constituent of such stochastic forcing [e.g., Moore and Kleeman, 1999a].

[79] There are many controversial aspects regarding possible effects of the MJO on ENSO [Zhang *et al.*, 2001]. For example, whether stochastic forcing is needed at all for the ENSO cycle and its prediction, whether the MJO plays any unique role in stochastic forcing, and whether ENSO prediction may benefit from a better understanding of the MJO are all topics of debate. The sources of the controversies are in many cases model configurations and assumptions on which different conclusions are based.

[80] To help navigate the discussion through many different opinions, one can consider the ENSO cycle to be governed by the following simple dynamic system, extended from the one used by Penland and Sardeshmukh [1995],

$$\frac{d\Psi(t)}{dt} = L\Psi + N(\Psi) + [G(\Psi) + A]f(t), \quad (1)$$

where  $t$  is time,  $\Psi(t)$  represents the state vector of the interannual component of the coupled system,  $L$  is a linear matrix and  $N(\Psi)$  is a nonlinear operator, both representing basin-scale coupled dynamics on the interannual timescale,  $f(t)$  represents atmospheric variability independent of  $L$  and  $N(\Psi)$ , which is referred to as noise or stochastic forcing,  $G(\Psi)$  represents the modulation of  $f(t)$  by  $\Psi(t)$ , and  $A$  is independent of  $\Psi(t)$ . If  $f(t)$  is completely independent of  $\Psi$ , namely,  $G(\Psi) = 0$  and  $A \neq 0$ , it is referred to as “additive”; while if  $f(t)$  is modulated by  $\Psi(t)$  (i.e.,  $G(\Psi) \neq 0$ ;  $A = 0$ ), it is “multiplicative” [Sancho *et al.*, 1982]. Possible effects of the MJO on ENSO are included in  $f(t)$ . Considering the observed interannual variability of the MJO under the influence of ENSO SST (section 2.9), the MJO is likely to be multiplicative stochastic forcing to ENSO to a certain degree ( $G(\Psi) \neq 0$ ;  $A \neq 0$ ).

[81] The coupled system in the equatorial Pacific could be in a dynamically stable (damped), neutral, or unstable regime [e.g., Neelin *et al.*, 1998], determined by  $L$  and  $N(\Psi)$ . In an unstable regime, the ENSO cycle is mainly driven by  $L$  and  $N(\Psi)$ . Central to the instability are, among others, the equatorial wave propagation [e.g., McCreary, 1983; Battisti, 1988; Suarez and Schopf, 1988] and energy buildup and release in the upper ocean [Wyrski, 1985; Jin,

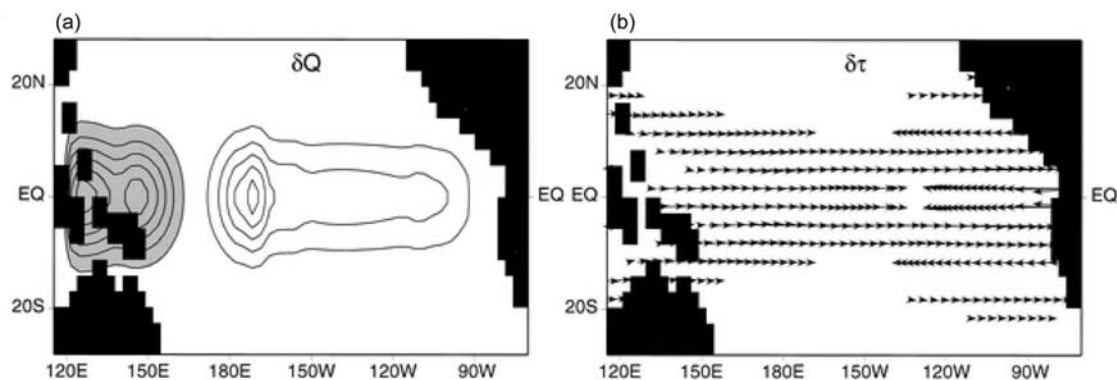


**Figure 19.** (a) Contours of surface heat flux and (b) surface wind stress vectors for the most disruptive stochastic optimal of a coupled model. From *Moore and Kleeman* [1999a].

1997]. Stochastic forcing in this regime may modulate the behavior of ENSO, such as its irregularity [e.g., *Blanke et al.*, 1997], but is not essential for its existence [e.g., *Zebiak*, 1989; *Chen et al.*, 2004]. When the coupled system is in a weakly unstable, neutral, or damped regime, the ENSO cycle is maintained only by stochastic forcing  $f(t)$  [e.g., *Chang et al.*, 1996; *Penland*, 1996]. As the strength of the instability varies on decadal timescales with factors such as the mean state of the coupled system, so does the effectiveness of stochastic forcing and ENSO predictability [Kurtman and Schopf, 1998]. However, it has been argued that variability in stochastic forcing itself can result in decadal changes in ENSO predictability [Flügel et al., 2004].

[82] The MJO-ENSO problem consists of the following questions: Does the MJO make any unique contribution irreplaceable by other types of stochastic forcing to the detailed evolution of ENSO warm events when the coupled system is in an unstable dynamic regime and to the sustenance of the ENSO cycle when the coupled system is in a neutral or stable regime? What are the mechanisms by which the MJO affects ENSO? Can ENSO prediction

benefit from an inclusion of the MJO in ENSO prediction models?

### 6.1. Uniqueness of the MJO

[83] When stochastic forcing  $f(t)$  is assumed to be completely random (white) in time and space [e.g., *Thompson and Battisti*, 2000], it includes all types of high-frequency weather variability, such as tropical cyclones, waves, and westerly wind bursts as well as the MJO. None of them should be more special than others. Some studies suggested that  $f(t)$  should be spatially coherent with a special structure in order to be the most efficient; such a structure is referred to as the stochastic optimal of the coupled system [e.g., *Kleeman and Moore*, 1997]. In one coupled model of intermediate complexity [Moore and Kleeman, 1999a, 1999b] the stochastic optimal is a planetary-scale dipole in the surface zonal stress and surface heat flux in the equatorial Pacific (Figure 19). Even for a model whose stochastic optimal maximizes away from the equator, stochastic forcing in zonal stress that matters the most to ENSO predictability concentrates along the equator in the western and central Pacific (Figure 20). In both cases the

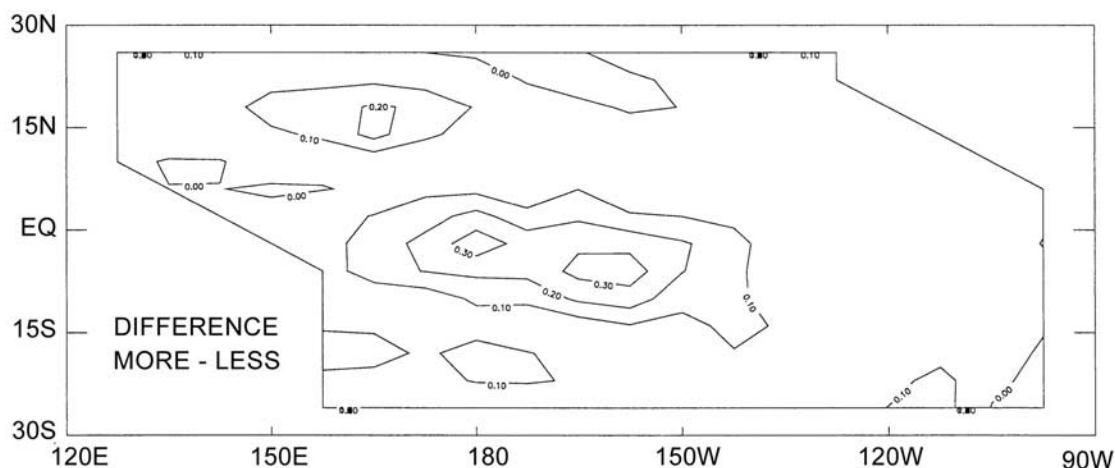


**Figure 20.** Difference between noise variance in zonal stress for periods of more and less predictable ENSO based on a prediction experiment by a coupled model of intermediate complexity in a linear stable dynamic regime. From *Flügel et al.* [2004].

MJO is the best candidate to explain the most effective patterns of stochastic forcing.

[84] In a coupled model that produces ENSO-like interannual fluctuations in equatorial SST only when  $f(t)$  is included, 71% of the variance induced by  $f(t)$  can be attributed to its leading modes representing only 28% of its total variance [Zavala-Garay *et al.*, 2003]. These leading modes, with the same spatial structures of the stochastic optimals, affect the ocean mainly by exciting equatorial Kelvin waves. The MJO component of  $f(t)$  alone can reproduce most of the ENSO-like variability; the interannual variability induced solely by the non-MJO component of  $f(t)$  is much weaker [Zavala-Garay *et al.*, 2005]. In observations the interannual variability of Kelvin wave forcing by the MJO component of wind stress is much greater than by non-MJO wind stress [Zhang and Gottschalek, 2002]. The relative importance of the MJO compared to other types of stochastic forcing of ENSO, such as westerly wind bursts independent of the MJO [Vecchi and Harrison, 2000], is a subject under debate and needs to be further scrutinized quantitatively.

## 6.2. Mechanisms for the MJO Effect

[85] The MJO may affect an ENSO warm event by helping reduce the zonal gradient of SST. Three processes can be involved (section 5). Mean SST in the western Pacific can be reduced by net cooling due to the MJO [e.g., Kessler and Kleeman, 2000; Shinoda and Hendon, 2002]. Zonal current forced by the MJO westerly wind advects eastward the eastern edge of the western Pacific warm pool [Kessler *et al.*, 1995; Picaut *et al.*, 1996]. Oceanic Kelvin waves forced by the MJO propagate into the eastern Pacific, where they suppress the thermocline, reduce cooling due to the upwelling, and induce warm anomalies at the surface [Zhang, 2001].

[86] From a linear point of view, the MJO contributes significantly to sustain the ENSO variability only if its low-frequency energy is strong [Syu and Neelin, 2000; Zavala-Garay *et al.*, 2003]. Intraseasonal SST anomalies associated with individual Kelvin waves ( $\leq 0.3^\circ\text{C}$ ) are on average an order magnitude smaller than the typical SST anomalies associated with ENSO warm events [Johnson and McPhaden, 1993a]. The low-frequency energy of the MJO in  $f(t)$ , mainly from its interannual fluctuations (section 2.9), must be amplified by air-sea coupling ( $L$  and  $N(\Psi)$ ) to sustain the ENSO variability [Zavala-Garay *et al.*, 2005].

[87] Nonlinear processes can transfer energy from intra-seasonal to interannual timescales. Several nonlinear mechanisms of rectification have been proposed. One is the *Ekman effect*, which makes the equatorial oceanic current responses stronger to westerly wind forcing than to easterly wind forcing [Kessler and Kleeman, 2000]. Another is surface wind speed, whose mean can be enhanced by about  $1 \text{ m s}^{-1}$  over a cycle of the MJO and therefore can promote a net increase in surface heat flux to cool the warm pool [Kessler and Kleeman, 2000; Shinoda and Hendon, 2002]. The nonlinearity can also come from the fact that the MJO is more a pulse-like phenomenon, whose westerly wind is

much stronger than its easterly wind (hence westerly wind bursts not easterly wind bursts) [Yano *et al.*, 2004], as are its forced downwelling ocean Kelvin waves [e.g., Lukas *et al.*, 1984].

[88] A positive feedback mechanism between the MJO and ENSO has been suggested [Kessler *et al.*, 1995; Bergman *et al.*, 2001]: Thermal advection by the MJO-forced oceanic Kelvin waves results in an eastward expansion of the western Pacific warm pool, which allows the MJO to propagate farther into the central Pacific. A longer zonal fetch of wind forcing would generate a stronger Kelvin wave. This progressive eastward penetration of the MJO is commonly observed during the onset and development stages of ENSO warm events [e.g., Anyamba and Weare, 1995; Hendon *et al.*, 1999]. This possible feedback between the MJO and ENSO SST is manifested by the observed correlation between the local MJO in the Pacific and ENSO SST indices [Kessler, 2001], in contrast to the interannual variability of the global MJO that is independent of ENSO SST [Slingo *et al.*, 1999; Hendon *et al.*, 1999]. Observed correlation between ENSO and MJO forcing of the Kelvin waves in the equatorial Pacific (Figure 21) also suggests a possible role of the MJO in enhancing ENSO warming at its very early stage.

[89] If forcing the oceanic Kelvin wave is central to the MJO influence on ENSO, then only in the *equatorial waveguide* can the strength in zonal stress of the MJO determine the efficiency of this influence. This may explain why not all MJO events, even some strong ones, necessarily lead to a warm event of ENSO [Bergman *et al.*, 2001]. Other possible explanations are the following: The susceptibility of ENSO to the influences of the MJO depends on the mean state of the coupled system and on the timing of the MJO relative to the phase of ENSO [Fedorov, 2000]. ENSO is perhaps influenced more effectively by the seasonal activity of the MJO than by any individual MJO event [Zhang and Gottschalek, 2002], as implied by the importance of the seasonal cycle of stochastic forcing [Penland and Sardeshmukh, 1995; Penland, 1996].

## 6.3. Implications for ENSO Prediction

[90] Numerical studies have demonstrated the effect of the MJO on individual ENSO warm events by prescribing through model integrations wind anomalies associated with the MJO, equivalent to  $f(t)$  with  $G(\Psi) = 0$  in equation (1). Thermal advection by intraseasonal downwelling Kelvin waves forced in the western Pacific could have contributed substantially to simulated positive SST anomalies during the 1982 El Niño event [Harrison and Schopf, 1984]. Oceanic responses to a westerly wind event lasting for a month in the western Pacific have led to SST anomalies persisting for 12 months in a coupled model [Latif *et al.*, 1988]. Many simulations have particularly demonstrated the roles of westerly wind events associated with the MJO in the onset and growth of the 1997–1998 El Niño [Kessler and Kleeman, 2000; Perigaud and Cassou, 2000; Lengaigne *et al.*, 2003; Boulanger *et al.*, 2004]. These results suggest

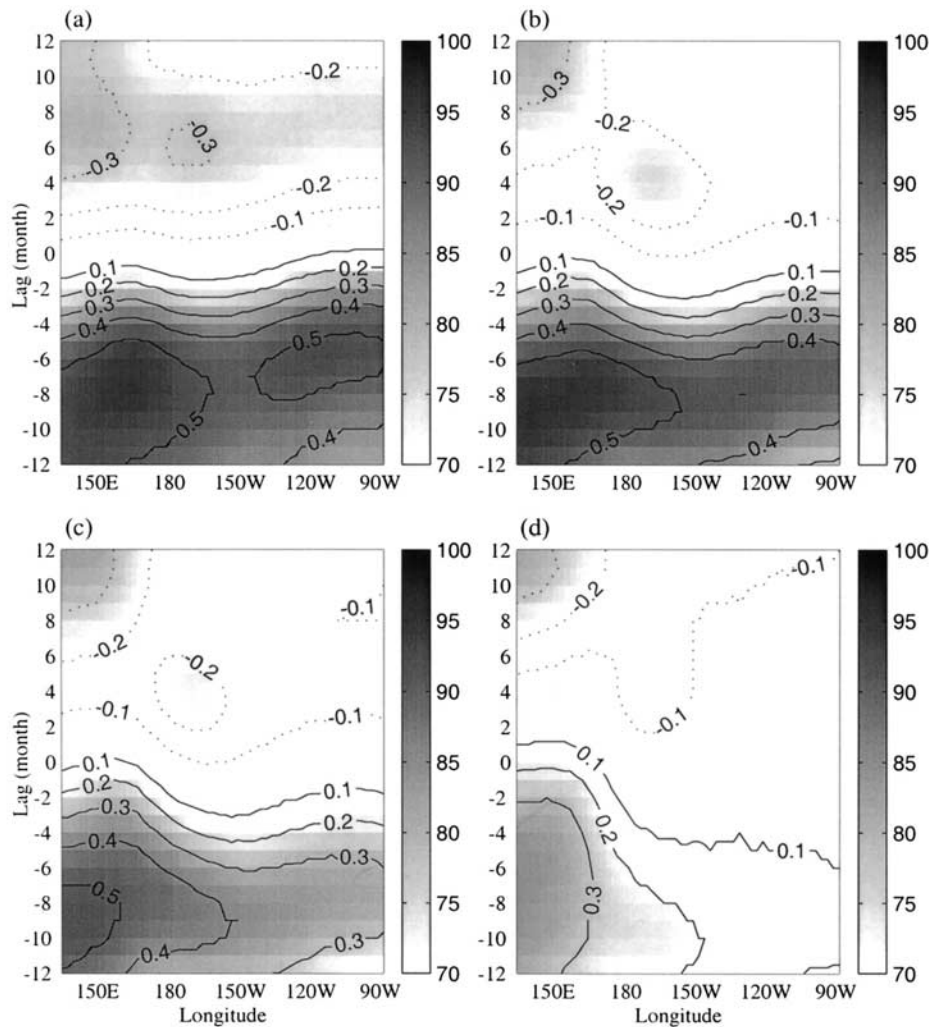


**Figure 21.** Coefficients (contours) and confidence levels (shading) of lag correlation between interannual anomalies in seasonal variance of Kelvin-wave forcing by the MJO in the Pacific as a function of longitude and interannual anomalies in SST in regions of (a) Niño1+2 ( $80^{\circ}$ – $90^{\circ}$ W and  $0^{\circ}$ – $10^{\circ}$ S), (b) Niño3 ( $90^{\circ}$ – $150^{\circ}$ W and  $5^{\circ}$ N– $5^{\circ}$ S), (c) Niño3.4 ( $120^{\circ}$ – $170^{\circ}$ W and  $5^{\circ}$ N– $5^{\circ}$ S), and (d) Niño4 ( $150^{\circ}$ W– $160^{\circ}$ E and  $5^{\circ}$ N– $5^{\circ}$ S) for the time period from 1980 through 1999. Dashed contours are for negative correlation coefficients. Negative lags indicate positive anomalies in MJO forcing of the Kelvin waves leading positive anomalies in SST. Maximum correlation is located at  $167.5^{\circ}$ E and lag  $-8$  in Figure 21a,  $152.5^{\circ}$ E and lag  $-9$  in Figure 21b,  $137.5^{\circ}$ E and lag  $-10$  in Figure 21c, and  $140^{\circ}$ E and lag  $-7$  in Figure 21d. From Zhang and Gottschalck [2002].

that the timing and amplitude of an ENSO warm event might be better predicted should MJO activities be known.

[91] With its current prediction skill limited to 15–20 days (section 4.3), the MJO is unpredictable on interannual timescales [Slingo *et al.*, 1999; Waliser *et al.*, 2001]. This implies that any significant effect from the MJO on ENSO might, as other types of stochastic forcing, limit the ENSO predictability. Better knowledge of the characteristics of the MJO (e.g., its structure, geographic preference, and seasonal cycle) might help determine more realistic spread of the uncertainties in probabilistic predictions of ENSO subject to stochastic forcing [Fedorov *et al.*, 2003]. If stochastic forcing of the MJO is indeed multiplicative, then it is conceivable that an ENSO prediction model with a capability of producing realistic MJO statistics and its relationship with ENSO SST would do better than a comparable

model but without any MJO signals. The observed lag correlation between anomalies in seasonal MJO activities in the western Pacific and in ENSO SST (Figure 21) and some ENSO simulations with prescribed wind events (discussed earlier in this section) both suggest that to benefit 6- to 12-month ENSO prediction by models able to produce MJO signals, it is perhaps more important for the models to maintain a realistic level of seasonal activities of the MJO at the initial time than to forecast the MJO 6–12 months into the future. ENSO prediction assisted by including MJO activities remains an uncharted territory.

## 7. CONCLUDING REMARKS

[92] The study of the MJO has undergone expeditious progress during the past decade. Observationally, the most

noticeable advancements have been made in its multiscale structure, large-scale vertical structure, and air-sea interaction. Observations of the MJO, however, still face several challenges. The traditional way of describing the MJO as sinusoidal perturbations with equal amplitudes in its active and inactive phases is inadequate. The properties of the MJO should be better described with each MJO episode treated as a discrete, pulse-like event [Salby and Hendon, 1994; Yano *et al.*, 2004]. The vertical structure of the MJO as we currently know is largely based on global model reanalysis products (section 2.5). New satellite data (e.g., data from the Atmospheric Infrared Sounders aboard the Earth Observation System (EOS) satellites Terra and Aqua) resolving high-resolution vertical profiles of water vapor and temperature provide unprecedented opportunities to validate the results from the global model reanalyses. Multiyear ground-based remote sensing products of cloud properties in the equatorial western Pacific provided by the Atmospheric Radiation Measurement Program [Mather *et al.*, 1998] open a new door to documenting the evolution of clouds, especially their vertical structure and diabatic heating rate of condensation/evaporation and radiation, through the life cycle of the MJO. Large uncertainties in the current estimates of the energy balance of the ocean mixed layer need to be reduced by better quantifying entrainment cooling and thermal advection.

[93] Theoretical study of the MJO has lately enjoyed a boost in one sense and suffered a stall in another. Many new ideas and hypotheses have been proposed to explain the MJO (section 3.3). Most of them, however, do not quantitatively predict the selection of the observed time and space scales and phase speed, let alone the structure, of the MJO. It is intriguing that the MJO can be produced by theoretical and idealized models tuned to represent specific but simplified mechanisms but not by many GCMs with more sophisticated treatment of physical processes. It is not obvious what is in the idealized models but missing in the GCMs that would make the MJO present in the former and absent in the latter. A successful theory of the MJO should not be judged solely by whether it produces an MJO. It must be able to quantitatively explain the difficulty of simulating the MJO by GCMs as well as the selection of the scales and phase speed of the MJO.

[94] Numerical simulations of the MJO by GCMs have evolved with slow but steady progress. The spread of models' capability of simulating the MJO is becoming wider, with commendable improvement made in some models (section 4.1), while others remaining completely inept. Our standard of evaluating MJO simulations should be constantly raised with improved observations. The risk is too high when GCMs giving unrealistic simulations of the MJO are used to study its dynamics. A GCM with known incapability of simulating the MJO is one with inexplicable deficiencies. Such a model can hardly produce reliable results on any phenomenon sensitively depending on model parameterizations. Simulations of the MJO are therefore measures of model fidelity in the tropics. We do not know well the reason for the sensitivity of MJO simulations to

model configurations (section 4.2). We do not have any evidence showing that models with less dependence on cumulus parameterizations (e.g., mesoscale and cloud-resolving models) than GCMs can produce more realistic MJOs. These are not merely modeling problems. They are also issues of theoretical understanding. Failing to explain the modeling difficulties by existing MJO theories exposes a gaping hole in our knowledge. Improving numerical simulations in concert with advancing theories should be the highest priority of the study of the MJO.

[95] Many topics in the study of the MJO have been transfigured during the past decade. Its scale interactions, air-sea interaction, prediction, interaction with ENSO, modulation of tropical cyclones, interaction with the monsoons, and influences on higher-latitude weather have received probably the most rapidly increasing research attention. Only the first four are reviewed here. The MJO is interesting and important not only because of its special position in the tropical general circulation but also because of its broad impact on various aspects of weather and climate. The greatest significance of the MJO is perhaps its challenge to our understanding of the fundamental dynamics and physics of the tropical atmosphere. In this sense the MJO should be one of the central research themes in the study of tropical weather, circulation, and climate.

## GLOSSARY

**Baroclinic:** Variation with depth of motions associated with variation of density with depth. In this review this term describes vertical structures in which winds or currents reverse directions.

**Barotropic:** Part of the velocity field that is uniform with depth. This term is used in this review to describe vertical structures in which winds or currents maintain in the same direction.

**Barrier layer:** Layer between the base of the oceanic mixed layer and the top of thermocline, in which there is a strong vertical gradient in salinity (increasing with the depth) but a relative constant temperature profile. The salinity gradient tends to prevent turbulence mixing from penetrating downward through the barrier layer.

**CISK:** Conditional instability of the second kind, a concept in which low-level convergence in the wind field produces convection and cumulus formation, thereby releasing latent heat. Wave-CISK emphasizes the role of atmospheric waves in generating low-level convergence.

**Closure:** A critical step in cumulus parameterization where assumptions are made to link resolvable variables (wind, temperature, and humidity) to unresolvable variables (e.g., precipitation).

**Cloud-resolving model:** Numerical model with spatial resolutions sufficiently high ( $<1$  km) to explicitly resolve the gross structure of cloud. Cloud microphysics is still parameterized.

**Critical latitude:** Latitude at which the relative horizontal phase speed of a zonally propagating wave equals the mean zonal wind speed. As a wave approaches its

critical latitude, its energy is absorbed and transferred to the mean wind.

**Cumulus parameterization:** An approach to estimate the effects of convective processes, such as diabatic heating and precipitation, that cannot be resolved directly by coarse resolutions of a numerical model.

**Detrainment:** Turbulent transfer of air from cloud to the surrounding atmosphere.

**Diabatic heating:** Heating due to latent heat release or radiation.

**Downwelling:** Downward motion of water.

**Easterly:** Wind from the east.

**Ekman effect:** Effect of viscosity or friction that makes wind or current veer toward low pressure as a result of its balance with the Coriolis and pressure gradient forces. Surface westerly winds of the Kelvin and Rossby waves are associated with high pressure at the equator and therefore tend to deviate away from the equator because of friction, resulting in Ekman divergence.

**Entrainment:** Turbulent transfer of air from the surrounding atmosphere into cloud or turbulent transfer of water into the ocean mixed layer across its base from below.

**Equatorial cold tongue:** A narrow strip of cold surface water along the equator extending from the eastern coast westward into the central Pacific (and Atlantic).

**Equatorial undercurrent:** A subsurface eastward current ( $1.5 \text{ m s}^{-1}$ ) along the equator at a depth of 200 m in the west and 40 m in the east in the Pacific.

**Equatorial waveguide:** An equatorial zone ( $5^{\circ}\text{S}$ – $5^{\circ}\text{N}$ ) in which equatorial waves exist.

**Equatorial waves:** Family of waves, in both the atmosphere and ocean, propagating zonally along the equator with their amplitude decaying exponentially with latitude. Also known as equatorially trapped waves. They include Kelvin waves (propagating eastward), Rossby waves (propagating westward), mixed Rossby-gravity waves (propagating either eastward or westward), and gravity waves (propagating both eastward and westward).

**Frictional convergence:** Wind convergence due to the Ekman effect on easterlies in the boundary layer.

**GPCP:** Global Precipitation Climate Project.

**Inertiogravity waves:** A wave disturbance caused by changes in buoyancy (or density) under the effect of Earth's rotation (the Coriolis force).

**Inversion:** Departure from a normal vertical profile of temperature. In the atmosphere an inversion is a temperature increase with height. In the ocean it is a temperature increase with depth.

**Kelvin waves:** Members of the equatorial waves, characterized by an eastward propagation and a zero component in meridional wind or current. In the atmosphere their low-level easterly (westerly) component is located in the region of low (high) surface pressure. There are several types of Kelvin waves. "Free" Kelvin waves are detached from their energy sources. Forced Kelvin waves constantly draw energy from their sources (e.g., independent convective heating for the atmospheric Kelvin waves and wind stress for the oceanic Kelvin waves). Convectively coupled

Kelvin waves draw energy from their interaction with atmospheric deep convection. A Kelvin wave component of the MJO refers to the zonal wind component east of its convective center. The gravest baroclinic Kelvin wave in the ocean changes the direction of its current only once in the vertical and has a greatest phase speed.

**Large scale:** Spatial scale of  $10^3$  –  $10^4$  km in the zonal direction.

**Melting level:** An altitude ( $\sim 5.5$  km in the tropical atmosphere) at which temperature is  $0^{\circ}\text{C}$ .

**Mesoscale:** Spatial scale of  $10^0$ – $10^2$  km.

**Mixed layer:** Layer within which atmospheric or oceanic properties are roughly uniform in vertical because of turbulence mixing, typically the lowest 1 km in the atmosphere and the upper 100 m (often shallower) in the ocean.

**Mixed Rossby-gravity waves:** Members of the equatorial waves that resemble gravity waves when propagating eastward but resemble Rossby waves when propagating westward.

**Moist convective adjustment:** Method of cumulus parameterization, which estimates the convective effects based on departures of actual temperature and humidity from their reference profiles.

**Moist stability:** Measure of the tendency for a moist air parcel to return to its original position after being displaced vertically.

**NCEP/NCAR reanalysis:** Product of assimilating together observations using a numerical model by the National Centers for Environmental Prediction (NCEP) and National Center for Atmospheric Research (NCAR).

**Optimal:** Spatial structure in stochastic forcing or initial perturbations for responses to have possibly the fastest growth.

**Planetary scale:** Spatial scale greater than  $10^4$  km in the zonal direction.

**Rossby waves:** Members of the equatorial waves, characterized by a westward propagation with zonal wind (current) dominant near the equator and gyral circulations on both sides of the equator. A different type of Rossby wave exists in the extratropics.

**Stratiform precipitation:** Precipitation (ice crystals, snow, hail, graupel, etc.) fall out of anvil clouds that extend horizontally from the top of deep convective clouds near the tropopause.

**Synoptic scale:** Spatial scale of  $10^2$ – $10^3$  km or a temporal scale of 2–10 days.

**Thermocline:** Layer of strong vertical temperature gradient separating the relative warm upper ocean from the cold abyss.

**Upwelling:** Upward motion of water.

**Westerly:** Wind from the west.

[96] **ACKNOWLEDGMENTS.** The author thanks Harry Hendon, George Kiladis, Sharan Majumdar, Eric Maloney, Mike McPhadden, Todd Mitchell, David Nolan, Jun-Ichi Yano, Javier Zavala-Garay, and anonymous reviewers for their careful and constructive comments on this article. This study was supported

by NSF grant ATM99122297 and by NOAA's Office of Global Programs through awards under cooperative agreement NA67RJO149 to CIMAS.

[97] The Editor responsible for this paper was Kendal McGuffie. He thanks two anonymous technical reviewers and one anonymous cross-disciplinary reviewer.

## REFERENCES

- Anderson, J. R., and D. E. Stevens (1987), The response of the tropical atmosphere to low frequency thermal forcing, *J. Atmos. Sci.*, **44**, 676–686.
- Anderson, S. P., R. A. Weller, and R. B. Lukas (1996), Surface buoyancy forcing and the mixed layer of the western Pacific warm pool: Observations and 1-D model results, *J. Clim.*, **9**, 3056–3085.
- Anyamba, E. K., and B. C. Weare (1995), Temporal variability of the 40–50-day oscillation in tropical convection, *Int. J. Climatol.*, **15**, 379–402.
- Anyamba, E., E. Williams, J. Susskind, A. Fraser-Smith, and M. Fullekrug (2000), The manifestation of the Madden-Julian Oscillation in global deep convection and in the Schumann resonance intensity, *J. Atmos. Sci.*, **57**, 1029–1044.
- Barnston, A. G., M. H. Glantz, and Y. He (1999), Predictive skill of statistical and dynamical climate models in SST forecast during the 1997–98 El Niño episode and the 1998 La Niña onset, *Bull. Am. Meteorol. Soc.*, **80**, 217–243.
- Battisti, D. S. (1988), The dynamics and thermodynamics of a warm event in the coupled atmosphere/ocean model, *J. Atmos. Sci.*, **45**, 2889–2919.
- Benestad, R. E., R. T. Sutton, and D. L. T. Anderson (2002), The effect of El Niño on intraseasonal Kelvin waves, *Q. J. R. Meteorol. Soc.*, **128**, 1277–1291.
- Bergman, J. W., and H. H. Hendon (2000), Cloud radiative forcing of the low latitude tropospheric circulation: Linear calculations, *J. Atmos. Sci.*, **57**, 2225–2245.
- Bergman, J. W., H. H. Hendon, and K. M. Weickmann (2001), Intraseasonal air-sea interactions at the onset of El Niño, *J. Clim.*, **14**, 1702–1719.
- Blade, I., and D. L. Hartmann (1993), Tropical intraseasonal oscillation in a simple nonlinear model, *J. Atmos. Sci.*, **50**, 2922–2939.
- Blanke, B., J. D. Neelin, and D. Gutzler (1997), Estimating the effect of stochastic wind stress forcing on ENSO irregularity, *J. Clim.*, **10**, 1473–1486.
- Bond, N. A., and G. A. Vecchi (2003), The influence of the Madden-Julian Oscillation on precipitation in Oregon and Washington, *Weather Forecasting*, **18**, 600–613.
- Boulanger, J.-P., and C. Menkes (1995), Propagation and reflection of long equatorial waves in the Pacific Ocean during the 1992–1993 El Niño, *J. Geophys. Res.*, **100**, 25,041–25,059.
- Boulanger, J.-P., C. Menkes, and M. Lengaigne (2004), Role of high- and low-frequency winds and wave reflection in the onset, growth and termination of the 1997–1998 El Niño, *Clim. Dyn.*, **22**, 267–280, doi:10.1007/s00382-0003-0383-8.
- Brown, R. G., and C. Zhang (1997), Variability of midtropospheric humidity and its effect on cloud-top height distribution during TOGA COARE, *J. Atmos. Sci.*, **54**, 2760–2774.
- Cane, M. A., and E. Sarachik (1981), The response of linear baroclinic equatorial ocean to periodic forcing, *J. Mar. Res.*, **39**, 651–693.
- Chang, C. P. (1977), Viscous internal gravity waves and low-frequency oscillations in the tropics, *J. Atmos. Sci.*, **34**, 901–910.
- Chang, C. P., and H. Lim (1988), Kelvin wave-CISK: A possible mechanism for the 30–50 day oscillations, *J. Atmos. Sci.*, **45**, 1709–1720.
- Chang, P., L. Ji, H. Li, and M. Flugel (1996), Chaotic dynamics versus stochastic processes in El Niño–Southern Oscillation in coupled ocean-atmosphere models, *Physica D*, **98**, 301–320.
- Chao, W. C. (1987), On the origin of the tropical intraseasonal oscillation, *J. Atmos. Sci.*, **44**, 1940–1949.
- Chao, W. C., and S.-J. Lin (1994), Tropical intraseasonal oscillations, super cloud clusters, and cumulus convective schemes, *J. Atmos. Sci.*, **51**, 1282–1297.
- Charney, J. G., and A. Eliassen (1964), On the growth of the hurricane depression, *J. Atmos. Sci.*, **21**, 68–75.
- Chen, D., M. A. Cane, A. Kaplan, S. E. Zebiak, and D. Huang (2004), Predictability of El Niño over the past 148 years, *Nature*, **428**, 733–735.
- Chen, S. S., and R. A. Houze Jr. (1997), Diurnal variation of deep convective systems over the tropical Pacific warm pool, *Q. J. R. Meteorol. Soc.*, **123**, 357–388.
- Chen, S. S., B. E. Mapes, and R. A. Houze Jr. (1996), Multiscale variability of deep convection in relation to large-scale circulation in TOGA COARE, *J. Atmos. Sci.*, **53**, 1380–1409.
- Chen, T. C., and J. M. Chen (1997), On the relationship between the streamfunction and velocity potential of the Madden-Julian Oscillation, *J. Atmos. Sci.*, **54**, 679–685.
- Chen, T. C., and M. C. Yen (1991), A study of the diabatic heating associated with the Madden-Julian Oscillation, *J. Geophys. Res.*, **96**, 13,163–13,177.
- Clayton, C. A., B. Strahl, and J. Schrage (2002), 2–3-day convective variability in the tropical western Pacific, *Mon. Weather Rev.*, **130**, 529–548.
- Colon, E., J. Lindesay, and M. J. Suarez (2002), The impact of surface flux- and circulation-driven feedbacks on simulated Madden-Julian Oscillations, *J. Clim.*, **15**, 624–641.
- Compo, G. P., G. N. Kiladis, and P. J. Webster (1999), The horizontal and vertical structure of east Asian winter monsoon pressure surges, *Q. J. R. Meteorol. Soc.*, **125**, 29–54.
- Cravatte, S., J. Picaut, and G. Eldin (2003), Second and first baroclinic Kelvin modes in the equatorial Pacific at intraseasonal timescales, *J. Geophys. Res.*, **108**(C8), 3266, doi:10.1029/2002JC001511.
- Cronin, M. F., and M. J. McPhaden (1997), The upper ocean heat balance in the western equatorial Pacific warm pool during September–December 1992, *J. Geophys. Res.*, **102**, 8533–8553.
- Cronin, M. F., and M. J. McPhaden (1998), Upper ocean salinity balance in the western equatorial Pacific, *J. Geophys. Res.*, **103**, 27,567–27,587.
- Cronin, M. F., and M. J. McPhaden (2002), Barrier layer formation during westerly wind bursts, *J. Geophys. Res.*, **107**(C12), 8020, doi:10.1029/2001JC001171.
- Crum, F. X., and T. J. Dunkerton (1992), Analytic and numerical models of wave-CISK with conditional heating, *J. Atmos. Sci.*, **49**, 1693–1708.
- Davey, M. K. (1989), A simple tropical moist model applied to the ‘40-day’ wave, *Q. J. R. Meteorol. Soc.*, **115**, 1071–1107.
- Delcroix, T., J. Picaut, and G. Eldin (1991), Equatorial Kelvin and Rossby waves evidenced in the Pacific Ocean through Geosat sea level and surface current anomalies, *J. Geophys. Res.*, **96**, 3249–3262.
- Duffe, P. B., B. Govindasamy, J. P. Iorio, J. Milovich, K. R. Sperber, K. E. Taylor, M. F. Wehner, and S. L. Thompson (2003), High-resolution simulation of global climate, part 1: Present climate, *Clim. Dyn.*, **21**, 371–390.
- Dunkerton, T. J., and F. X. Crum (1995), Eastward propagating ~2- to 15-day equatorial convection and its relation to the tropical intraseasonal oscillation, *J. Geophys. Res.*, **100**, 25,781–25,790.
- European Centre for Medium-Range Weather Forecasts (2004), *Proceedings of a ECMWF/CLIVAR Workshop on Simulation and Prediction of Intra-Seasonal Variability With Emphasis on the MJO*, 3–6 November 2003, 269 pp., Eur. Cent. for Medium-Range Weather Forecasts, Reading, UK.
- Emanuel, K. A. (1987), An air-sea interaction model of intraseasonal oscillations in the tropics, *J. Atmos. Sci.*, **44**, 2324–2340.
- Emanuel, K. A., J. D. Neelin, and C. S. Bretherton (1994), On large-scale circulations in convecting atmospheres, *Q. J. R. Meteorol. Soc.*, **120**, 1111–1143.

- Enfield, D. B. (1987), The intraseasonal oscillation in eastern Pacific sea levels: How is it forced?, *J. Phys. Oceanogr.*, *17*, 1860–1876.
- Esbensen, S. (1978), Bulk thermodynamic effects and properties of small tropical cumuli, *J. Atmos. Sci.*, *35*, 826–831.
- Fasullo, J., and P. J. Webster (2000), Atmospheric and surface variations during westerly wind bursts in the tropical western Pacific, *Q. J. R. Meteorol. Soc.*, *126*, 899–924.
- Fedorov, A. V. (2000), The response of the coupled tropical ocean-atmosphere to westerly wind bursts, *Q. J. R. Meteorol. Soc.*, *128*, 1–23.
- Fedorov, A. V., S. L. Harper, S. G. Philander, B. Winter, and A. Wittenberg (2003), How predictable is El Niño?, *Bull. Am. Meteorol. Soc.*, *84*, 911–919.
- Feng, M., R. Lukas, P. Hacker, R. A. Weller, and S. P. Anderson (2000), Upper-ocean heat and salt balances in the western equatorial Pacific in response to the intraseasonal oscillation during TOGA COARE, *J. Clim.*, *13*, 2409–2427.
- Ferranti, L., T. N. Palmer, F. Molteni, and E. Klinker (1990), Tropical-extratropical interaction associated with the 30–60 day oscillation and its impact on medium and extended range prediction, *J. Atmos. Sci.*, *47*, 2177–2199.
- Fink, A., and P. Speth (1997), Some potential forcing mechanisms of the year-to-year variability of the tropical convection and its intraseasonal ( $25 \pm 70$ -day) variability, *Int. J. Climatol.*, *17*, 1513–1534.
- Finney, B. (1994), *Voyage of Rediscovery*, 401 pp., Univ. of Calif. Press, Berkeley.
- Flatau, M., P. J. Flatau, P. Phoebus, and P. P. Niiler (1997), The feedback between equatorial convection and local radiative and evaporative processes: The implications for intraseasonal oscillations, *J. Atmos. Sci.*, *54*, 2373–2386.
- Flügel, M., P. Chang, and C. Penland (2004), The role of stochastic forcing in modulating ENSO predictability, *J. Clim.*, *15*, 3125–3140.
- Foltz, G. R., and M. J. McPhaden (2004), The 30–70 day oscillations in the tropical Atlantic, *Geophys. Res. Lett.*, *31*, L15205, doi:10.1029/2004GL020023.
- Frederiksen, J. S., and C. S. Frederiksen (1997), Mechanisms of the formation of intraseasonal oscillations and Australian monsoon disturbances: The roles of latent heat, barotropic and baroclinic instability, *Contrib. Atmos. Phys.*, *70*, 39–56.
- Giese, G. S., and D. E. Harrison (1990), Aspects of the Kelvin wave response to episodic wind forcing, *J. Geophys. Res.*, *95*, 7289–7312.
- Ghil, M., and K. Mo (1991), Intraseasonal oscillations in the global atmosphere. part I: Northern Hemisphere and tropics, *J. Atmos. Sci.*, *48*, 752–779.
- Godfrey, J. S., and E. J. Lindstrom (1989), The heat budget of the equatorial western Pacific surface mixed layer, *J. Geophys. Res.*, *94*, 8007–8017.
- Goswami, P., and R. K. Rao (1994), A dynamical mechanism for selective excitation of the Kelvin mode at timescale of 30–50 days, *J. Atmos. Sci.*, *51*, 2769–2779.
- Grabowski, W. W. (2001), Coupling cloud processes with the large-scale dynamics using the cloud-resolving convective parameterization (CRCP), *J. Atmos. Sci.*, *58*, 978–997.
- Grabowski, W. W. (2003), MJO-like coherent structures: Sensitivity simulations using the cloud-resolving convection parameterization (CRCP), *J. Atmos. Sci.*, *60*, 847–864.
- Grabowski, W. W., and M. W. Moncrieff (2001), Large-scale organization of tropical convection in two-dimensional explicit numerical simulations, *Q. J. R. Meteorol. Soc.*, *127*, 445–468.
- Grabowski, W. W., and M. W. Moncrieff (2005), Moisture-convective feedback in the tropics, *Q. J. R. Meteorol. Soc.*, *130*, 3081–3104.
- Gualdi, S., A. Navarra, and H. von Storch (1997), Tropical intraseasonal oscillation appearing in operational analyses and in a family of general circulation models, *J. Atmos. Sci.*, *54*, 1185–1202.
- Gualdi, S., A. Navarra, and G. Tinarelli (1999), The interannual variability of the Madden-Julian Oscillation in an ensemble of GCM simulations, *Clim. Dyn.*, *15*, 643–658.
- Gustafson, W. I., and B. C. Weare (2004a), MM5 modeling of the Madden-Julian Oscillation in the Indian and west Pacific oceans: Model description and control run results, *J. Clim.*, *17*, 1320–1337.
- Gustafson, W. I., and B. C. Weare (2004b), MM5 modeling of the Madden-Julian Oscillation in the Indian and west Pacific oceans: Implications of 30–70 day boundary effects on MJO development, *J. Clim.*, *17*, 1338–1351.
- Gutzler, D. S. (1991), Interannual fluctuations of intraseasonal variance of near-equatorial zonal winds, *J. Geophys. Res.*, *96*, 3173–3185.
- Gutzler, D. S., and R. A. Madden (1989), Seasonal variations in the spatial structure of intraseasonal tropical wind fluctuations, *J. Atmos. Sci.*, *46*, 641–660.
- Gutzler, D. S., and R. M. Ponte (1990), Exchange of momentum among atmosphere, ocean, and solid earth associated with the Madden-Julian Oscillation, *J. Geophys. Res.*, *95*, 18,679–18,686.
- Haertel, P. T., and G. N. Kiladis (2004), Dynamics of 2-day equatorial waves, *J. Atmos. Sci.*, *61*, 2707–2721.
- Hall, J. D., A. J. Matthews, and D. J. Karoly (2001), The modulation of tropical cyclone activity in the Australian region by the Madden-Julian Oscillation, *Mon. Weather Rev.*, *129*, 2970–2982.
- Harrison, D. E., and P. S. Schopf (1984), Kelvin-wave-induced anomalous advection and the onset of surface warming in El Niño events, *Mon. Weather Rev.*, *112*, 923–933.
- Harrison, D. E., and G. A. Vecchi (1997), Westerly wind events in the tropical Pacific 1986–1995, *J. Clim.*, *10*, 3131–3156.
- Hartmann, D. L., H. H. Hendon, and R. A. Houze Jr. (1984), Some implications of the mesoscale circulations in tropical cloud clusters for large-scale dynamics and climate, *J. Atmos. Sci.*, *41*, 113–121.
- Hartten, L. M. (1996), Synoptic settings of westerly wind bursts, *J. Geophys. Res.*, *101*, 16,997–17,019.
- Hayashi, Y. (1979), A generalized method of resolving transient disturbances into standing and traveling waves by space-time spectral analysis, *J. Atmos. Sci.*, *36*, 1017–1029.
- Hayashi, Y., and A. Sumi (1986), The 30–40 day oscillations simulated in an “Aqua-planet” model, *J. Meteorol. Soc. Jpn.*, *64*, 451–467.
- Hayashi, Y., and D. G. Golder (1986), Tropical intraseasonal oscillation appearing in the GFDL general circulation model and FGGE data. Part I: Phase propagation, *J. Atmos. Sci.*, *43*, 3058–3067.
- Hayashi, Y., and D. G. Golder (1997), United mechanisms for the generation of low- and high-frequency tropical waves. Part I: Control experiments with moist convective adjustment, *J. Atmos. Sci.*, *54*, 1262–1276.
- Hendon, H. H. (1988), A simple model of the 40–50 day oscillation, *J. Atmos. Sci.*, *45*, 569–584.
- Hendon, H. H. (2000), Impact of air-sea coupling on the Madden-Julian Oscillation in a general circulation model, *J. Atmos. Sci.*, *57*, 3939–3952.
- Hendon, H. H. (2005), Air-sea interaction, in *Intraseasonal Variability in the Atmosphere-Ocean Climate System*, edited by W. K. M. Lau and D. E. Waliser, pp. 221–246, Praxis, Chichester, U.K.
- Hendon, H. H., and J. Glick (1997), Intraseasonal air-sea interaction in the tropical Indian and Pacific oceans, *J. Clim.*, *10*, 647–661.
- Hendon, H. H., and B. Liebmann (1990), The intraseasonal (30–50 day) oscillation of the Australian summer monsoon, *J. Atmos. Sci.*, *47*, 2909–2923.
- Hendon, H. H., and B. Liebmann (1994), Organization of convection within the Madden-Julian Oscillation, *J. Geophys. Res.*, *99*, 8073–8083.
- Hendon, H. H., and M. L. Salby (1994), The life cycle of the Madden-Julian Oscillation, *J. Atmos. Sci.*, *51*, 2225–2237.

- Hendon, H. H., B. Liebmann, and J. Glick (1998), Oceanic Kelvin waves and the Madden-Julian Oscillation, *J. Atmos. Sci.*, **55**, 88–101.
- Hendon, H. H., C. Zhang, and J. D. Glick (1999), Interannual variation of the Madden-Julian Oscillation during Austral summer, *J. Clim.*, **12**, 2538–2550.
- Hendon, H. H., B. Liebmann, M. E. Newman, J. D. Glick, and J. E. Schemm (2000), Medium-range forecast errors associated with active episodes of the Madden-Julian Oscillation, *Mon. Weather Rev.*, **128**, 69–86.
- Higgins, R. W., and W. Shi (2001), Intercomparison of the principal modes of interannual and intraseasonal variability of the North American monsoon system, *J. Clim.*, **14**, 403–417.
- Hirst, A. C., and K.-M. Lau (1990), Intraseasonal and interannual oscillations in coupled ocean-atmosphere modes, *J. Clim.*, **3**, 713–725.
- Hostetter, C. (1991), *Star Trek to Hawa-i'i: Mesopotamia to Polynesia*, 208 pp., Diamond Press, San Luis Obispo, Calif.
- Houze, R. A., Jr. (1989), Observed structure of mesoscale convective systems and implications for large-scale heating, *Q. J. R. Meteorol. Soc.*, **115**, 425–461.
- Houze, R. A., Jr., S. S. Chen, and D. E. Kingsmill (2000), Convection over the Pacific warm pool in relation to the atmospheric Kelvin-Rossby wave, *J. Atmos. Sci.*, **57**, 3058–3089.
- Hsu, H.-H. (1996), Global view of the intraseasonal oscillation during northern winter, *J. Clim.*, **9**, 2386–2406.
- Hsu, H.-H., B. J. Hoskins, and F.-F. Jin (1990), The 1985/86 intraseasonal oscillation and the role of the extratropics, *J. Atmos. Sci.*, **47**, 823–839.
- Hu, Q., and D. A. Randall (1994), Low-frequency oscillations in radiative-convective systems, *J. Atmos. Sci.*, **51**, 1089–1099.
- Hu, Q., and D. A. Randall (1995), Low-frequency oscillations in radiative-convective systems. Part II: An idealized model, *J. Atmos. Sci.*, **52**, 478–490.
- Huffman, G. J., R. F. Adler, P. Arkin, A. Chang, R. Ferraro, A. Gruber, J. Janowiak, A. McNab, B. Rudolph, and U. Schneider (1997), The Global Precipitation Climatology Project (GPCP) combined precipitation dataset, *Bull. Am. Meteorol. Soc.*, **78**, 5–20.
- Inness, P. M., and J. M. Slingo (2003), Simulation of the Madden-Julian Oscillation in a coupled general circulation model. Part I: Comparisons with observations and an atmosphere-only GCM, *J. Clim.*, **16**, 345–364.
- Inness, P. M., J. M. Slingo, S. J. Woolnough, R. B. Neale, and V. D. Pope (2001), Organization of tropical convection in a GCM with varying vertical resolution: Implications for the simulation of the Madden-Julian Oscillation, *Clim. Dyn.*, **17**, 777–793.
- Inness, P. M., J. M. Slingo, E. Guilyardi, and J. Cole (2003), Simulation of the Madden-Julian Oscillation in a coupled general circulation model. Part II: The role of the basic state, *J. Clim.*, **16**, 365–382.
- Itoh, H. (1989), The mechanism for the scale selection of tropical intraseasonal oscillations. Part I: Selection of wavenumber 1 and the three-scale structure, *J. Atmos. Sci.*, **46**, 1779–1798.
- Jin, F. F. (1997), An equatorial ocean recharge paradigm for ENSO. part I: Conceptual model, *J. Atmos. Sci.*, **54**, 811–829.
- Jin, F.-F., D. Neelin, and M. Ghil (1996), El Niño/Southern Oscillation and the annual cycle: Subharmonic frequency locking and aperiodicity, *Physica D*, **98**, 442–465.
- Johnson, E. S., and M. J. McPhaden (1993a), Structure of intraseasonal Kelvin waves in the equatorial Pacific Ocean, *J. Phys. Oceanogr.*, **23**, 608–625.
- Johnson, E. S., and M. J. McPhaden (1993b), Effects of a three-dimensional mean flow on intraseasonal Kelvin waves in the equatorial Pacific Ocean, *J. Geophys. Res.*, **98**, 10,185–10,194.
- Johnson, R. H., T. M. Rickenbach, S. A. Rutledge, P. E. Ciesielski, and W. H. Schubert (1999), Trimodal characteristics of tropical convection, *J. Clim.*, **12**, 2397–2418.
- Jones, C. (2000), Occurrence of extreme precipitation events in California and relationships with the Madden-Julian Oscillation, *J. Clim.*, **13**, 3576–3587.
- Jones, C., and J.-K. E. Schemm (2000), The influence of intraseasonal variations on medium-range weather forecast over South America, *Mon. Weather Rev.*, **128**, 486–494.
- Jones, C., and B. C. Weare (1996), The role of low-level moisture convergence and ocean latent heat flux in the Madden-Julian Oscillation: An observational analysis using ISCCP data and ECMWF analyses, *J. Clim.*, **9**, 3086–3104.
- Jones, C., D. E. Waliser, and C. Gautier (1998), The influence of the Madden-Julian Oscillation on ocean surface heat fluxes and sea surface temperature, *J. Clim.*, **11**, 1057–1072.
- Jones, C., D. E. Waliser, J.-K. E. Schemm, and W. K. M. Lau (2000), Prediction skill of the Madden and Julian Oscillation in dynamical extended range forecasts, *Clim. Dyn.*, **16**, 273–289.
- Jones, C., D. E. Waliser, K. M. Lau, and W. Stern (2004), Global occurrences of extreme precipitation events and the Madden-Julian Oscillation: Observations and predictability, *J. Clim.*, **17**, 4575–4589.
- Kalnay, E., et al. (1996), NCEP/NCAR 40-year reanalysis project, *Bull. Am. Meteorol. Soc.*, **77**, 437–471.
- Kawamura, R. (1991), Air-sea coupled modes on intraseasonal and interannual time scales over the tropical western Pacific, *J. Geophys. Res.*, **96**, 3165–3172.
- Kayano, M. T., and V. E. Kousky (1998), Zonally symmetric and asymmetric features of the tropospheric Madden-Julian Oscillation, *J. Geophys. Res.*, **103**, 13,703–13,712.
- Keen, R. A. (1982), The role of cross-equatorial tropical cyclone pairs in the Southern Oscillation, *Mon. Weather Rev.*, **110**, 1405–1416.
- Kemball-Cook, S. R., and B. C. Weare (2001), The onset of convection in the Madden Julian Oscillation, *J. Clim.*, **14**, 780–793.
- Kemball-Cook, S., B. Wang, and X. Fu (2002), Simulation of the intraseasonal oscillation in the ECHAM-4 model: The impact of coupling with an ocean model, *J. Atmos. Sci.*, **59**, 1433–1453.
- Kessler, W. S. (2001), EOF representation of the Madden-Julian Oscillation and its connection with ENSO, *J. Clim.*, **14**, 3055–3061.
- Kessler, W. S., and R. Kleeman (2000), Rectification of the Madden-Julian Oscillation into the ENSO cycle, *J. Clim.*, **15**, 3560–3575.
- Kessler, W. S., and M. J. McPhaden (1995), The 1991–93 El Niño in the central Pacific, *Deep Sea Res., Part II*, **42**, 295–333.
- Kessler, W. S., M. J. McPhaden, and K. M. Weickmann (1995), Forcing of intraseasonal Kelvin waves in the equatorial Pacific, *J. Geophys. Res.*, **100**, 10,613–10,631.
- Khairoutdinov, M. F., and D. A. Randall (2001), A cloud-resolving model as a cloud parameterization in the NCAR Community Climate System Model: Preliminary results, *Geophys. Res. Lett.*, **28**, 3617–3620.
- Kiladis, G. N., K. H. Straub, and P. T. Haertel (2005), Zonal and vertical structure of the Madden-Julian Oscillation, *J. Atmos. Sci.*, in press.
- Kingsmill, D. E., and R. A. Houze Jr. (1999), Kinematic characteristics of air flowing into and out of precipitating convection over the west Pacific warm pool: An airborne Doppler radar survey, *Q. J. R. Meteorol. Soc.*, **125**, 1165–1207.
- Kindle, J. C., and P. A. Phoebus (1995), The ocean response to operational westerly wind bursts during the 1991–1992 El Niño, *J. Geophys. Res.*, **100**, 4893–4920.
- Kleeman, R., and A. M. Moore (1997), A theory for the limitation of ENSO predictability due to stochastic atmospheric transients, *J. Atmos. Sci.*, **54**, 753–767.
- Knutson, R. R., K. M. Weickmann, and J. E. Kutzbach (1986), Global-scale intraseasonal oscillations of outgoing longwave radiation and 250 mb zonal wind during Northern Hemisphere summer, *Mon. Weather Rev.*, **114**, 605–623.
- Knutson, T. R., and K. M. Weickmann (1987), 30–60 day atmospheric oscillations: Composite life cycles of convection

- and circulation anomalies, *Mon. Weather Rev.*, **115**, 1407–1436.
- Krishnamurti, T. N., P. K. Jayakumar, J. Sheng, N. Surgi, and A. Kumar (1985), Divergent circulations on the 30 to 50 day time scale, *J. Atmos. Sci.*, **42**, 364–375.
- Krishnamurti, T. N., D. K. Oosterhof, and A. V. Mehta (1988), Air-sea interaction on the time scale of 30 to 50 days, *J. Atmos. Sci.*, **45**, 1304–1322.
- Kurtman, B. P., and P. S. Schopf (1998), Decadal variability in ENSO predictability and prediction, *J. Clim.*, **11**, 2804–2822.
- Kutsuwada, K., and M. J. McPhaden (2002), Intraseasonal variations in the upper equatorial Pacific Ocean prior to and during the 1997–98 El Niño, *J. Phys. Oceanogr.*, **32**, 1133–1149.
- Landsea, C. W., and J. A. Knaff (2000), How much skill was there in forecasting the very strong 1997–98 El Niño?, *Bull. Am. Meteorol. Soc.*, **81**, 2107–2119.
- Langley, R. B., R. W. King, I. I. Shapiro, R. D. Rosen, and D. A. Salstein (1981), Atmospheric angular momentum and the length of the day: A common fluctuation with a period of 50 days, *Nature*, **294**, 730–732.
- Latif, M., J. Biercamp, and H. von Storch (1988), The response of a coupled ocean-atmosphere general circulation model to wind bursts, *J. Atmos. Sci.*, **45**, 964–979.
- Latif, M., D. Anderson, T. Barnett, M. Cane, R. Kleeman, A. Leetmaa, J. O'Brien, A. Rosati, and E. Schneider (1998), A review of the predictability and prediction of ENSO, *J. Geophys. Res.*, **103**, 14,375–14,393.
- Lau, K.-M. (1985), Elements of a stochastic-dynamical theory of the El Niño/Southern Oscillation, *J. Atmos. Sci.*, **42**, 1552–1558.
- Lau, K.-M., and P. H. Chan (1985), Aspects of the 40–50 day oscillation during the northern winter as inferred from outgoing longwave radiation, *Mon. Weather Rev.*, **113**, 1889–1909.
- Lau, K.-M., and P. H. Chan (1986), Aspects of the 40–50 day oscillation during the northern summer as inferred from outgoing longwave radiation, *Mon. Weather Rev.*, **114**, 1354–1367.
- Lau, K.-M., and P. H. Chan (1988), Intraseasonal and interannual variations of tropical convection: A possible link between the 40–50 day oscillation and ENSO?, *J. Atmos. Sci.*, **45**, 506–521.
- Lau, K.-M., and F. C. Chang (1992), Tropical intraseasonal oscillation and its prediction by the NMC operational model, *J. Clim.*, **5**, 1365–1378.
- Lau, K.-M., and L. Peng (1987), Origin of low-frequency (intraseasonal) oscillations in the tropical atmosphere. Part I: Basic theory, *J. Atmos. Sci.*, **44**, 950–972.
- Lau, K.-M., and S. Shen (1988), On the dynamics of intraseasonal oscillations and ENSO, *J. Atmos. Sci.*, **45**, 1781–1797.
- Lau, K.-M., and C.-H. Sui (1997), Mechanisms of short-term sea surface temperature regulation: Observations during TOGA COARE, *J. Clim.*, **10**, 465–472.
- Lau, K.-M., and D. E. Waliser (2005), *Intraseasonal Variability in the Atmosphere-Ocean Climate System*, 436 pp., Praxis, Chichester, U.K.
- Lau, K.-M., L. Peng, C. H. Sui, and T. Nakazawa (1989), Dynamics of super cloud clusters, westerly wind bursts, 30–60 day oscillations and ENSO: An unified view, *J. Meteorol. Soc. Jpn.*, **67**, 205–219.
- Lau, K.-M., P.-J. Sheu, and I.-S. Kang (1994), Multiscale low-frequency circulation modes in the global atmosphere, *J. Atmos. Sci.*, **51**, 1169–1193.
- Lau, N. C., and K.-M. Lau (1986), Structure and propagation of intraseasonal oscillations appearing in a GFDL GCM, *J. Atmos. Sci.*, **43**, 2023–2047.
- Lau, N. C., I. M. Held, and J. D. Neelin (1988), The Madden-Julian Oscillation in an idealized general circulation model, *J. Atmos. Sci.*, **45**, 3810–3832.
- Lawrence, D. M., and P. J. Webster (2002), The boreal summer intraseasonal oscillation: Relationship between northward and eastward movement of convection, *J. Atmos. Sci.*, **59**, 1593–1606.
- Lengaigne, M., J.-P. Boulanger, C. Menkes, G. Madec, and P. Delecluse (2003), The March 1997 westerly wind event and the onset of the 1997/98 El Niño: Understanding the role of the atmospheric response, *J. Clim.*, **16**, 3330–3343.
- Liebmann, B., and D. L. Hartmann (1984), An observational study of tropical-midlatitude interaction on intraseasonal time scales during winter, *J. Atmos. Sci.*, **41**, 3333–3350.
- Liebmann, B., H. Hendon, and J. Glick (1994), The relationship between tropical cyclones of the western Pacific and Indian oceans and the Madden-Julian Oscillation, *J. Meteorol. Soc. Jpn.*, **72**, 401–411.
- Liebmann, B., H. H. Hendon, and J. D. Glick (1997), On the generation of two-day convective disturbances across the western equatorial Pacific, *J. Meteorol. Soc. Jpn.*, **75**, 939–946.
- Liebmann, B., G. N. Kiladis, C. S. Vera, A. C. Saulo, and L. M. V. Carvalho (2004), Subseasonal variations of rainfall in the vicinity of the South American low-level jet stream and comparison to those in the South Atlantic Convergence Zone, *J. Clim.*, **17**, 3829–3842.
- Liess, S., and L. Bengtsson (2004), The intraseasonal oscillation in ECHAM4 part II: Sensitivity studies, *Clim. Dyn.*, **22**, 671–688, doi:10.1007/s00382-004-0407-z.
- Liess, S., L. Bengtsson, and K. Arpe (2004), The intraseasonal oscillation in ECHAM4 part I: Coupled to a comprehensive ocean model, *Clim. Dyn.*, **22**, 653–669, doi:10.1007/s00382-004-0406-0.
- Lin, J., B. E. Mapes, M. Zhang, and M. Newman (2004), Stratiform precipitation, vertical heating profiles, and the Madden-Julian Oscillation, *J. Atmos. Sci.*, **61**, 296–309.
- Lin, J. W.-B., J. D. Neelin, and N. Zeng (2000), Maintenance of tropical intraseasonal variability: Impact of evaporation-wind feedback and midlatitude storms, *J. Atmos. Sci.*, **57**, 2793–2823.
- Lin, X., and R. H. Johnson (1996a), Kinematic and thermodynamic characteristics of the flow over the western Pacific warm pool during TOGA COARE, *J. Atmos. Sci.*, **53**, 695–715.
- Lin, X., and R. H. Johnson (1996b), Heating, moistening, and rainfall over the western Pacific warm pool during TOGA COARE, *J. Atmos. Sci.*, **53**, 3367–3383.
- Lindstrom, E., R. Lukas, R. Fine, E. Firing, J. S. Godfrey, G. Meyers, and M. Tsuchiya (1987), The western equatorial Pacific Ocean circulation study, *Nature*, **330**, 533–537.
- Lindzen, R. S. (1974), Wave-CISK in the tropics, *J. Atmos. Sci.*, **31**, 156–179.
- Lo, F., and H. H. Hendon (2000), Empirical extended-range forecasting of the Madden-Julian Oscillation, *Mon. Weather Rev.*, **128**, 2528–2543.
- Lukas, R., and E. Lindstrom (1991), The mixed layer of the western equatorial Pacific Ocean, *J. Geophys. Res.*, **96**, 3343–3357.
- Lukas, R., S. P. Hayes, and K. Wyrki (1984), Equatorial sea level response during the 1982–1983 El Niño, *J. Geophys. Res.*, **89**, 10,425–10,430.
- Luther, D. S., D. E. Harrison, and R. A. Knox (1983), Zonal winds in the central equatorial Pacific and El Niño, *Science*, **222**, 327–330.
- Madden, R. A. (1986), Seasonal variations of the 40–50 day oscillation in the tropics, *J. Atmos. Sci.*, **43**, 3138–3158.
- Madden, R. A., and P. R. Julian (1971), Detection of a 40–50 day oscillation in the zonal wind in the tropical Pacific, *J. Atmos. Sci.*, **28**, 702–708.
- Madden, R. A., and P. R. Julian (1972), Description of global-scale circulation cells in the tropics with a 40–50 day period, *J. Atmos. Sci.*, **29**, 1109–1123.
- Madden, R. A., and P. R. Julian (1994), Observations of the 40–50 day tropical oscillation: A review, *Mon. Weather Rev.*, **112**, 814–837.
- Magana, V., and M. Yanai (1991), Tropical-midlatitude interaction on the time scale of 30 to 60 days during the northern summer of 1979, *J. Clim.*, **4**, 180–201.
- Majda, A. J., and J. A. Biello (2004), A multiscale model for tropical intraseasonal oscillation, *Proc. Natl. Acad. Sci. U. S. A.*, **101**, 4736–4741.

- Mak, M. K. (1969), Laterally driven stochastic motions in the equatorial area, *J. Atmos. Sci.*, 26, 41–64.
- Maloney, E. D. (2002), An intraseasonal oscillation composite life cycle in the NCAR CCM3.6 with modified convection, *J. Clim.*, 15, 964–982.
- Maloney, E. D., and D. L. Hartmann (1998), Frictional moisture convergence in a composite life cycle of the Madden-Julian Oscillation, *J. Clim.*, 11, 2387–2403.
- Maloney, E. D., and D. L. Hartmann (2000), Modulation of eastern North Pacific hurricanes by the Madden-Julian Oscillation, *J. Clim.*, 13, 1451–1460.
- Maloney, E. D., and D. L. Hartmann (2001), The sensitivity of intraseasonal variability in the NCAR CCM3 to changes in convective parameterization, *J. Clim.*, 14, 2015–2034.
- Maloney, E. D., and J. T. Kiehl (2002), MJO related SST variations over the tropical eastern Pacific during Northern Hemisphere summer, *J. Clim.*, 15, 675–689.
- Maloney, E. D., and A. H. Sobel (2004), Surface fluxes and ocean coupling in the tropical intraseasonal oscillation, *J. Clim.*, 17, 4368–4386.
- Mapes, B. E. (2000), Convective inhibition, subgridscale triggering, and stratiform instability in a toy tropical wave model, *J. Atmos. Sci.*, 57, 1515–1535.
- Mapes, B. E., and R. A. Houze Jr. (1993), Cloud clusters and superclusters over the oceanic warm pool, *Mon. Weather Rev.*, 121, 1398–1415.
- Mather, J. H., T. P. Ackerman, W. E. Clements, F. J. Barnes, M. D. Ivey, L. D. Hatfield, and R. M. Reynolds (1998), An atmospheric radiation and cloud station in the tropical western Pacific, *Bull. Am. Meteorol. Soc.*, 79, 627–642.
- Matsuno, T. (1966), Quasi-geostrophic motions in the equatorial area, *J. Meteorol. Soc. Jpn.*, 44, 25–43.
- Matthews, A. J. (2000), Propagation mechanisms for the Madden-Julian Oscillation, *Q. J. R. Meteorol. Soc.*, 126, 2637–2651.
- Matthews, A. J. (2004), Intraseasonal variability over tropical Africa during northern summer, *J. Clim.*, 17, 2427–2440.
- Matthews, A. J., and G. N. Kiladis (1999), The tropical-extratropical interaction between high-frequency transients and the Madden-Julian Oscillation, *Mon. Weather Rev.*, 127, 661–677.
- Matthews, A. J., B. J. Hoskins, and J. M. Slingo (1996), Development of convection along the SPCZ within a Madden-Julian Oscillation, *Q. J. R. Meteorol. Soc.*, 122, 669–688.
- McCreary, J. P. (1983), A model of tropical ocean-atmosphere interaction, *Mon. Weather Rev.*, 111, 370–387.
- McPhaden, M. J. (1999), Genesis and evolution of the 1997–98 El Niño, *Science*, 283, 950–954.
- McPhaden, M. J. (2002), Mixed layer temperature balance on intraseasonal timescales in the equatorial Pacific Ocean, *J. Clim.*, 15, 2632–2647.
- McPhaden, M. J. (2004), Evolution of the 2002/2003 El Niño, *Bull. Am. Meteorol. Soc.*, 85, 677–695.
- McPhaden, M. J., and B. A. Taft (1988), On the dynamics of seasonal and intraseasonal variability in the eastern equatorial Pacific, *J. Phys. Oceanogr.*, 18, 1713–1732.
- McPhaden, M. J., H. P. Freitag, S. P. Hayes, B. A. Taft, Z. Chen, and K. Wyrtki (1988), The response of the equatorial Pacific Ocean to a westerly wind burst in May 1986, *J. Geophys. Res.*, 93, 10,589–10,603.
- McPhaden, M. J., F. Bahr, Y. Du Penhoat, E. Firing, S. P. Hayes, P. P. Niiler, P. L. Richardson, and J. M. Toole (1992), The response of the western equatorial Pacific ocean to westerly wind bursts during November 1989 to January 1990, *J. Geophys. Res.*, 97, 14,289–14,303.
- McPhaden, M. J., et al. (1998), The Tropical Ocean-Global Atmosphere observing system: A decade of progress, *J. Geophys. Res.*, 103, 14,169–14,240.
- Mechem, D. B., S. S. Chen, and R. A. Houze Jr. (2005), Momentum transport processes in the stratiform regions of mesoscale convective systems over the western Pacific warm pool, *Q. J. R. Meteorol. Soc.*, in press.
- Meyers, G., J. R. Donguy, and R. K. Reed (1986), Evaporative cooling of the western equatorial Pacific Ocean by anomalous winds, *Nature*, 323, 523–526.
- Milliff, R. F., and R. A. Madden (1996), The existence and vertical structure of fast, eastward-moving disturbances in the equatorial troposphere, *J. Atmos. Sci.*, 53, 586–597.
- Min, S.-K., S. Legutke, A. Hense, and W.-T. Kwon (2004), Climatology and internal variability in a 1000-year control simulation with the coupled climate model ECHO-G, *Tech. Rep. 2*, 67 pp., Model and Data Group, Max Planck Inst. for Meteorol., Hamburg, Germany.
- Mo, K., and R. W. Higgins (1998), Tropical convection and precipitation regimes in the western United States, *J. Clim.*, 10, 3028–3046.
- Moncrieff, M. (2004), Analytic representation of the large-scale organization of tropical convection, *J. Atmos. Sci.*, 61, 1521–1538.
- Moore, A. M., and R. Kleeman (1999a), Stochastic forcing of ENSO by the intraseasonal oscillation, *J. Clim.*, 12, 1199–1220.
- Moore, A. M., and R. Kleeman (1999b), The nonnormal nature of El Niño and intraseasonal variability, *J. Clim.*, 12, 2965–2982.
- Moskowitz, B., and C. S. Bretherton (2000), An analysis of frictional feedback on a moist equatorial Kelvin mode, *J. Atmos. Sci.*, 57, 2188–2206.
- Mote, P. W., H. L. Clark, T. J. Dunkerton, R. S. Harwood, and H. C. Pumphrey (2000), Intraseasonal variations of water vapor in the tropical upper troposphere and tropopause region, *J. Geophys. Res.*, 105, 17,457–17,470.
- Myers, D. S., and D. E. Waliser (2003), Three-dimensional water vapor and cloud variations associated with the Madden-Julian Oscillation during Northern Hemisphere winter, *J. Clim.*, 16, 929–950.
- Nakazawa, T. (1988), Tropical super clusters within intraseasonal variations over the western Pacific, *J. Meteorol. Soc. Jpn.*, 66, 823–836.
- Neelin, J. D., and J.-Y. Yu (1994), Modes of tropical variability under convective adjustment and the Madden-Julian Oscillation. Part I. Analytical theory, *J. Atmos. Sci.*, 51, 1876–1894.
- Neelin, J. D., I. M. Held, and K. H. Cook (1987), Evaporation-wind feedback and low-frequency variability in the tropical atmosphere, *J. Atmos. Sci.*, 44, 2341–2348.
- Neelin, J. D., D. S. Battisti, A. C. Hirst, F.-F. Jin, Y. Wakata, T. Yamagata, and S. E. Zebiak (1998), ENSO theory, *J. Geophys. Res.*, 103, 14,261–14,290.
- Newman, M., P. D. Sardeshmukh, C. R. Winkler, and J. S. Whitaker (2003), A study of subseasonal predictability, *Mon. Weather Rev.*, 131, 1715–1732.
- Nieto Ferreira, R., W. H. Schubert, and J. J. Hack (1996), Dynamical aspects of twin tropical cyclones associated with the Madden-Julian Oscillation, *J. Atmos. Sci.*, 53, 929–945.
- Nogués-Paegle, J., B.-C. Lee, and V. E. Kousky (1989), Observed modal characteristics of the intraseasonal oscillation, *J. Clim.*, 2, 496–507.
- North, G. R., T. L. Bell, R. F. Cahalan, and F. J. Moeng (1982), Sampling errors in the estimation of empirical orthogonal functions, *Mon. Weather Rev.*, 110, 699–706.
- Ooyama, K. (1964), A dynamical model for the study of tropical cyclone development, *Geophys. Int.*, 4, 187–198.
- Paegle, J. N., L. A. Byerle, and K. C. Mo (2000), Intraseasonal modulation of South American summer precipitation, *Mon. Weather Rev.*, 128, 837–850.
- Park, C.-K., D. M. Straus, and K.-M. Lau (1990), An evaluation of the structure of tropical intraseasonal oscillations in three general circulation models, *J. Meteorol. Soc. Jpn.*, 68, 403–417.
- Penland, C. (1996), A stochastic model of Indo-Pacific sea surface temperature anomalies, *Physica D*, 98, 534–558.
- Penland, C., and P. D. Sardeshmukh (1995), The optimal growth of tropical sea surface temperature anomalies, *J. Clim.*, 8, 1999–2024.

- Perigaud, C. M., and C. Cassou (2000), Importance of oceanic decadal trends and westerly wind bursts for forecasting El Niño, *Geophys. Res. Lett.*, **27**, 389–392.
- Picaut, J., M. Ioualalen, C. Menkes, T. Delcroix, and M. J. McPhaden (1996), Mechanism of the zonal displacements of the Pacific warm pool: Implications for ENSO, *Science*, **274**, 1486–1489.
- Randall, D., M. Khairoutdinov, A. Arakawa, and W. Grabowski (2003), Breaking the cloud parameterization deadlock, *Bull. Am. Meteorol. Soc.*, **84**, 1547–1564.
- Raymond, D. J. (1994), Cumulus convection and the Madden-Julian Oscillation in the tropical troposphere, *Physica D*, **77**, 1–22.
- Raymond, D. J. (2001), A new model of the Madden-Julian Oscillation, *J. Atmos. Sci.*, **58**, 2807–2819.
- Ripa, P. (1985), Nonlinear effects in the propagation of Kelvin pulses across the Pacific Ocean, in *Advances in Nonlinear Waves*, vol. II, edited by L. Debnath, pp. 43–55, Pitman, London.
- Rui, H., and B. Wang (1990), Development characteristics and dynamic structure of tropical intraseasonal convection anomalies, *J. Atmos. Sci.*, **47**, 357–379.
- Salby, M. L., and R. R. Garcia (1987), Transient response to localized episodic heating in the tropics. Part I: Excitation and short-time, near-field behavior, *J. Atmos. Sci.*, **44**, 458–498.
- Salby, M. L., and H. H. Hendon (1994), Intraseasonal behavior of clouds, temperature, and winds in the tropics, *J. Atmos. Sci.*, **51**, 2207–2224.
- Salby, M. L., R. R. Garcia, and H. H. Hendon (1994), Planetary-scale circulations in the presence of climatological and wave-induced heating, *J. Atmos. Sci.*, **51**, 2344–2367.
- Sancho, J. M., M. San Miguel, S. L. Katz, and J. D. Gunton (1982), Analytical and numerical studies of multiplicative noise, *Phys. Rev. A*, **26**, 1589–1609.
- Schneider, E. K., and R. S. Lindzen (1977), Axially symmetric steady-state models of the basic state for instability and climate studies. Part I: Linearized calculations, *J. Atmos. Sci.*, **34**, 263–279.
- Seo, K.-H., and K.-Y. Kim (2003), Propagation and initiation mechanisms of the Madden-Julian Oscillation, *J. Geophys. Res.*, **108**(D13), 4384, doi:10.1029/2002JD002876.
- Shinoda, T., and H. H. Hendon (1998), Mixed layer modeling of intraseasonal variability in the tropical western Pacific and Indian Oceans, *J. Clim.*, **11**, 2668–2685.
- Shinoda, T., and H. H. Hendon (2001), Upper-ocean heat budget in response to the Madden-Julian Oscillation in the western equatorial Pacific, *J. Clim.*, **14**, 4147–4165.
- Shinoda, T., and H. H. Hendon (2002), Rectified wind forcing and latent heat flux produced by the Madden-Julian Oscillation, *J. Clim.*, **15**, 3500–3508.
- Shinoda, T., H. H. Hendon, and J. Glick (1998), Intraseasonal variability of surface fluxes and sea surface temperature in the tropical Indian and Pacific oceans, *J. Clim.*, **11**, 1685–1702.
- Shinoda, T., H. H. Hendon, and J. Glick (1999), Intraseasonal surface fluxes in the tropical western Pacific and Indian oceans from NCEP reanalyses, *Mon. Weather Rev.*, **127**, 678–693.
- Slingo, J. M., et al. (1996), Intraseasonal oscillations in 15 atmospheric general circulation models: Results from an AMIP diagnostic subproject, *Clim. Dyn.*, **12**, 325–357.
- Slingo, J. M., D. P. Rowell, K. R. Sperber, and F. Nortley (1999), On the predictability of the interannual behavior of the Madden-Julian Oscillation and its relationship with El Niño, *Q. J. R. Meteorol. Soc.*, **125**, 583–610.
- Slingo, J. M., P. Inness, R. Neale, S. Woolnough, and G.-Y. Yang (2003), Scale interactions on diurnal to seasonal timescales and their relevance to model systematic errors, *Ann. Geophys.*, **46**, 139–155.
- Smyth, W. D., D. Hebert, and J. N. Moum (1996), Local ocean response to a multiphase westerly wind burst. Part II: Thermal and freshwater responses, *J. Geophys. Res.*, **101**, 22,513–22,533.
- Song, X., and C. A. Friehe (1997), Surface air-sea fluxes and upper ocean heat budget at 156°E, 4°S during the Tropical Ocean-Global Atmosphere Coupled Ocean Atmosphere Response Experiment, *J. Geophys. Res.*, **102**, 23,109–23,129.
- Sperber, K. R. (2003), Propagation and the vertical structure of the Madden-Julian Oscillation, *Mon. Weather Rev.*, **131**, 3018–3037.
- Sperber, K. R. (2004), Madden-Julian variability in NCAR CAM2.0 and CCSM2.0, *Clim. Dyn.*, **23**, 259–278.
- Sperber, K. R., J. M. Slingo, P. M. Inness, and K. M. Lau (1997), On the maintenance and initiation of the intraseasonal oscillation in the NCEP/NCAR reanalysis and the GLA and UKMO AMIP simulations, *Clim. Dyn.*, **13**, 769–795.
- Sprintall, J., and M. Tomczak (1992), Evidence of the barrier layer in a surface layer of the tropics, *J. Geophys. Res.*, **97**, 7305–7316.
- Sprintall, J., and M. J. McPhaden (1994), Surface layer variations observed in multiyear time series measurements from the western equatorial Pacific, *J. Geophys. Res.*, **99**, 963–979.
- Straub, K. H., and G. N. Kiladis (2002), Observations of a convectively coupled Kelvin wave in the eastern Pacific ITCZ, *J. Atmos. Sci.*, **59**, 30–53.
- Straus, D. M., and R. S. Lindzen (2000), Planetary-scale baroclinic instability and the MJO, *J. Atmos. Sci.*, **57**, 3609–3626.
- Suarez, M. J., and P. S. Schopf (1988), A delayed action oscillator for ENSO, *J. Atmos. Sci.*, **45**, 3283–3287.
- Sui, C.-H., and K.-M. Lau (1989), Origin of low-frequency (intraseasonal) oscillations in the tropical atmosphere. Part II: Structure and propagation of mobile wave-CISK modes and their modification by lower boundary forcings, *J. Atmos. Sci.*, **46**, 37–56.
- Sui, C.-H., and K. M. Lau (1992), Multiple phenomena in the tropical atmosphere over the western Pacific, *Mon. Weather Rev.*, **120**, 407–430.
- Sui, C.-H., X. Li, K.-M. Lau, and D. Adamec (1997), Multiscale air–sea interactions during TOGA COARE, *Mon. Weather Rev.*, **125**, 448–462.
- Swinbank, R., T. N. Palmer, and M. K. Davey (1988), Numerical simulations of the Madden and Julian Oscillation, *J. Atmos. Sci.*, **45**, 774–788.
- Syu, H.-H., and J. D. Neelin (2000), ENSO in a hybrid coupled model. part II: Prediction with piggyback data assimilation, *Clim. Dyn.*, **16**, 35–48.
- Takayabu, Y. N. (1994), Large-scale cloud disturbances associated with equatorial waves. part II: Westward-propagating inertio-gravity waves, *J. Meteorol. Soc. Jpn.*, **72**, 451–465.
- Takayabu, Y. N., T. Iguchi, M. Kachi, A. Shibata, and H. Kanzawa (1999), Abrupt termination of the 1997–98 El Niño in response to a Madden-Julian Oscillation, *Nature*, **402**, 279–282, doi:10.1038/46254.
- Thompson, C. J., and D. S. Battisti (2000), A linear stochastic dynamical model of ENSO. Part I: Model development, *J. Clim.*, **13**, 2818–2832.
- Tompkins, A. M. (2001), Organization of tropical convection in low vertical wind shears: The role of water vapor, *J. Atmos. Sci.*, **58**, 529–545.
- Van Tuyl, A. H. (1987), Nonlinearities in low-frequency equatorial waves, *J. Atmos. Sci.*, **44**, 2478–2492.
- Vecchi, G., and D. E. Harrison (2000), Tropical Pacific sea surface temperature anomalies, El Niño, and equatorial westerly wind events, *J. Clim.*, **13**, 1814–1830.
- Waliser, D. E., C. Jones, J.-K. Schemm, and N. E. Graham (1999a), A statistical extended-range tropical forecast model based on the slow evolution of the Madden-Julian Oscillation, *J. Clim.*, **12**, 1918–1939.
- Waliser, D. E., K. M. Lau, and J. H. Kim (1999b), The influence of coupled sea surface temperatures on the Madden-Julian Oscillation: A model perturbation experiment, *J. Atmos. Sci.*, **56**, 333–358.
- Waliser, D. E., Z. Z. Zhang, K. M. Lau, and J. H. Kim (2001), Interannual sea surface temperature variability and the predictability of tropical intraseasonal variability, *J. Atmos. Sci.*, **58**, 2596–2615.

- Waliser, D. E., K. M. Lau, W. Stern, and C. Jones (2003a), Potential predictability of the Madden-Julian Oscillation, *Bull. Am. Meteorol. Soc.*, **84**, 33–50.
- Waliser, D. E., R. Murtugudde, and L. E. Lucas (2003b), Indo-Pacific Ocean response to atmospheric intraseasonal variability: 1. Austral summer and the Madden-Julian Oscillation, *J. Geophys. Res.*, **108**(C5), 3160, doi:10.1029/2002JC001620.
- Wang, B. (1988a), Dynamics of tropical low-frequency waves: An analysis of the moist Kelvin wave, *J. Atmos. Sci.*, **45**, 2051–2065.
- Wang, B. (1988b), Comments on “An air-sea interaction model of intraseasonal oscillation in the tropics,” *J. Atmos. Sci.*, **45**, 3521–3525.
- Wang, B. (2005), Theory, in *Intraseasonal Variability in the Atmosphere-Ocean Climate System*, edited by W. K. M. Lau and D. E. Waliser, pp. 307–360, Praxis, Chichester, U.K.
- Wang, B., and T. Li (1994), Convective interaction with boundary-layer dynamics in the development of the tropical intraseasonal system, *J. Atmos. Sci.*, **51**, 1386–1400.
- Wang, B., and H. Rui (1990a), Dynamics of the coupled moist Kelvin-Rossby wave on an equatorial beta plane, *J. Atmos. Sci.*, **47**, 397–413.
- Wang, B., and H. Rui (1990b), Synoptic climatology of transient tropical intraseasonal convective anomalies: 1975–1985, *Meteorol. Atmos. Phys.*, **44**, 43–61.
- Wang, B., and X. Xie (1997), Coupled modes of the warm pool climate system. Part I: The role of air-sea interaction in maintaining Madden-Julian Oscillation, *J. Clim.*, **8**, 2116–2135.
- Wang, B., and Y. Xue (1992), Behavior of a moist Kelvin wave packet with nonlinear heating, *J. Atmos. Sci.*, **49**, 549–559.
- Wang, C., and R. H. Weisberg (2000), The 1997–98 El Niño evolution relative to previous El Niño events, *J. Clim.*, **13**, 488–501.
- Wang, G., O. Alves, and N. Smith (2005), BAM3.0 tropical surface flux simulation and its impact on SST drift in a coupled model, *BMRC Res. Rep.* **107**, Bur. of Meteorol. Res. Cent., Melbourne, Victoria, Australia.
- Wang, W., and M. E. Schlesinger (1999), The dependence on convective parameterization of the tropical intraseasonal oscillation simulated by the UIUC 11-layer atmospheric GCM, *J. Clim.*, **12**, 1423–1457.
- Wang, W., S. Saha, H.-L. Pan, S. Nadiga, and G. White (2005), Simulation of ENSO in the new NCEP Coupled Forecast System Model (CFS03), *Mon. Weather Rev.*, in press.
- Watterson, I. G. (2002), The sensitivity of subannual and intraseasonal tropical variability to model ocean mixed layer depth, *J. Geophys. Res.*, **107**(D2), 4020, doi:10.1029/2001JD000671.
- Weare, B. C. (2003), Composite singular value decomposition analysis of moisture variations associated with the Madden-Julian Oscillation, *J. Clim.*, **16**, 3779–3792.
- Webster, P. J. (1983), Mechanisms of monsoon low-frequency variability: Surface hydrological effects, *J. Atmos. Sci.*, **40**, 2110–2124.
- Webster, P. J., and J. R. Holton (1982), Cross-equatorial response to middle-latitude forcing in a zonally varying basic state, *J. Atmos. Sci.*, **39**, 722–733.
- Webster, P. J., and R. Lukas (1992), TOGA COARE: The Coupled Ocean-Atmosphere Response Experiment, *Bull. Am. Meteorol. Soc.*, **73**, 1377–1416.
- Weickmann, K. M. (1983), Intraseasonal circulation and outgoing longwave radiation modes during Northern Hemisphere winter, *Mon. Weather Rev.*, **111**, 1838–1858.
- Weickmann, K. M., and S. J. S. Khalsa (1990), The shift of convection from the Indian Ocean to the western Pacific Ocean during a 30–60 day oscillation, *Mon. Weather Rev.*, **118**, 964–978.
- Weickmann, K. M., G. R. Lussky, and J. E. Kutzbach (1985), Intraseasonal (30–60 day) fluctuations of outgoing longwave radiation and 250 mb stream function during northern winter, *Mon. Weather Rev.*, **113**, 941–961.
- Weickmann, K. M., G. N. Kiladis, and P. D. Sardeshmukh (1997), The dynamics of intraseasonal atmospheric angular momentum oscillations, *J. Atmos. Sci.*, **54**, 1445–1461.
- Wheeler, M., and H. H. Hendon (2004), An all-season real-time multivariate MJO index: Development of an index for monitoring and prediction, *Mon. Weather Rev.*, **132**, 1917–1932.
- Wheeler, M., and G. N. Kiladis (1999), Convectively coupled equatorial waves: Analysis of clouds and temperature in the wavenumber-frequency domain, *J. Atmos. Sci.*, **56**, 374–399.
- Wheeler, M., and K. M. Weickmann (2001), Real-time monitoring and prediction of modes of coherent synoptic to intraseasonal tropical variability, *Mon. Weather Rev.*, **129**, 2677–2694.
- Wijesekera, H. W., and M. C. Gregg (1996), Surface layer response to weak winds, westerly bursts, and rain squalls in the western Pacific warm pool, *J. Geophys. Res.*, **101**, 977–997.
- Woolnough, S. J., J. M. Slingo, and B. J. Hoskins (2000), The relationship between convection and sea surface temperature on intraseasonal timescales, *J. Clim.*, **13**, 2086–2104.
- Wu, Z. (2003), A shallow CISK, deep equilibrium mechanism for the interaction between large-scale convection and large-scale circulations in the tropics, *J. Atmos. Sci.*, **60**, 377–392.
- Wu, Z., E. S. Sarachik, and D. S. Battisti (2000), Vertical structure of convective heating and the three-dimensional structure of the forced circulation on an equatorial beta plane, *J. Atmos. Sci.*, **57**, 2169–2187.
- Wu, Z., E. S. Sarachik, and D. S. Battisti (2001), Thermally driven tropical circulations under Rayleigh friction and Newtonian cooling: Analytic solutions, *J. Atmos. Sci.*, **58**, 724–741.
- Wyrtki, K. (1985), Water displacements in the Pacific and the genesis of El Niño cycles, *J. Geophys. Res.*, **90**, 7129–7132.
- Xie, P., and P. A. Arkin (1997), Global precipitation: A 17-year monthly analysis based on gauge observations, satellite estimates, and numerical model outputs, *Bull. Am. Meteorol. Soc.*, **78**, 2539–2558.
- Yamagata, T., and Y. Hayashi (1984), A simple diagnostic model for the 30–50 day oscillation in the tropics, *J. Meteorol. Soc. Jpn.*, **62**, 709–717.
- Yanai, M., and M.-M. Lu (1983), Equatorially trapped waves at 200 mb and their association with meridional convergence of wave energy flux, *J. Atmos. Sci.*, **40**, 2785–2803.
- Yanai, M., B. Chen, and W. W. Tung (2000), The Madden-Julian Oscillation observed during the TOGA COARE IOP: Global view, *J. Atmos. Sci.*, **57**, 2374–2396.
- Yano, J.-I., and K. Emanuel (1991), An improved model of the equatorial troposphere and its coupling with stratosphere, *Atmos. Sci.*, **48**, 377–389.
- Yano, J.-I., R. Blender, C. Zhang, and K. Fraedrich (2004), 1/f noise and pulse-like events in the tropical atmospheric surface variabilities, *Q. J. R. Meteorol. Soc.*, **130**, 1697–1721.
- Yasunari, T. (1979), Cloudiness fluctuations associated with the Northern Hemisphere summer monsoon, *J. Meteorol. Soc. Jpn.*, **57**, 227–242.
- Yoshida, K. (1959), A theory of the Cromwell Current and equatorial upwelling, *J. Oceanogr. Soc. Jpn.*, **15**, 154–170.
- Yu, J.-Y., and J. D. Neelin (1994), Modes of tropical variability under convective adjustment and the Madden-Julian Oscillation. Part II: Numerical results, *J. Atmos. Sci.*, **51**, 1895–1914.
- Zavala-Garay, J., A. M. Moore, and C. L. Perez (2003), The response of a coupled model of ENSO to observed estimates of stochastic forcing, *J. Clim.*, **16**, 2827–2842.
- Zavala-Garay, J., C. Zhang, A. M. Moore, and R. Kleeman (2005), On the linear response of ENSO to the Madden-Julian Oscillation, *J. Clim.*, in press.
- Zebiak, S. E. (1989), On the 30–60 day oscillation and the prediction of El Niño, *J. Clim.*, **2**, 1381–1387.
- Zhang, C. (1996), Atmospheric intraseasonal variability at the surface in the western Pacific Ocean, *J. Atmos. Sci.*, **53**, 739–785.
- Zhang, C. (1997), Intraseasonal variability of the upper-ocean temperature structure observed at 0° and 165°E, *J. Clim.*, **10**, 3077–3092.

- Zhang, C. (2001), Intraseasonal perturbations in sea surface temperatures of the equatorial eastern Pacific and their association with the Madden-Julian Oscillation, *J. Clim.*, *14*, 1309–1322.
- Zhang, C., and S. P. Anderson (2003), Sensitivity of intraseasonal perturbations in SST to the structure of the MJO, *J. Atmos. Sci.*, *60*, 2196–2207.
- Zhang, C., and M.-D. Chou (1999), Variability of water vapor, infrared radiative cooling, and atmospheric instability for deep convection in the equatorial western Pacific, *J. Atmos. Sci.*, *56*, 711–723.
- Zhang, C., and M. Dong (2004), Seasonality of the Madden-Julian Oscillation, *J. Clim.*, *17*, 3169–3180.
- Zhang, C., and J. Gottschalck (2002), SST anomalies of ENSO and the Madden-Julian Oscillation in the equatorial Pacific, *J. Clim.*, *15*, 2429–2445.
- Zhang, C., and H. H. Hendon (1997), On propagating and stationary components of the intraseasonal oscillation in tropical convection, *J. Atmos. Sci.*, *54*, 741–752.
- Zhang, C., and M. J. McPhaden (2000), Intraseasonal surface cooling in the equatorial western Pacific, *J. Clim.*, *13*, 2261–2276.
- Zhang, C., H. H. Hendon, W. S. Kessler, and A. Rosati (2001), A workshop on the MJO and ENSO, *Bull. Am. Meteorol. Soc.*, *82*, 971–976.
- Zhu, B., and B. Wang (1993), The 30–60-day convection seesaw between the tropical Indian and western Pacific oceans, *J. Atmos. Sci.*, *50*, 184–199.
- Zipser, E. J. (1969), The role of organized unsaturated convective downdrafts in the structure and rapid decay of an equatorial disturbance, *J. Appl. Meteorol.*, *8*, 799–814.

---

C. Zhang, Rosenstiel School of Marine and Atmospheric Science, University of Miami, 4600 Rickenbacker Causeway, Miami, FL 33149-1089, USA. (czhang@rsmas.miami.edu)